Title
CONVENTIONAL AND SEMIAUTOMATIC DATA PROCESSING AND INTERPRETATION

Authors
Alston, Margaret
Franck, Jack V.
Kerth, Leroy T.

Publication Date
1965-01-26

University of California

Ernest O. Lawrence Radiation Laboratory

CONVENTIAL & SEMIAUTOMIC DATA PROCESSING & INTERPRETATION

Berkeley, California

DISCLAIMER

Submitted for publication as Chapter 8 [illegible] in book "Bubble Chambers and Spark Chambers"

UCRL-11869

UNIVERSITY OF CALIFORNIA

Lawrence Radiation Laboratory
Berkeley, California

AEC Contract No. W-7405-eng-48

CONVENTIONAL AND SEMIAUTOMATIC DATA PROCESSING AND INTERPRETATION

Margaret Alston, Jack V. Franck, and Leroy T. Kerth

January 26, 1965

Publ. in Bubble and Spark Chambers
(Academic Press, New York, 1967), vol. II, ch 2.

CONVENTIONAL AND SEMIAUTOMATIC DATA PROCESSING AND INTERPRETATION

Contents

CONVENTIONAL AND SEMIAUTOMATIC DATA PROCESSING AND INTERPRETATION

Margaret Alston, Jack V. Franck, and Leroy T. Kerth

Lawrence Radiation Laboratory
University of California, Berkeley, California

January 26, 1965

I. GENERAL

A. Data Processing for Bubble Chambers and Spark Chambers

1. Introduction

Data analysis for bubble chambers and spark chambers serves both to identify the events recorded on film, and also to interpret the overall behavior of physical quantities obtained from each event. Events can be identified either by requiring a definite signature in a secondary array of counters, or by scanning the film for the required topology, making coordinate measurements along the tracks, and then making a mathematical reconstruction of the tracks and a kinematic analysis of the event to identify the particles. The first method is often used for spark chambers, but bubble chambers require the second method because the pictures are used to study many reactions simultaneously. The second part of the analysis requires calculation of various physical quantities from the observations as well as interpretation of physics results.

The approach to the problems of data analysis for the two types of chambers is strongly influenced by basic differences in the way the devices are used as well as by differences in the devices themselves.

A bubble chamber is a large, expensive piece of equipment that changes its configuration very little from one experiment to the next. Many different reactions, both simple and complex, can be studied using the same film; in addition, the method of analysis is very similar for all types of experiments and chambers. To analyze bubble-chamber data, several large complex systems of machines, people, and computer programs have been

built up in many laboratories over the past several years. In fact, these systems have occupied many engineers and programmers, and much of the physicist manpower spent in bubble-chamber physics. Each system is usually very flexible and can be used to analyze data from almost any chamber or experiment.

The spark-chamber experiment, on the other hand, is often designed to study only one particular reaction with high statistical accuracy. The chamber can be triggered by external devices to record only the required events and the configuration of the chambers can be tailored to suit the experiment. Each experiment, therefore, may present a whole new data-reduction problem, and the techniques used may be different for each experiment. Consequently, the data-analysis systems used for spark chambers are less sophisticated than those for bubble chambers. Compensation for this lack of sophistication in the analysis system can be obtained by a careful, and sometimes ingenious, arrangement of spark chambers, triggering logic, and optics.

This chapter describes some systems and techniques used in data processing. Unfortunately, much of the information is unpublished, making the compilation of a comprehensive bibliography extremely difficult. However, additional information can be found in the proceedings of several meetings (International Conference on Instrumentation for High Energy Physics 1960, 1963; Informal Meeting on Track Data Processing, 1962). We have also drawn extensively from the review article of Rosenfeld and Humphrey (1963).

2. Recording the Track Images

The track images are recorded on high-speed, high-contrast film with as fine a grain as possible. A bubble chamber is illuminated with high-intensity flash tubes in such a way as to produce either dark- or bright-field illumination; dark-field illumination is more popular. For

spark chambers the sparks themselves provide the illumination so that the pictures are always dark-field. In general, it is the negatives that are scanned and measured; therefore most pictures appear as dark traces on a transparent background.

Since the aperture of the camera lenses must be small to provide adequate depth of focus, the bubble or spark images are enlarged by diffraction. Bubble images are typically 20 to 30 microns in diameter on the film; the size of a spark image varies considerably, depending upon the arrangement of the plates and the magnification of the picture.

To make stereo reconstruction calculations as easy as possible, the simplest camera arrangement is preferred. For bubble chambers there are usually three views of each picture, the camera lenses being arranged on the corners of either a right angle or equilateral triangle and having their lens axes parallel. Parallel-plate spark chambers can be photographed with two camera lenses whose axes are perpendicular to each other and parallel to the surfaces of the plates. In either case the pictures can be taken on a separate film strip for each view, or all stereo views can be recorded on one film strip. For cylindrical-plate spark chambers, the two "views" are obtained by placing a tilted mirror below the chamber, giving the direct and reflected images on the same exposure.

3. Scanning

Negatives of the pictures are scanned for interesting topologies by human scanners, who recognize the patterns made by the tracks and classify them into event types. Each view is projected onto a two-dimensional screen (either reflecting or transmitting) and carefully examined. Usually the views of the stereo combination can be projected onto the screen either singly or concurrently so that the views can be easily compared.

After the scanner has found an interesting event, he records its topology and whereabouts in some coded format so that the event can be recorded on the master list of the experiment for subsequent evaluation. Great care must be taken to educate the scanners so that they record not only the event types for which they are looking but also those they do not understand; otherwise, unusual events will be lost.

4. Measuring

For bubble-chamber pictures, scanning and measuring may be done separately or concurrently. In most experiments, only the more interesting events are measured because of limited measuring facilities. The frequency of events requiring measurement depends upon the interactions being studied and may be one or more events per picture for simple events or as few as one in many thousands of pictures in the case of unusual interactions. Although some work has been done in reprojecting and measuring in three-dimensional space, the most popular technique is to make two-dimensional measurements of points along the tracks in at least two of the stereo views. The track measurements are made relative to two or more reference marks (fiducials) which are usually crosses engraved on the windows of the chamber. About 10 points are measured along each track in either Cartesian or polar coordinates. The time required to measure each event depends not only upon its complexity, but also upon the design of the measuring machine and how well the operator and machine have been integrated.

For spark chambers, the scanning and measuring problem is somewhat simpler than for bubble chambers. There are several reasons for this: The total amount of information on each picture is less; a spark chamber often has no magnetic field, and consequently the tracks are

straight; and the measurement need not be so accurate. Spark-chamber pictures are often measured with an x, y, θ device with a precision that is 1/5 to 1/10 that of bubble-chamber measurements.

5. Reconstruction and Identification

For accurate spatial reconstruction of the tracks, two-dimensional measurements on at least two stereo views must be made. Provided that corresponding identifiable points (i. e., a definite spark or bubble) are measured, two views are sufficient for accurate reconstruction of any track. Bubble-chamber tracks do not usually have sufficient distinguishing features to make this practical. If random points are measured and the track lies in a direction parallel to the line joining the two camera lenses (the stereo axis), it is impossible to find the depth of the track; the depth measurement is also very poor if the track makes a small angle with this direction. Consequently, if random points along each track are measured and only two views are used in the spatial-reconstruction program, the pair of views which gives optimum stereo reconstruction should be chosen by the measurer or the computer program.

If no magnetic field is applied to the chamber, the trajectory of each particle will be a straight line; however, in this case, no momentum measurement is obtained for any of the particles. In most bubble chambers and some spark chambers a high magnetic field is applied with its lines of force parallel to the optical axes of the camera lenses. The trajectory of each particle is then approximately a helix in space with its axis parallel to the lens axes, and the momentum is proportional to the radius of curvature of this helix.

Events can be identified by either (1) a special signature observed in external triggering devices, or (2) kinematics calculations made at each

vertex. The first method is normally used with spark chambers, the second for bubble chambers. When a kinematic analysis is used, a mass identity is assigned to each track and the four equations of momentum and energy conservation are used as constraints in the calculations. One can then calculate χ^2 for this hypothesis and hence find the probability that this particular physical interpretation of the event is correct. In general the hypothesis with the best χ^2 is accepted as correct unless this interpretation is overruled by the ionization of the tracks or other considerations.

6. Display of Physical Quantities and Interpretation

After an event has been consigned to a physical interpretation, the physical quantities required in the experiment are calculated. For example, the angle of the scattered particle with respect to its incident direction, or the invariant mass of two out-going particles might be required. Distributions of these calculated variables are then displayed for the physicist so that he can attempt to interpret the results. For example, the physicist might wish to examine the angular distribution of the scattered particle. These displays are usually in the form of histograms, ideograms, or scatter plots and can either be made by means of printout or by photographing a display on an oscilloscope attached to the computer.

From these displays the physicist attempts a further interpretation of the observations. To do this he requires additional physics-oriented computer programs. These programs may perform minimizing procedures, phase-space calculations for multibody final states, or any other physics calculations required.

7. Data Storage and Retrieval

All the raw data and the results of calculations must be filed so that they can be retrieved easily whenever additional calculations are

required. When only a few hundred events comprise the whole experiment, it is usually quite easy to keep a record of their current status and then construct tallies or histograms by hand. However, when the number of events increases to several thousands, this becomes very tedious and leads to many human errors. The best solution to this problem is a library system which uses a computer to store the data on magnetic tape or other storage media and also to retrieve the data when required. This library system contains scanning information, measuring information, physics information, and also the current status of each event. Tallies, lists, histograms, and plots can be obtained from this library as required.

B. History of Development

1. Equipment

Some of the first bubble-chamber experiments adopted techniques of analysis used previously for cloud-chamber experiments. One of these methods was to use a "space table." This was a screen mounted in such a way that it could be moved into any orientation in three dimensions. To reproduce the event in space, the two stereo views of a picture were replaced accurately in the camera and projected through the camera lenses. The screen could then be moved until the two images of any track were concurrent over its surface. The space table was particularly useful for events in which all the tracks were coplanar (e.g. elastic scatters). In this case, by properly positioning the screen, the two images of all tracks could be brought into coincidence on the table at the same time, and space angles, ranges and curvatures could be measured directly on the surface of the table, using a protractor, ruler, and curvature templates. Another method of using a "space table" was to obtain coincidence of the two images of one track with a line on the table. The dip and azimuthal angles of the track

could then be measured by protractors attached to the table.

The use of a space table for bubble-chamber analysis was very tedious, slow, and inaccurate. It was also seriously limited because the images were reprojected into air whereas the tracks were originally formed in a medium with a refractive index not equal to one. Consequently, a correction had to be applied to all dip angles. This correction, although quite small for liquid hydrogen ($\mu = 1.06$), is quite large for "heavy-liquid" chambers. Because of this correction and the tedium of the method, an easier way to analyze bubble-chamber pictures is to make coordinate measurements along the track images on each view separately and then calculate the position of the track in space. This method is currently used. At first, the pictures were either projected onto a screen and measurements made on the projected image using a ruler and protractor, or measurements were made on the film itself using a two-dimensional traveling microscope. The choice of method depended upon the accuracy required, and in either case the measurements were recorded manually. Later the coordinates of a measured point were automatically digitized and punched on cards. Devices such as those just described are still used quite frequently at installations where only a few thousand events are analyzed in each experiment and speed is not too important.

To speed up the measuring process, projection microscopes were introduced which made the measuring less fatiguing for the operator. The precision engine was guided by a servomechanism which sampled the track signal and kept the reticle tracking along the chosen track image. This device was invented and first constructed at Berkeley and is colloquially called a "Franckenstein." Projection microscopes both with and without automatic track following are now in use all over the world and have

accounted for most of the bubble-chamber data measured during the past six or seven years. These conventional measuring projectors will be described in detail later in this chapter.

In the past year more automatic devices have been put into operation for bubble-chamber analysis. These include the spiral reader, scanning and measuring projectors (SMP), and flying-spot digitizer (FSD), all at Berkeley, and the Hough-Powell device (HPD) at Brookhaven and CERN. All of these devices attempt to relieve the human operator of some or all of his chores and consequently speed up the measuring operation. The FSD may also be used ultimately to automatically scan and measure. Another device designed for this purpose is the precision encoder and pattern-recognition device (PEPR) currently being built at MIT. All of these devices are described in detail in Chapter IX.

Spark-chamber measurements usually need not be as accurate as those for bubble chambers. Consequently, scanning and measuring of spark-chamber film are usually done on the same machine. The measuring projectors currently in use are not so highly developed as for bubble-chamber measurements.

Recently several new devices using an oscilloscope for the automatic scanning and measuring of spark-chamber pictures have been put into operation at MIT and Chicago (CHLOE). The SASS project is under construction at Berkeley. These devices are described in detail in Chapter IX.

2. Computation

In the early days of bubble-chamber analysis little computation was required. Events were identified by making simple measurements on a scanning projector and comparing the measured quantities with graphical plots of kinematic functions and ionization. Transformation of measured quantities to the center-of-mass system could also be performed

graphically or by hand calculation. However, as the number of events increased, this procedure became too clumsy, and computer programs were required to cope with the volume of data.

The first programs which were written performed the spatial reconstruction of tracks from measurements on the film or projected image, since these calculations were most tedious to calculate manually. The azimuth and dip angle of each track were output and the event was plotted on a Woolf chart [1] to obtain the geometric three-dimensional properties of the event. Comparisons could then be made with kinematic plots as before. After an event had been identified, various quantities were punched onto cards or paper tape for input to programs that calculated the required physics information.

The next important advance, made about six years ago, was the writing of programs for the kinematics calculations and the classification of the event. Several versions of these programs exist and are described later.

The most recent advances have been in the areas of data manipulation: (1) programs to generate histograms and scatter plots, and (2) library routines. These latter routines are most important because they make a more coherent system out of the many unrelated programs.

The computations required for spark chambers are in general simpler than those for bubble chambers. Spark chambers have only existed for the past four or five years and no large data-reduction systems have been constructed. However, the growth of spark-chamber analysis has been similar to that of bubble chambers, and it is clear that many of the operations, particularly data manipulation and physics calculations, are identical in the two cases.

In general, the data-analysis ability in both spark-chamber and

bubble-chamber physics has lagged behind the output of the detecting device; only the more interesting events have been processed, and many experiments are completed years after the exposure has been made. However, with the advent of the more automatic devices described in Chapter IX, this should no longer be the case.

II. INTERPRETATION OF EXPERIMENTAL DATA

A. Types of Experiments

Most bubble chambers and spark chambers have been used in conjunction with large accelerators, primarily at Berkeley, Brookhaven, and CERN, in the study of high-energy-particle phenomena. In this chapter we do not attempt to review the field since this would obviously be impossible; rather we give the reader a brief outline of the type of experiments performed and techniques used in bubble- and spark-chamber data analysis. The bibliography we present is incomplete and merely gives examples of analysis techniques. The review articles quoted contain comprehensive bibliographies.

Most strange particles had already been discovered prior to the advent of the bubble chamber. However, many of their properties, such as mass, lifetime, decay modes, spin and parity, etc., have been determined using bubble- and spark-chamber techniques (Adair and Fowler, 1963).

A phenomenon that has been investigated very intensively in the past four years is that of particle resonant states, both between strange and non-strange particles. (See for example Dalitz, 1963; Puppi, 1963; and Rosenfeld, 1963.) Many resonances have already been discovered and many more will probably be found in the future. The technique most often used when searching for resonances in the final state is to plot histograms in M

(the invariant mass of the combination of particles) or M^2, and scatter diagrams in M^2. A resonance will appear as a peak in the mass spectrum and a clustering of points in the scatter plot. Resonances can also be found in the initial state by observing "bumps" in the total or partial cross sections and by investigating the behavior of angular distributions with incident momentum. Since the "lifetime" of a resonance is extremely short, a "resonant particle" does not travel an observable distance, and its existence can only be inferred. Determination of spin, parity, etc., for both particles and resonant states often requires examination of angular distributions and polarizations (Adair, 1955; Trieman and Yang, 1962; Byers and Fenster, 1963; Gatto and Stapp, 1961; and Capps, 1961). The existence of definite production or decay mechanisms, together with conservation laws, can also be used.

Many bubble and spark chamber experiments have been performed to investigate the properties of weak interactions (International Conference on Weak Interactions, 1963; Feinberg and Lederman, 1963). These experiments usually involve the observation of rare leptonic decay modes of particles and the interactions of muons and neutrinos with matter. Rare decay modes can be conveniently observed in bubble and spark chambers because the signature of the event is often unusual; a kinematic analysis can be made to identify the event. Information concerning the interactions of neutrinos with matter has been very limited in the past due to the very small cross sections involved ($\sim 10^{-38}$ cm^2) and the difficulty of this type of experiment. However, large fluxes of high-energy neutrinos are now available from the accelerators at Brookhaven and CERN, and the age of "high-energy neutrino physics" has just begun.

In all experiments it is customary to determine the cross sections

for the various reactions that occur. It may be difficult to obtain absolute cross sections from bubble chambers if the incident beam is contaminated with other particles, because it is hard to estimate the appropriate incident path length. Bubble chambers are always useful for finding relative partial cross sections. Total cross sections can be obtained quite easily from spark-chamber or counter experiments where a time-of-flight method and Čerenkov counters can be conveniently used to identify each incident particle.

B. Methods for Displaying Data

1. Histograms and Ideograms

Many data can be conveniently displayed in the form of histograms or ideograms. A histogram is a plot of the number of events that have a value (x_i) of variable (x) falling within cells of chosen size (Δx). The plot is independent of the calculated error (δx_i) on each value (x_i), although it is usual to choose $\Delta x >> \delta x_i$. A Gaussian ideogram, on the other hand, takes into account the value of δx_i. Each event is assigned a probability described by a normalized Gaussian centered at x_i and with standard deviation δx_i. Probabilities for all the events are then added together and plotted. It is important to estimate the value of δx_i correctly, and in bubble chamber experiments one must often increase the calculated errors by a factor a (see Section IIID).

The variables most often represented are mass or $(\text{mass})^2$ and angles of production or decay (angular distributions, Fig. 1). The distribution in M^2 is often preferred because it is the projection of a Dalitz plot (Fig. 2); also it can be shown the M^2 is nearly Gaussian distributed whereas M has a skew distribution (Rosenfeld and Humphrey, 1963).

Histograms are in general superior to ideograms because they are a straightforward representation of the data, whereas in an ideogram

some information is lost. Consequently, histograms afford a better feeling for statistical effects in the data, and it is easy to combine the results of many experiments. However, ideograms are useful for finding the resolution function in a mass distribution. In this case an ideogram can be made of the events in which the central value for each point is set equal to an arbitrary mass. Then the width of this ideogram gives the experimental resolution function.

2. Scatter Plots

a. Dalitz plot. A very convenient way of displaying the properties of three bodies in a final state is to plot each event as a point on a Dalitz plot (see Fig. 2). This is a scatter plot of either T_i vs T_j or M_{jk}^2 vs M_{ik}^2, where T_i is the kinetic energy of the ith particle in the center of mass of the three-body system, and M_{jk} is the invariant mass of the diparticle consisting of particles j and k, namely,

$$M_{jk}^2 = (E_j + E_k)^2 - (P_j + P_k)^2.$$

The available area of the Dalitz plot lies within an envelope determined by momentum conservation and the total energy of the three-body system (E^*). It can be shown that unit area within this envelope is proportional to the Lorentz-invariant phase space. Consequently, if there are no correlations between the three particles, the Dalitz plot for a particular center-of-mass energy will be uniformly populated. A resonant state between two of the particles will produce a bunching of points along the horizontal or vertical line corresponding to the mass of the resonance.

The Dalitz plot contains no information about the direction of the incident particle. This momentum merely determines the total energy available in the system, and consequently, the size of the envelope.

The choice of the variable M^2 or T is optional, since they are

linearly related by the expression $T_i = [(E^* - M_i)^2 - M_{jk}^2]/2E^*$. If a resonance in the final state is being investigated, it is convenient to use the M^2 representation, because all events, regardless of incident momentum, can be added together on one plot and will show the resonant effect at the same place. If, on the other hand, correlation between particles produced in a decay (for example, ω decay) is of interest, the variable T or a linear combination of T's is often used, and the coordinates are normalized so that the envelope for each event coincides as nearly as possible.

b. Triangle plot. A four-body final state is much harder to represent since there are five internal variables in addition to the beam momentum and direction. A plot sometimes made is a scatter diagram of M_{ij} versus M_{kl}. This is called a triangle plot because the outer envelope is a right triangle. Unfortunately, in this plot unit area is not proportional to Lorentz-invariant phase space. As in a Dalitz plot, a resonance between two particles shows as a clustering of points. However, since only two pairs of particles can be plotted at a time, some prior knowledge of the most useful pairing is required. Any additional correlations are not displayed and may produce spurious effects in the mass plots.

c. Chew-Low plot. Another type of scatter diagram is the Chew-Low plot (Chew and Low, 1959). This is used when "one-particle exchange" mechanisms are being investigated. Each event is represented as a point on the plane of Δ^2 versus ω^2, where Δ is the four-momentum transfer to the nucleon and ω is the invariant mass of the exchanged particle combined with the incident particle. If one-particle exchange takes place in the reaction considered, the points show a bunching towards low Δ.

C. Analysis of Experiments

1. Minimizing Procedures

Having obtained values and plots of various physical quantities, one must attempt to interpret those experimental data. This usually involves parameterization of the problem in terms of some currently favored theory. It is then necessary to find the values of these parameters which best describe the data. Two commonly used optimizing procedures are the maximum-likelihood and least-squares methods. These methods have been described in detail by Solmitz (1964).

All the "fitting procedures" consist of using the measured variables $\underline{x}$ and attempting to find good estimates ($\underline{a}^*$) of the true values ($\underline{a}$) of all the parameters describing the problem. In the "maximum-likelihood" method the required estimator (a_λ^*) is that value of the parameter (a_λ) for which the likelihood function (L) has its greatest value, i. e.

$$\frac{\partial}{\partial \underline{a}} [\ell n\, L(\underline{x}, \underline{a})] = 0.$$

For a sufficiently large sample, the distribution of a_λ^* is approximately Gaussian with its mean at a_λ. In the special case of Gaussian variable $\underline{x}$, we have

$$L \propto \exp[-\tfrac{1}{2} \chi^2(\underline{x}, \underline{a})]$$

and

$$\chi^2(\underline{x}, \underline{a}) = [\underline{x} - \underline{f}(\underline{a})]^+ \cdot \underline{G}^{-1} \cdot [\underline{x} - \underline{f}(\underline{a})];$$

therefore the maximum-likelihood estimate occurs at the minimum value of χ^2. The minimization of χ^2, called the least-squares method, is often used instead of the maximum-likelihood method. In many cases the least-squares criterion may provide a reasonable estimate even if the measured variables $\underline{x}$ are not exactly Gaussian. In addition, one need not know the

moment matrix (G) precisely since a small error in G will have only a second-order effect on the standard deviations of $\underline{a}$. In particular, the numerical computation can often be greatly simplified by neglecting small correlations between the variables. (Note that if all the variables (x_{ij}) are independent, G is diagonal and χ^2 is a sum of squares).

Of course, the choice of method depends largely on the problem to be solved. In both methods described above the best values of the parameters are those that occur at an extreme value of a function. The maximum-likelihood method requires finding a maximum; however, the sign of the likelihood function can be changed, and both methods then require a minimizing procedure. Since the required calculations are very complicated and tedious, computers are usually used, and analyses that would have been prohibitive in the past are now possible.

The actual minimizing procedures most frequently used fall into two classes: iteration procedures in which repeated attempts are made to reach a minimum in one step, and stepping procedures in which an attempt is made to reach a minimum through a series of small steps. The iteration method is usually easier to perform and is used for straight-forward problems in which the first, and possibly the second, derivative of the function can be evaluated with respect to all parameters. For example, consider the least-squares fit where the functions $\underline{f}(\underline{a})$ are only approximately linear. If the nonlinearities are small within the region of the maximum in the likelihood function, it is often adequate to represent the functions by

$$f_i(a_\lambda) \approx f_i(a_\lambda^0) + \sum_{\lambda=1}^{r} (a_\lambda - a_\lambda^0) \left(\frac{\partial f_i}{\partial a_\lambda} \right)_{a_\lambda^0} ,$$

where a_λ^0 is the value of a_λ near the minimum of χ^2, found by some method of approximation. If this approximation is inadequate, a new value a_λ' can be found by minimizing χ^2, using the above equation for $f(a_\lambda)$. This process can be repeated until a minimum value of χ^2 is obtained giving a value a_λ^*.

The stepping procedure is usually preferred if the function is expected to behave in a complex way--for example, to have multiple minima or unallowable regions--or require numerical evaluation of the gradient. In this case it is advantageous to be able to follow each step and make certain that no extraneous minima are encountered. A procedure frequently used is the "ravine method." The hunting procedure consists of a sequence of two types of steps: an overstep along (and down) a "ravine" in the contour lines of the function to be minimized, followed by a side-step across the ravine (i. e., perpendicular to the overstep). A minimum along the direction across the ravine is then calculated and used to give the direction down the ravine for the following step (see Rosenfeld and Humphrey, 1963). The actual position of the local minimum in the function is determined by reducing the step size and reversing the direction each time an increase in the value of the function is encountered. At Berkeley a Fortran program called MINFUN (Humphrey (1962)) is used to seek a minimum according to the ravine method.

The minimizing procedures described are used for fitting theoretical parameters to many types of experimentally determined distributions, for example, angular and polarization distributions, lifetimes, and partial and total cross sections. In addition, these procedures--particularly the least-squares method--have many applications in experimental physics such as the parameterization of magnetic-field values, particle-orbit fitting, and determination of atomic constants. The least-squares method, using Lagrangian multipliers, is extensively employed for kinematic analysis of

events occurring in bubble chambers (see Section IIIC).

2. Monte Carlo Techniques

It is frequently necessary to investigate biases in an experiment or in the analysis system. A convenient way of accomplishing this is by generating track measurements, event measurements, or distributions according to some prescriptions using the Monte Carlo method. The analysis of these simulated events by the techniques used in the experiment then show up any biases or errors that are being introduced into the experiment. These techniques can also be used for designing or investigating the feasibility of future experiments. Some examples of computer programs that have been written at Berkeley to accomplish the simulation are described.

Simulation of track measurements can be used to study the biases introduced by track-fitting procedures. These simulated measurements are also useful in many other ways: for example, to adjust uncertain parameters used in the reconstruction, study correlations between track variables, study the limitations of track reconstruction methods, and "debug" new programs. The SIMULATE programs (Zarian, 1962) have been written to generate actual coordinate-point measurements along tracks as accurately as possible and produce a sample of events for input to the track-reconstruction program. The program generates a particle orbit within the chamber by adding together short track segments. The origin, initial orientation, momentum, and mass of the particle are specified. Each additional segment is calculated, taking into account coulomb scattering and magnetic-field variations in the chamber, and these segments are added together until the track is of a specified length or the particle stops. Points along the track are then traced through the optics to the film plane on each of several views, and typical measurement uncertainties are imposed to

generate measured film points.

One of the most important and distressing biases in an experiment is introduced by the misidentification of events. This may occur during scanning, or in the case of bubble-chamber analysis, may often be caused by acceptable kinematic fits of interesting hypotheses being made to background events. Corrections for the misidentification of events during scanning are usually applied by estimating the scanning inefficiency from a rescan of all or a sample of the pictures (see Section IIIA). Misfitting during the kinematic analysis can be simulated by generating a sample of typical events due to a certain reaction and then analyzing them with the appropriate kinematic fitting routines. The frequency and type of spurious fits can then be easily determined. The Fortran program FAKE (Lynch et al., 1962) uses the Monte Carlo method to generate the track parameters of events occurring in the chamber. The events are of a specified type and can be generated according to a phase-space distribution or any other distribution which can be written analytically. Each event is constructed within the chamber, and the momentum (p), azimuth (θ), and dip(λ) are calculated for each track. Using the errors that the track reconstruction program would have given to these quantities, FAKE then modifies the values to simulate measured events. Kinematic analysis of the FAKE output shows how often one type of event will "fake" another. The effect of these spurious events upon various experimental distributions can also be determined. In some cases, it is easier to use a sample of real events than to FAKE them. For example, to find how often events that are really examples of the reaction $K^- + p \rightarrow \Sigma^{\pm} + \pi^{\mp} + \pi^0 + \pi^0$ will fit the reaction $K^- + p \rightarrow \Sigma^{\pm} + \pi^{\mp} + \pi^0$, we can either use the FAKE program to generate the events, or use a sample of real events of the type $K^- + p \rightarrow \Sigma^{\pm} + \pi^{\mp} + \pi^+ + \pi^-$ by ignoring the

measurements of a pair of unlike-charged pion tracks during the kinematic fit.

FAKE output can also be made directly into histograms by using the program SUMX (see Section III). This is very convenient for displaying expected distributions or for calculating correction factors--for example, investigating the shape of a particular center-of-mass distribution as seen in the laboratory system, or calculating escape corrections. One particular application of this method is the generation of "phase-space" curves. These represent the expected distributions of various quantities (a) if the particles in the final state are distributed according to phase space, or (b) if the interactions between them are given by explicit matrix elements.

One further Monte Carlo program called GAME (Lynch, 1963) can be used for evaluating experimental distributions. This program generates many independent distributions for a particular number of events according to a prescribed equation and plots them as histograms. These simulated distributions are very helpful in understanding the statistical significance of any observed deviations from a theoretically predicted distribution.

III. BUBBLE CHAMBER DATA PROCESSING

A. Scanning

1. The Scanning Operation

The object of scanning is to find and record interesting events on the film. The track images are projected onto an opaque table or a screen which is either transmitting or reflecting. At least two views of each picture should be carefully examined unless it is obvious from the first view that there are no interesting interactions or decays on the picture.

Many different scans are usually made on the film. In fact, one roll of film is often put in the scanning projector 10 to 20 times during the course of an experiment. Since the number of pictures is large, routine scanning is usually performed by nonscientist scanners who are specially trained for the job. Nowadays it is normal for physicists and graduate students to look at only unusual or difficult events after routine scanning has been done. Scanning is much easier and the efficiency is higher if there are not too many incident tracks; fifteen seems a good average.

The first scanning in an experiment is usually a beam scan to determine the characteristics and composition of the incident beam of particles, so that the beam-transport system can be changed if necessary. Of course, it is also wise to make a quality scan of a small sample throughout the film soon after exposure so that difficulties in the chamber operation and conditions, light intensity, photographic processing, etc., can be rectified as soon as possible.

The first routine scan (Section IIIA2) usually starts soon after the exposure. Since this type of scanning is done by nonscientists, it is usually topological. The scanner has to recognize the pattern made by the tracks, and to classify and record it. To determine the scanning efficiency (Section IIIA5), part or all of the film is rescanned and the two scans compared.

In addition to the routine scans, many special scans are often made on the film. These are discussed in Section IIIA3.

2. Routine Scanning

Two schools of thought exist as to the procedure that should be adopted in routine scanning. In the first method the film is scanned for all the topological-event types of general interest in the experiment. For

example, this might be all beam-track interactions, or all beam-track interactions more complicated than an event with two outgoing prongs. In the second method the film is scanned for each topology separately. Method I usually makes the scanning instructions rather complicated and arguments have been advanced that the scanning efficiency is higher if Method II is used, because the scanner is less confused and can concentrate on one particular configuration. Method II has the disadvantage that an interaction can easily be identified as two different events in two different scans, and it is very difficult to resolve this problem in the bookkeeping. Even worse, a particularly interesting but unclassified event can be completely overlooked. However, if one of the prime objectives of an experiment is an attempt to find a new particle or a reaction which makes a very distinctive topology, then Method II is adopted, since performing an overall scan and recording all events would take too long.

As already mentioned, most routine scanning is performed by nonscientists whose knowledge of physics is rudimentary. Consequently, scanning is usually oriented toward a topological classification of the events, in which the scanner is not expected to identify the type of particle which made each track. For example, all beam interactions in which two charged prongs and a V are produced would be classified as belonging to the same event type, regardless of whether or not the V can be identified as a K^0 or Λ. The computer programs would then allow all possible mass assignments for each track and identify the event by kinematic analysis (see Section IIIC).

3. Special Scans

These scans involve reexamination of events found during the routine scan or rescan. This scanning is done by physicists, graduate students, and the most experienced scanners, because it often requires an

advanced application of scanning technique, a knowledge of track characteristics, and considerable knowledge of particle physics. In a routine scan the scanners are not expected to identify each particle reaction occurring in the bubble chamber. Rather, they need only recognize and record special characteristics of an event which can be determined with the minimum of equipment--for example, circular templates for momentum measurements, curves of track density versus momentum or energy, and templates of stopping tracks for the correct magnetic field, or curves of range-momentum or range-energy relations. In special scans, however, in addition to the above capabilities, it is often necessary to use kinematics plots and be familiar with all the reactions that can possibly occur for the particular incident particle and incident momentum. Most special scans are determined by the nature of the experiment; however, some reasons for special scans are common to many experiments.

Many rescans are the result of poor scanning instructions in the original routine scan. This unfortunate state of affairs can best be avoided by very carefully prepared scanning instructions for the routine scans, although it is usually impossible to cover all eventualities, particularly when these scans are topological.

Three other reasons for rescanning occur very often. The first is to reduce the number of events that require measurement. This is necessary if there is a shortage of measuring capability and involves selecting a sample of events with special characteristics from a particular topology. For example, if we have a large number of events in which K^0's and Λ's are produced and we are very anxious to measure only the events with K^0's, then the events can be reexamined on the scanning table and those events where the V is a possible K^0 can be selected for measurement.

Events may also be reexamined if they have failed measurement. This often reveals misidentified events or even unusual events such as three-body V decays or neutral interactions. A third reason for a rescan is a "conflict" scan on all or a sample of film that has been second scanned. This scan is made to resolve the "conflicts" between the two scans, and is used to determine the scanning efficiency (see Section IIIA5).

In addition to the above special scans, it is very important to reexamine all the ZOONS, i.e., those strange events that were not understood by the original scanner, or events for which there was no assigned event type. Most of the ZOONS usually turn out to be uninteresting; however, they must be reexamined in case some unpredicted interaction has occurred. In addition, events with rare but predicted topologies are usually reexamined because they are often misidentified.

Another special scan is often necessary to determine the incident path length accurately for cross-section measurements. For pion beams the number of background particles that produce interactions is very small, so that the number of interactions, appropriately corrected for small-angle scatters, can be normalized to the published total cross-section data, which is usually obtained from counters. For K and $\bar{p}$ beams the pion contamination is very troublesome. However, this contamination can often be estimated from a particular interaction, which is easy to distinguish, for example, $\pi^- + p \rightarrow K^0 + \Lambda$ or from the number of large δ-rays (see Appendix). The number of interactions due to K's can then be found, and the partial cross sections normalized to the published value of the total K-p cross section. Another method of obtaining the K path length is to count the τ decays in the incident beam. Care must be taken when using this method, because in many cases genuine τ decays cannot be distinguished from decays that

produce a Dalitz pair and one charged particle. It is important to count all events with three outgoing prongs and then correct for the Dalitz-pair contamination.

4. Recording of Scanning Information

One important aspect of scanning is the manner in which the data are recorded, since this information forms a master list of the experiment. For this purpose a record of each event must be kept. This includes its indicative data (roll and frame number), its location, its event-type assignment, and often any additional physics information that may be required. The identity and whereabouts of an event is also required during the measuring phase so that the event can be relocated.

For small experiments of a few hundred events, it is possible to keep the lists on hand-written sheets and to make sketches of the events requiring measurement. However, for large experiments this is impractical, and the scanning information is coded so that a computer can easily do the bookkeeping. As an example of a large operation, we will describe the method used by the Alvarez Group at Berkeley.

The location of the event is partially defined by the roll and frame numbers. To distinguish events on a frame, each event is assigned a unique beam-track number so that no two events in an experiment can have the same identification number. To obtain the location of the event within the frame, a grid is projected onto the scanning table and the appropriate zone number assigned to each vertex of the event. This information is very helpful for relocating the event during the measurement or in subsequent special scans, although it is obviously not necessary for identification.

An event-type number is assigned to each topology. For example, all events where an incident particle produced two charged outgoing tracks

and a neutral, which subsequently decayed to form a V, are called primary event type 32. This number, together with the experiment number, controls the processing of the event in later analysis (Section IIIC). In addition, physics information is inserted by means of binary switches and decimal-code numbers.

The procedure adopted is as follows. When the scanner finds an event, he switches on the grid on view 2 and positions it correctly. Then he records the relevant data on a printed form similar to a computer-program coding form. An example is shown in Fig. 3. The headings of the columns are mostly self explanatory; the grid locations on view 2 for each vertex in the primary event are entered in x, y; F_1 and F_2 are decimal-flag digits which give the configuration of any secondary interactions not included in the primary event type. The binary-code switches and decimal codes are preassigned to have special meanings in each experiment. The hand-written data are keypunched onto holorith cards and merged with the master list of the experiment (Section IIIC6) to form a scanning-information library.

Another method of recording the data is tape-recording the scanner's description of the event. The tape can then be played back by a keypunch operator and the data punched onto cards. This method has proven very efficient for recording simple events that occur frequently (Anderson and Laney, 1964).

5. Scanning Efficiency

To measure scanning efficiency, all or part of the film is re-scanned. Scans one and two are then compared and frames which have a conflict between the two scans are reexamined on the scanning table. After this "conflict" scan, the master list is updated with the "conflictor's" decisions. Then, for a total number of events N, the number of events

found by scanner 1 correctly is $N_1 = E_1N$, those found by scanner 2 correctly is $N_2 = E_2N$, and the number common to scans 1 and 2 is $N_{12} = E_1E_2N$; where the scanning efficiency of scan 1 is $E_1 = N_1/N = N_{12}/N_2$ and that of scan 2 is $E_2 = N_2/N = N_{12}/N_1$. Then the total number of events (N) is N_1N_2/N_{12}, and the total events found is $N_1 + N_2 - N_{12}$. The efficiency of scan 1 + scan 2 is $(N_1 + N_2 - N_{12})N_{12}/N_1N_2 = E_1 + E_2 - E_1E_2$. In practice the efficiency for most topologies is greater than 90%, so that the efficiency of a double scan is about 99%. In some experiments all the film is scanned twice to pick up the extra events. However, as experiments become larger, this becomes rather uneconomical, and a correction can be applied. It should be pointed out that the above estimation of the scanning efficiency is meaningless if either or both scans are biased in some way. For example, if the scanning efficiency of both scanners is low for a particular topology or configuration of the tracks, the value of the scanning efficiency obtained by the above method will be optimistically high.

There are many causes of inefficiency. The most frequent are (a) missing the whole event completely, (b) misidentifying it, or (c) misrecording it. The first is usually completely random and probably caused by tiredness or some other distraction of the scanner. The latter two, however, can be biased. They are often caused by poor scanning instructions which are either unclear or ambiguous, and also by poor training of the scanning personnel. This is particularly true of physics information recorded by means of binary switches. In some cases the efficiency for recording this information properly may be as low as 50%, simply because the scanners did not understand the importance of this physics information to the physicist.

B. Measuring

1. The Measuring Operation

The basic purpose of measuring is to reduce the quantitative data contained in a photograph to digital form. Firstly, these digital data are used for identification of the event by space reconstruction and kinematic analysis, since the event is usually unrecognizable on the scan table. Secondly, the physical quantities pertaining to this event which will be required in the interpretation of the experiment are calculated from the measurements. In most laboratories there is a shortage of measuring capability, and only the more interesting events are measured.

Events can be measured in a variety of ways. If there is no magnetic field in the chamber, the tracks are straight, and a simple measurement of a point on the track and the track's direction will suffice. However, when there is a magnetic field the tracks are curved, and points must be measured along at least two images of each track in an event, so that each track can be reconstructed in space and its momentum and space angles determined. If only two views are measured, they should be chosen to obtain the best stereo reconstruction. Measurements, sometimes in r, θ but usually in x,y coordinates, are made with respect to the images of fiducial marks within the chamber.

Two methods of measurement are used. In the first method, the film is placed on the precision stage of a microscope and measurements made essentially in the film plane, although in many instances the measuring machine is a projection microscope and the operator looks at a projected image. For the second method the film is projected and the measurements made on the projected image. Method two is inherently less accurate because of distortions in the projection optics; consequently the

measuring machines using this method are usually simpler and cheaper than those for method one. Method two is often used for measurements of events in heavy liquids where great accuracy in the measurements is not necessary because of the large uncertainties introduced by multiple scattering. This method is also particularly useful if there is no magnetic field in the chamber because a simple drafting-machine arrangement can be used to obtain adequate r, θ coordinates.

At many laboratories the ionization is measured on some or all tracks. This may be a special precision measurement of the gap lengths along the tracks (see Appendix) using a microscope. The track density can also be found from any pulse-height information obtained during routine measurement. Pulse-height analysis is used frequently with the more advanced types of measuring equipment (see Chapter IX).

2. Measuring Techniques

Of course, the measuring techniques used vary appreciably depending upon the type of measuring machine. Measuring is a routine task performed by specially trained technicians. In almost all conventional measuring machines a reticle is moved along the track (or vice versa) and positioned as accurately and quickly as is reasonable, commensurate with the accuracy of the machine. The operator is expected to choose clear points along the track for measurement, to choose the views to be measured, to perform the measurements of the fiducials and tracks in the correct order, and to insert all necessary indicative data for the event. When measurement is not required to great accuracy, relatively crude techniques and machines can be used. However, when an accuracy of a few microns is required, precise machines and good measuring technique is essential.

The conventional precision measuring machines currently in use

are often very complicated and are designed to assist the operator as much as possible (see Section IIIE3). Some form of projection microscope is usually used. The operator views the picture on a transmission screen which has a stationary reticle projected on it. He moves the measuring stage carrying the film by means of hand wheels and (or) a joystick. Since moving the measuring stage and centering the track image on the reticle is a tedious process, there is often a servo system to keep the track centered so that coordinate measurements can be made "on the fly." In addition all data are recorded as automatically as possible and are output directly onto paper tape, magnetic tape, or punched cards.

To illustrate the measuring technique required to operate such a machine, the methods used on the automated Franckensteins at Berkeley are described. When a physicist decides that a certain sample of events should be measured, he makes a measurement request. The library program then abstracts the locations of the required events from the experiment master list in the form of a listing and measurement control cards. These contain the indicative data, event type, zone numbers of the vertices, and many other data required in the measurement. The film is loaded onto the Franckenstein, and the first control card placed in the card reader. Any relevant data are displayed to the operator by means of lights. The film is advanced to the required frame automatically, and the stage moves so that the first vertex to be measured is close to the reticle. The operator then looks at the event on all three views to make sure that he can measure it and also decides which views of each track he will measure. He then pushes a button which enters the indicative data on the control card onto the output paper or magnetic tape. This also causes the stage to position itself automatically for fiducial measurements. After the operator has measured the fiducials, the stage returns to the vicinity of the first vertex. The operator

measures this vertex and all tracks radiating from it, using the servo to control the motion of the stage. Next he measures the tracks from any other vertex requiring measurement on the first view and then repeats the process on the other two views. The machine is capable of sequencing itself correctly and entering the identification of each track so that the operator can concentrate on measuring the points accurately. All vertex points are measured, and the neutral tracks are inserted in the computer program. The measuring rate for strange-particle, two-vertex events using this technique is seven to nine events per hour. With less automated machines it is about five events per hour or less.

Errors that occur during measuring fall into two categories. In the first case the error is catastrophic, and the event is rejected early in processing. Many of the errors of this type are due to operator mistakes: for example, choosing the wrong pair of views for good stereo reconstruction; not measuring two views at all; or measuring tracks in the wrong order. In addition, some of the catastrophic errors may be due to machine errors such as bad sequencing or incorrect data transfer. This type of error, which makes the event fail completely, usually amounts to about 10%. The events should be unbiased and most of them pass when remeasured.

The second type of error is caused by poor measurements. These occur when the operator does not measure accurately enough and particularly if he records a point when the servo is not centered correctly. These errors are hard to detect but are indicated by high values of χ^2 obtained in the kinematic fitting program. The number of failures varies considerably dependent upon the quality of the track images and the complexity of the events.

C. Computations

1. Data Flow

Digital computers are used extensively in the analysis of bubble-chamber pictures. In fact, the volume of data is now so large that it would be impossible to do bubble-chamber physics without the aid of a large general-purpose computer. The computer analysis of the data divides itself naturally into six phases: (1) spacial reconstruction of each track in an event, (2) kinematic analysis at each vertex, (3) interpretation of each event, (4) calculation of physical quantities for each event, (5) analysis of the whole experiment, including the display of experimental data, and (6) a library program which organizes the data into an orderly system and compiles records of the progress of the experiment.

Several large analysis systems exist. At Berkeley there are the PANAL, PACKAGE, WRING, EXAMINE, SUMX, LINGO system designed by members of the Alvarez Group (see Rosenfeld, 1963) and the FOG, CLOUDY, FAIR system (designed by White (White, 1960 and 1961, and White et al., 1960). There are also THRESH, GRIND, BAKE, SLICE, and SUMX at CERN, and variations and combinations of these programs that are used at other laboratories. Most of these programs have already been described in detail. In this chapter we do not attempt to describe any of these systems extensively or compare them, but rather, give the reader some idea of the philosophy underlying the programs. As an example of a large data-analysis system, we discuss the Alvarez Group programs used at Berkeley (see Fig. 4).

2. Spacial Reconstruction of Tracks

The first computation is the spacial reconstruction of the bubble-chamber tracks. The information input to this program from the measuring

machine consists of indicative information for the event, fiducial measurements, track-coordinate measurements, and an identification word for each track. In addition there may be bubble-density information and a flag on each track indicating whether or not it stopped in the chamber. The quantities calculated include at least the position, momentum, and orientation of each end of each track, its length, and the estimated errors on these quantities. To do this calculation in great detail is not really sensible because it requires too much computer time; however, various compromises and approximations based on three slightly different philosophies are in use.

In the older programs PANG (Humphrey, 1959), FOG (White, 1960), and TRED (Thorndike, 1958), the method of corresponding points is used. This method of reconstruction relies upon the fact that if a particular bubble is measured in two views, the two light rays traced backwards from the film through the optical system intersect at the position of the bubble. In practice, measurements of corresponding bubbles are not made because this is too time-consuming. Instead, the points are measured at random along the images in the two views. Consequently, it is necessary to generate an artificial corresponding point in one of the views by interpolation between two measured points. The calculations would be very simple for a pin-hole lens and no refracting media. The actual situation is somewhat more complicated due to lens distortion, film shrinkage, tilted mirrors, and refracting media between the lens and bubbles. The corresponding point is actually found by iterating once from the point found by using "ideal" optics. The calculation is done in two parts. First, view A is chosen as the principal view, and points on view B corresponding to the measured points in view A are found by interpolation. From this the coordinates of a string of space points lying along the track can be calculated. The second part consists of

fitting a curve to these space points by using a least-squares fitting procedure. The method is then repeated, using B as the principal view and interpolating on A. The parameters of the two fitted curves are then used to calculate the properties of the track. The shape of the fitted curve is very complicated but is basically either a parabola or a circle in projection. In addition, the fitted curve must take into account corrections for variations in magnetic field and the energy loss of the particle. Since the latter is mass dependent, it is customary to repeat the fitting procedure for all possible particle identifications for the track, thus obtaining mass-dependent fits.

In PANG two independent power series are used to parameterize the space curve:

$$x = x$$

$$y = y\,(x, a_1, a_2, a_3)$$

$$z = z(x, a_4, a_5),$$

where z is the direction of the magnetic field at the center of the chamber. The curve for y involves terms to the fourth power, and for z, terms to the third power.

The PANG method has several disadvantages: (a) Information from only two views is used. (b) The interpolation of the corresponding point is very inaccurate if the direction of the track makes only a small angle with the stereo axis and is impossible if this angle is zero. Consequently, the two views used for the reconstruction are chosen to give the best stereo angle. This choice is made either by the measurer who measures only two views, or, if more than two views are measured, the choice of the pair of views used for the reconstruction is made by the program. In addition, if the track turns through a large angle, it is often impossible

or very inaccurate to make the stereo reconstruction using only two views, because the direction of the track gets too close to the stereo axis for some part of its length. In this case only the first part of the track can be reconstructed using the appropriate pair of views and the end is chopped off. This problem becomes more severe for large chambers with large magnetic fields. (c) Track extrapolation is very dangerous and usually is avoided. (d) One of the worst problems is in the estimation of the errors, both of the coordinates of the space points and also the fitted parameters of the curve. The main advantage of this method is that it is relatively simple. The optical reconstruction is done once, and then a complicated fitting procedure can be made to the space points for each mass interpretation of the track without using too much computer time.

To overcome some of the difficulties of the corresponding-point method of reconstruction, newer programs, for example THRESH (Moorhead, 1960), employ a method which describes the track in space by a helix, corrected for magnetic-field variations and momentum loss. This curve is then fitted to sets of rays traced through the optics into the chamber from each measured film point in each of the measured views. This is done by finding a first approximation for the helix by using a few measured points and then representing each ray by two intersecting planes. A short segment of the helix near the ray will usually intersect the two planes in two points, or in one point if the helix and ray actually intersect. The angular separation of the two intersection points on the helix is then used in a minimizing procedure to calculate optimum parameters for the fitted curve. This method has many advantages over previous methods, but it is still hard to relate the uncertainties in the parameters of the helix to the setting error on the film.

An alternative method using a helix has been devised by Solmitz (1960). Two versions have been coded, one at the Rutherford Laboratory (Burren and Sparrow, 1963) and another called TVGP at Berkeley. This method consists of projecting a helix in space (corrected as before for changes in curvature) onto the film in each view. The deviations between the projected helix and the measured points are then minimized by varying the parameters of the helix. The first approximation to the helix is obtained by the method of corresponding points, but all views are used and weighted appropriately for stereo angle. This method has the advantage that the errors in the track parameters can be calculated rather easily, all views are used in the reconstruction, and there are no problems of extrapolation and interpolation.

The information on each mass interpretation of each track output from the space-reconstruction program contains the position, orientation, and curvature of each end of each track. In addition, the momentum calculated from the range of the track in the chamber is included and is used in the subsequent programs if the track stops in the chamber. In practice a variable proportional to momentum^{-1} is preferred over momentum because for most tracks this variable is more nearly Gaussian distributed than the momentum itself.

3. Kinematic Fits of Vertices

The variables calculated by track-reconstruction programs are concerned only with the geometric properties of each mass interpretation of each track and not with the physical interpretation of the tracks or the event as a whole. Since all physically possible mass interpretations of each track are tried, many of the values of the variables calculated have no physical

meaning because momentum and energy conservation at the vertex will be violated. However, if all tracks at a vertex have been identified correctly, then the calculated variables should conserve energy and momentum, subject to the uncertainties in these variables. The kinematic requirements at each vertex can therefore be used to choose the most probable interpretation of an event and also to reduce the uncertainties in the kinematic variables assigned to each particle. The conservation of energy and momentum (in three mutually perpendicular directions) can impose up to four equations of constraint on the track variables at any vertex. A vertex at which all quantities are measured is subject to four constraints and is classified colloquially as a "4C fit." If the momentum of one track is unmeasured, one conservation equation must be used to calculate this momentum, and only three constraints (3C) remain. Similarly 2C and 1C fits can be classified. In each of the above cases a least-squares fit can be performed; however, if four variables are unmeasured, the problem is unconstrained. Note that if there is one unobserved or unmeasured track at a vertex the fit is at best "1C." In the kinematic fitting procedure each track is assigned a mass identity, and the fitting program then attempts to perform a least-squares fit to the variables calculated by the geometry program, minimizing χ^2 subject to the constraints required by energy and momentum conservation.

The Alvarez Group program GUTS (Berge et al., 1961, and Berge, 1959) uses the method of Lagrangian multipliers (a_k) to apply the kinematic constraints. An attempt is made to minimize the function:

$$M = \sum_{\substack{i=1 \\ j=1}}^{I} (x_j - x_j^m)\, G_{ij}\, (x_j - x_j^m) + 2 \sum_{k=1}^{L} a_k F_k(x),$$

where I is the number of measured track variables, L is the number of constraints, x_j is the jth variable with a measured value x_j^m, $G_{ij}^{-1} = \langle \delta x_i^m \ \delta x_j^m \rangle$, and δx_j, the error on the jth variable, is assumed to be Gaussian. The kinematic constraints are applied by $F_k(x_i) = 0$ for $k = 1, 2, \ldots L$. The variables actually used in GUTS are the azimuthal angle (ϕ), tanλ (where λ is the dip angle), and curvature. (Obviously tanλ is not normally distributed, but it is convenient to use).

The fitting procedure would be simple if the F_λ functions were linear in the parameters x_j, because then the problem would reduce to the solution of L simultaneous linear equations. In practice this is unfortunately not true, and it is necessary to iterate. The fitting procedure may obtain (a) an acceptably small χ^2; or (b) a χ^2 that is too large to be acceptable by some predetermined criteria. Cases (b) are classed as rejects, and only a small amount of data are output. However, if the vertex is acceptable, the fitted-track variables are output.

GUTS was originally written for single-vertex events, but the coding has been extended to make an overall fit to the more common two-vertex configurations. Multivertex configurations can be fitted as a chain of single-vertex fits by "swimming" the values of the variables and errors of any charged connecting track to the second vertex. The whole kinematic program which incorporates GUTS and does the chaining of fits is called KICK.

The GUTS method has three disadvantages: (1) only the last vertex fitted uses all the input data and consequently best values for parameters at previously fitted vertices can only be found by refitting, (2) it is hard to find an overall χ^2 for the whole event, (3) there are some multivertex chains in which one vertex is undetermined although the whole

event is overdetermined.

To overcome these problems the CERN kinematics program GRIND has been written by R. Bock (1962). In this program the event is first fitted as individual vertices and then automatically as a whole. This provides a well-defined χ^2 for the fitted hypothesis of the whole event and also gets the best values of all the parameters simultaneously. The actual fitting program incorporated into GRIND is called FIT. This routine uses a method similar to that of GUTS for the minimizing procedure. However, it has the advantage that it attempts to use even poorly measured parameters (with appropriate errors), whereas GUTS treats the parameter as unmeasured if the error is greater than an aribitrarily assigned percentage, because otherwise the method may become numerically unstable.

In addition to kinematic fitting at a vertex, it is often desirable to perform a "missing mass" calculation. This can only be done if there are four constraints at the vertex. From the unbalance in energy and momentum and by using the measured parameters of the visible tracks, a calculation is made of the invariant mass of any unobserved particle or collection of particles.

The minimizing routines GUTS and FIT are incorporated into large kinematics programs which perform the chaining together of vertices and also the assigning of a mass identity to each track. This latter can be done in two ways: Either a physicist can write a subroutine which performs the task explicitly, or the physically possible assignments can be made automatically by the program using the conservation laws for baryons, strangeness, etc. This latter method is used in CLOUDY and GRIND. It is easier to write an event-type subroutine using this method; however, it is liable to become very complicated and wasteful of computer time

unless it is used with discretion.

The kinematics program KICK (Rosenfeld, 1961; Rosenfeld and Snyder, 1962; Harvey, 1962; and Dahl, 1963) is basically a collection of subroutines (including GUTS) which can be called by an event-type subroutine. Each topology has a different event-type number and the program branches to the correct event-type subroutine by testing the event-type number of each event. The event-type subroutine is designed by a physicist who is familiar with the physics of the experiment. Vertices can be fitted in any order provided they are not underdetermined. The vertex that is required with greatest accuracy is usually fitted last. To avoid extra tape handling the PANG and KICK programs have been combined together and are called PACKAGE (Fig. 5). This program contains about 28,000 words of machine language coding (including storage). A mixed sample of events can be processed at the rate of about 10 to 20 events per minute on an IBM 7094.

The output from kinematic routines is in the form of a binary tape for use as input to subsequent programs. Each vertex fit that is successful (i.e., has an acceptable value of χ^2) contains information such as the χ^2 for the mass interpretations used; momentum, azimuth, and dip angles for each track at the fitted vertex; and a matrix of the errors on the fitted quantities. A shorter record is output if the vertex fit failed. Using PACKAGE a complicated event currently produces about 2000 words of 36 bits each.

An additional tape-editing pass named WRING (Johnson, 1962) is now made on the PACKAGE output tape. This program condenses the data to about 600 words per event by ignoring redundant elements in the

error matrix and packing some of the data. In particular, it greatly reduces the data from a "failing" vertex. WRING is run as a separate pass because PACKAGE and WRING together overflow the core of the IBM 7094. The WRING output is our library of fitted data.

4. Interpretation of an Event

To find the most probable interpretation of the whole event, a comparison is made of all the values of χ^2 obtained in the fitting procedures. Of course, the numerical values of the χ^2 cannot be compared directly; account must be taken of the number of constraints in the fit. The interpretation of an event is much simpler if an overall χ^2 is obtained for the whole event, rather than a number of χ^2 from chains of single vertices. This is particularly true if there are several physical interpretations of the event with similar probability. If bubble-density information is available, this can sometimes resolve the ambiguities. The criterion used for interpretation is defined by the physicist and may take into account a scaling of the χ^2 values (see Section IIID).

In many instances no interpretation has an acceptably small probability. This can be caused by bad measurement or bad distortion of the tracks, or be simply because the correct physical interpretation of the event was not tried during the fitting procedure. This latter problem must always occur when more than one unobserved particle is produced at any vertex, because the vertex is then undetermined and a fit cannot be made. In this case, the "missing mass" calculated at the vertex can be used, since if the missing mass is greater than the sum of the masses of the two lightest unobserved particles that can possible be produced, the event can be accepted and classified.

Once the most acceptable interpretation of the event has been determined, the physical variables interesting to the physicist can be calculated. These variables are such quantities as the momentum and direction cosines of each track and their errors (in one or several rest frames). In addition such quantities as invariant masses of groups of particles and their errors may be required.

One Alvarez Group program which selects the most probable interpretation of each event and then calculates any required variables is called EXAMIN (Johnson, 1961). This program consists of a large selection of FORTRAN subroutines that perform Lorentz transformation, calculate missing masses, etc. The physicist writes a FORTRAN control routine which calls the subroutines and does any additional arithmetic and logic required to process the event. EXAMIN produces an output tape called a "Data Summary Tape" which is the library of experimental physics quantities and usually consists of about 200 words (36 bits each) per event.

Recently a new sequence of programs has been written which perform the functions of EXAMIN (Dahl and Kalbfleisch, 1963). These new programs use the same subroutines as EXAMIN. The first program AFREET reads WRING output and determines the most probable interpretation for the event. A second program DST-EXAM calculates physical quantities required by the physicist.

5. Interpretation of an Experiment

Before a physicist can interpret the results from an experiment, the information from all the events in a required category must be gathered together and displayed. The form of this display depends upon the type of experiment, but histograms and scatter plots are usually the most popular.

These plots can be obtained from the "data summary" information. The program SUMX (Champomier, 1964) is used at both Berkeley and CERN for this purpose. This program contains a number of FORTRAN subroutines which make histograms, ideograms, and scatter plots. The required subroutines are called by data cards placed behind the program deck. Scatter plots are displayed on the CRT connected to the 7094 and photographed, and histograms are printed. This program is general and can be used for preparing displays of any type of data. FAIR is a similar type of program used by the White group.

In addition to the displays of data, the physicist requires lists and tallies of all the events in the experiment. These are prepared by the library system (next section).

Other routines are also available to the physicist. These include routines for least-squares fitting, phase space, and Monte Carlo calculations (see Section II). Of course, many special-purpose routines are also written for each experiment.

6. Data Storage and Retrieval

A library serves two main functions: first, to store all the relevant measurement and physics data in an orderly way for easy data retrieval; and second, to keep a status report of each event in an event catalogue so that tallies, lists, etc., can be easily supplied to the physicist on request. Now that all calculations are done with computers, the data are stored on punched cards, or more frequently, magnetic tape. Consequently, a system of tape editing, condensing, ordering, and merging routines is required to keep the data tidy. The bookkeeping function can quite easily be done with pencil-and-paper techniques if there are only a

few hundred events in the experiment. However, with ever increasing volumes of data, it becomes imperative to have more automatic library procedures.

Two different approaches to this problem are described here. In one used by LINGO (Penny, 1962), an event catalogue or master list is kept which contains a current status report for each event in the experiment. It can be used to control some of the functions in the event processing and is also used for producing lists and tallies. It only communicates with the other programs and data when being updated. A schematic diagram of the Alvarez Group data-processing system including LINGO is shown in Fig. 6. Scan data is entered onto the master list from the scan cards containing information written down by the scanning technician. From the current master list and using measurement-request criteria supplied by the physicist, the "measurement request processor" generates measurement-request cards which initiate measurement on the Franckenstein. The output from the Franckensteins then goes to PANAL (Alston et al., 1961) which checks for gross errors in the data and condenses it. This data is then input to PACKAGE whose output is geometrical quantities from PANG together with the fitted data for each track at each vertex (from KICK). The condensed-results tapes from EXAMIN or AFREET are then run against the library list to update the master list with the interpretation of the event and obtain a "clean" master summary tape which contains no duplicate measurements. In this way the master list always knows the current status of an event and can be used to initiate further processing, for example, to generate a remeasurement request if the event failed the previous measurement. Modifications can be made to the master list deliberately by means of the routine "Modify."

In a second approach to library functions used by FOG, all information pertaining to one event is stored in a block on magnetic tape; for easy data retrieval the events are written in serial-number order. A schematic diagram of the FOG, CLOUDY, FAIR system is shown in Fig. 7. In this case the experiment data, scan data, and measurement data are all stored in the same record together with output from the FOG, CLOUDY, and FAIR programs. Again the library contains the status of each event and can be used to generate lists, tallies, and remeasurement requests.

One advantage of the LINGO system is that for lists etc., only the master list--which is quite short and contains only about 20 words per event--is read. In addition, data-summary information which is fairly short (~ 200 words per event) can easily be made into histograms etc., by the SUMX routines. It, however, has the disadvantage that retrieval of the voluminous data (measurement, PACKAGE output etc.) is difficult because it is not stored in a coherent way. FOG has an advantage in this respect because all data is stored neatly in serial-number order.

The volume of data handled by the library is increasing rapidly, and systems using magnetic tape as their storage medium will soon become saturated. In fact, data storage and retrieval is rapidly becoming the limiting factor in large-scale data analysis. There are plans at Berkeley to solve this problem by the use of a large random-access digital store where binary bits are permanently imaged onto photographic film as black and white spots. The volume of the store will be about 3×10^{11} binary bits and contain all the data for approximately five million bubble-chamber events on line to a large general-purpose computer. To obtain very fast access to the data in the store, an index of the location of each event within the store will be kept on the master list. A preliminary run will then be

made to abstract these addresses and arrange them in an order giving optimum access to the store. This list of addresses will then be used to access the data within the store as rapidly as possible. A study of the use of a mass store for bubble-chamber-data analysis has recently been made at Berkeley (Alston and Penny, 1964). Proposals to build a device on a special contract have been received from two commercial companies.[2] In addition to bubble-chamber analysis the mass store will be used to service requests from remote on-line inquiry stations.

7. On-Line Analysis

In any experiment there are always events that cannot be processed using the general programs. These may be events found during scanning that have a strange topology, or they may be events with a normal topology that will not fit the usual-event hypotheses. In these cases it is very tedious to write special computer programs for the kinematic analysis. Since these events are rare and often very interesting, it is useful to have an on-line kinematic program in which a physicist can direct the mathematical processing of the event by means of a typewriter connected to the computer and can decide what fits to attempt, depending upon the results already obtained.

At Berkeley the program QUEST (Alston et al., 1962 and 1963) has been written to fill this need. This is a reorganized version of PACKAGE in which the Pang and Kick event types are replaced by control routines that can be entered by means of a typewriter (or card reader) connected directly to the computer. The results of the kinematic fits and any required calculated data is written out on the typewriter. Coordinate data can be input from magnetic tape or from a Franckenstein. A

physicist sitting by the typewriter can then directly control the processing of the event without writing a program explicitly, but simply by typing in the necessary mass assignments for the tracks, the topology of each vertex, and the order in which vertices should be fitted.

The system (Fig. 8) has proved very useful for analyzing ZOONS and also those events which fail the regular topological event type due to some idiosyncrasy in the particular event.

D. Errors

1. Scaling of χ^2

One of the most difficult problems in data analysis is the estimation of random and systematic errors in the calculated quantities. These may be caused by coulomb scattering; measurement errors; distortions in the tracks due to liquid motion and optical effects; and various imperfections in the bubble-chamber camera and measuring machine which cause distortion of the track images. In addition, approximations in the fitting procedure and parameters describing the geometry and magnetic field may produce errors in the fitted data.

Incorrect determination of the errors leads to a χ^2 distribution from the kinematic fit whose width differs from the expected width by a factor of a^2. Since some causes of errors are likely to be omitted in the analysis, a^2 is usually greater than unity. In the experience of the Alvarez Group, the value of a^2 is usually in the range 1.4 to 1.8. The distribution of χ^2 scaled by $1/a^2$ has almost the theoretical shape, but has an excess of about 10% too many events in the tail of the distribution due to plural and single scattering, bad measurements, and wrong interpretations. The factor a determined from the χ^2 distribution should be applied to the uncertainties in the fitted quantities.

2. Distortion of Track Images

Track images may be distorted by poor optical components between the track and the film. The errors introduced by the optical components (i.e., windows, mirrors, and lenses) can in theory be measured and then corrected for by the computer programs because they should be constant if the optical components remain fixed. Unfortunately, it is difficult to measure them to the necessary accuracy and, in particular, it may be impossible to obtain a simple parameterized expression to describe them satisfactorily. The refractive effect of the windows can be calculated easily except for imperfections in the material; plastic is much inferior to glass in this respect and should be avoided. Mirrors, if sufficiently flat and mounted properly, do not produce distortions, but inadequate lenses can cause large and complicated distortions, particularly if they are used at large angles. The errors caused by the optical components are systematic, so it is desirable to minimize them as much as is practical.

In addition to distortion caused by optical components, there may be some optical turbulence in the chamber caused by local heating or cooling effects. This leads to local variations of refractive index and the tracks become "kinky." This effect is uncorrectable and merely increases the χ^2 for the particular event.

Nowadays with mylar-based photographic film, problems due to film shrinkage have been greatly reduced. Bulk changes due to development and storage are now of the order of one to five parts per thousand. Since measurements are always made with reference to at least two fiducial marks in the chamber, an overall change in the magnification of the film caused by aging, humidity, and temperature changes are not important.

However differential shrinkage can be troublesome and should be minimized as much as possible by stabilizing the film conditions during exposure, storage, and measurement. In particular, care should be taken to ensure that the film is clamped flat on the film platen in both the camera and measuring machine, or there will be bad localized distortions of the track images.

Distortion of the tracks can be caused by the motion of the chamber liquid in the interval of time between the passage of particles through the chamber and the light flash. This effect is hard to calculate because it is quite unpredictable. It is dependent upon the expansion system of the chamber and can vary from pulse to pulse or with location in the chamber. To reduce this error, a short bubble growth time should be used.

Another difficulty arises in estimating the central value and inhomogeneties in the magnetic field. In theory the field can be carefully mapped and the correct parameters calculated to describe the shape of the field. In practice, however, extensive measurement of the field can only be made at room temperature, and since the magnetic properties of the stainless steel of the chamber, vacuum tank, etc., change at low temperatures, it is never certain that the calculated parameters are correct under operating conditions.

Another effect that is hard to estimate is multiple coulomb scattering. One difficulty is that the theory usually used assumes that the distribution is gaussian. (See, for example, Bethe, 1953). This theory neglects single and plural scattering, and this effect probably accounts for some of the extra events in the high-value tail of the χ^2 distribution. In addition, the formulas must be modified to take account of scattering from atomic electrons. The approximation used (replacing Z^2 by $Z(Z + 1)$) is

particularly inaccurate for liquid hydrogen. A comprehensive study of coulomb scattering has been made by Gluckstein (1963).

3. Measurement Errors

Measurement inaccuracies arise from uncertainties in the measuring device and from setting errors. It is usually assumed that the measuring machine and operator combined contribute some arbitrarily chosen measurement error in the film plane transverse to the track direction and independent of the track. In practice, to account for possible errors caused by track distortions, the value chosen for the uncertainty in each coordinate measurement can be made larger than a simple estimation of measuring-machine accuracy and setting errors would indicate. This "external error" is propagated through the spacial-reconstruction program to form a first contribution to the uncertainties in the track variables. The "internal error"--the scatter of the measured points about a fitted curve--is not used to estimate the errors in the track variables. It can, however, be used to reject points, or the whole track image, if the measured points do not lie sufficiently close to any fitted curve.

The multiple coulomb-scattering contribution to the error is added to the estimated measurement error after the "mass-independent" spacial reconstruction, because the mass and momentum of the particle are required to perform the calculations. In PANG, a contribution is added to each of the estimated errors in the track angles to allow for errors in the optical parameters, distortions, etc. The value of this contribution is chosen so that the quoted uncertainties do not have unrealistically small values.

E. Hardware

1. Requirements for Scanning Machines

A scanning machine is a film projector used by a human operator to examine the stereo pictures of events occurring in a chamber. Although a three-dimensional representation of the picture is sometimes examined, most pictures are scanned by examining the stereo views of an exposure projected onto a plane surface, either reflecting or transmitting. The stereo views can be projected singly and concurrently onto the same surface area, or side by side for easy comparison. Many factors influence the design of a scanning machine. The more important factors are the size and arrangement of the stereo images of the chamber on the film or films, the reprojection magnification required, and the type of screen and viewing arrangement used. In particular, the degree to which all desirable features can be realized is limited by the amount of investment that can be justified.

Most bubble-chamber groups now use scanning tables with opaque screens mounted horizontally like a table top. The stereo images are projected onto the table via overhead mirrors and the operator sits at the end or side of the table. Although it may seem that the operator's head may cast a shadow, this is not the case with a carefully designed machine. The advantage of having a horizontal screen is evident when two people wish to scan at the same time, and when templates, protractors, rulers, etc., are used to make measurements on the projected image. In practice it is found better for the operator to sit in such a position that he can scan along the beam tracks rather than orthogonal to them, because "along-the-track" scanning makes it easier to find small-angle scatters and decays. In some scanning machines the viewing screen can be tilted such that the operator can view the track images at a grazing angle.

The size of the table is determined by the size of the picture on the film and the reprojection magnification desired. A magnification of 2/3 to 1-1/2 times the size of the original tracks in the chamber is usually preferred. Since the operator is only capable of making a detailed study of a picture projected on an area of the table within about two feet of his eyes, large pictures should be mounted on a movable film platen such that all parts of the picture can be projected onto the end of the table nearest the operator. Although it is then unnecessary for the table to be long enough to accomodate the whole picture, operators seem to prefer a table on which they can scan the whole picture superficially and then move the picture for detailed examination of the events.

The stereo views of each bubble-chamber picture are usually projected onto the same area of the screen either singly or concurrently. This is achieved by having solenoid-operated shutters in the light path of each view. In addition, it is advantageous to mount the projector lenses on movable stages so that the various stereo views can be superimposed at any depth in the bubble chamber; this facility is often used to determine whether a track stops in the chamber or goes out of the top or bottom.

The scanning projector should be designed for easy operation and maintenance. Control knobs and switches should be easily accessible and simple to operate. It should also be easy to load and remove film from the machine and to change projection lamps. The screen brightness should be sufficient for easy viewing in a semidark room, typically 20 foot-candles are adequate; less makes scanning tiring. The resolving power of the optical system should be close to six lines per millimeter on the viewing screen. A "crisp" image is advantageous since details--approximately a

bubble diameter in size--are often significant. The distortions in the projected image should be small so that it is possible to make crude momentum measurements by matching calibrated templates to the projected track images. Curvature measurements of a few per cent for tracks of about 1 BeV/c in a field of 15 to 20 kG should be easily achieved.

2. Description of Some Scanning Projectors

In the next few paragraphs we describe some of the scanning projectors currently in use at various laboratories throughout the world. Some are designed to handle only one specific film format, whereas others are easily adaptable to handle single and multiple films of any width.

Figure 9 shows the type of scanning projector designed and built at Berkeley and used by the Alvarez Group. This machine handles film from the Berkeley 25-inch and 72-inch hydrogen bubble chambers. In this format all three stereo views of each picture are interlaced on one film strip 46 mm wide and 800 to 1000 feet long. The film is threaded through the three film platens and clamped with solenoid-operated mechanical clamps. The correct spacing between views is obtained by looping the film around rollers. Each view is illuminated by a tungsten lamp and a condensing system placed underneath it and is projected via a Schneider Companon lens and two overhead mirrors onto the opaque white horizontal screen. The projector magnification is 10X, giving track images 2/3 their original size in the chamber. The resolving power is 60 to 100 lines per millimeter on the film. All three film platens are mounted on a common slider which can be moved parallel to the long axis of the table so that any portion of the picture can be projected onto the end of the screen nearest to the operator.

The three images can be projected onto the table simultaneously or singly by means of solenoid-operated shutters actuated by switches. The projector lenses for Views I and III are mounted on movable stages such that the stereo views can be easily superimposed. The fourth lens in Fig. 9 is used to project the image of an illuminated numbered grid onto the picture. The operator can use this grid to designate the approximate location of each vertex in an event.

The controls for image superposition, film advance, and rewind are situated near the operator's left hand, as are the switches for the selection of one or more pictures of a stereo combination and for controlling the projection of the grid. The knob for moving the film platens is on the operator's right.

Figure 10 shows a modification of the scanning projector described above. This model is used by the Powell-Birge and Goldhaber-Trilling Groups at Berkeley and is designed to handle up to three films 35 to 70 mm wide. Three films are shown loaded on the machine. The main modification to the previous model is a physical rearrangement of the components to allow easier film loading and projection-lamp changing. In addition, a more complex film advance, including a printed-circuit motor and clutch brake for each film is used to move all three films. An indexing system is available providing that appropriate indexing marks are on the films. A combined vacuum and mechanical film clamp is used to provide adequate clamping of large pictures. This projector was also designed and built by personnel at the Lawrence Radiation Laboratory, Berkeley.

The scanning tables pictured in Fig. 11 were designed and constructed at the Brookhaven National Laboratory. These machines also use opaque screens and overhead projection. They have a magnification

of approximately eight and project four 35-mm films simultaneously. The images are projected side by side rather than superimposed. The table can be tilted and pulled upwards to facilitate easy "along-the-track" scanning. To accomplish this the mirrors turn through half the angle of the table so that the image remains at the same place on the scanning surface.

Figure 12 pictures a scanning table used by the CERN Laboratory in Geneva, Switzerland. Opaque screen, table-top projection is used. This machine handles the two 35-mm, 400-ft spools from the CERN 80-cm hydrogen bubble chamber. The projected pictures can be superimposed by the operator, using controls that move the respective projection lens.

In addition to scanning tables designed and built by the experimental physics groups and laboratories, several designs are available from commercial sources.[3]

3. Requirements for Measuring Machines

A measuring machine is used to reduce the information contained in a photograph to digital form. Measurements may be made in xy, $r\theta$, or in any coordinate system that fits the problem. To do this effectively and efficiently, the measuring machine must combine several basic features and capabilities which are discussed in the next few paragraphs.

If the measuring errors are to be small compared to the other errors, the machine must measure to a precision of at least ±3 microns in the film plane for hydrogen-bubble-chamber pictures. The precision can be less (±10 microns) for heavy-liquid chambers because of deviations in the tracks caused by multiple scattering.

There should be some way, either through switches or a typewriter, to enter indicative data that describe the event to the computer

programs during analysis. In addition, there should be provision for entering auxiliary information which may be useful to the physicist during subsequent analysis.

To achieve any reasonable speed in measuring, the machine must have some type of automatic coordinate readout and recording. The output media usually takes the form of punched cards, paper tape, or magnetic tape.

There are many designs for measuring machines, but usually one of three approaches to the design problem is followed: (a) The optical system is held stationary. The film is moved, being fastened directly to a precision measuring engine. (b) The film and projection system are held stationary except for the lens which is fastened to and moved by a precision measuring engine. (c) The film and the projection systems are held stationary; measurements are made on the projected image.

Design method (a), where the complete optical system is held stationary and the film is mounted on and moved by a precision measuring engine, is usually considered to be the most desirable approach. The film is moved until the projected bubble image is coincident with a reticle on the projection screen. In this way the xy position of the film image is always determined using the same optical ray through the projection system. Consequently, lens and mirror distortions do not affect the measurements. The reticle is usually on the optical axis of the projection lens where the image resolution is a maximum. The precision of the measurements is limited only by the precision of the measuring engine and the ability of the operator to set the reticle on the proper point. When it is desired to measure to the maximum precision, this method is usually used. A precision of

one part in 100,000 over a length of 100 mm can be obtained by careful design.

Method (b), where the film and projection systems are held stationary and the lens is moved by a precision measuring engine, will produce measurements that are not quite as precise as can be obtained by using method (a), since the lens is used off-axis and different optical rays through the system are used. With a good lens the errors are small, but not negligible. The magnitude of the opto-mechanical-design problem is similar to that in method (a) except that the illumination system must now be made to track the projection-lens aperture and projection angle.

Design method (c), where both the film and the projection system are stationary and measurements are made on the projected image, is used when the required precision is about 1/10 the precision of that attainable in method (a). However, with perserverance and attention to detail, it is possible to approach the precision of method (a). Most of the inaccuracies in method (c) are due to the measurements being made off-axis of the lens. The resolving power always falls as one gets further off-axis, and this adversely affects the ability of the operator to set precisely. A more serious problem is the lens-field distortion, which can cause errors greater than one part in 1000. These errors can be corrected by measuring the distortions of each lens and correcting the data in the computer. With care, a precision of about one part in 10,000 is possible if corrections are made.

In methods (a) and (b) a precision engine is required since measurements are made directly in the film plane. The operator, however, usually views a magnified image. This is achieved by viewing a projected image in a projection microscope or by viewing through the eyepieces of a conventional microscope. The engine almost always measures in

Cartesian coordinates (x, y). The stages are usually moved by means of two lead screws, one for the x stage and one for the y stage, with a thread pitch of about 1 mm to 0.1 in. being typical. In some types of engines the stages are moved by hydraulic actuators.

The position of the stages can be measured in two ways: (1) by rotary encoders to measure the angular position of the screws if precision lead screws are used, (2) by means of linear encoders fastened to the stages (such as those using moire-fringe gratings, Guild, 1960) if the stages are moved hydraulically, or by recirculating ball screws.

In method (c) measurements are made on the projected-image plane. In this case the precision of the measurements can be less than in methods (a) and (b) because of the magnification of the projection system. The measuring device is usually some form of digitized drafting machine, although the SMP uses a very sophisticated method (see Chapter IX).

In all types of machines it is usually considered an advantage to be able to view all views simultaneously for comparison of different views of difficult events. In addition, it is advantageous to be able to superimpose the track images. This ability helps the operator to find the end of a track obscured by other tracks which cross the desired one at very small angles, or to locate small kinks in the tracks (decays) which may be virtually invisible on one or two views. Superposition of the images can be achieved by mounting the projection lenses on movable stages.

Magnification, resolving power, and image brightness are fundamental in their effect on the performance of any measuring machine. The magnification should be high so that accurate measurements can be made quickly. A large field of view is desirable so that the tracks to be measured can be found easily. The magnification that is most generally

found to be satisfactory is that which allows the operator to view the tracks at 2/3 to 2 times life size. Typically, this means viewing magnifications of from 7-1/2 to about 30 times the actual size of the image on the film. If these result in a viewed bubble image of approximately 1 mm diameter, the setting accuracy for the average operator will be about ±0.1 mm or about 0.1 bubble diameter. The advantages of high magnification and the ability to see a large area of the picture can be realized by using a high power projection system and also a projection system with a large-area viewing screen; or by using a zoom-microscope system.

The resolving power of the measuring-machine system can normally be made at least 70 lines/mm. This is adequate since the image quality is then limited by that on the film, where the diameter of a bubble image is usually about 30 microns. This size is determined by diffraction in the camera lens and is large because of the small lens aperture required to obtain good focusing throughout the depth of the chamber.

The image should be sufficiently bright that the operator's efficiency and speed are not impaired. The image can be so bright that it can cause physical discomfort, although this limit is not normally reached. Usable brightnesses for transmission screens vary from about 0.5 to about 5 foot-candles. For reflecting screens the range of usefulness is from about 5 to about 25 foot lamberts.

The numbers of films, their width, and the picture format vary considerably between bubble chambers. A measuring machine that is to be used to analyze pictures from several different chambers may have to handle three rolls of film in sizes up to 70 mm wide and pictures as long as 150 mm. Only a few per cent of the total machine time should be used for moving film. Loading film into the machine must be a convenient and rapid

operation, and of course the machine should not scratch, tear, distort, or damage the film.

Since measurements to a few microns are necessary, the film must be clamped securely. This is usually accomplished by using a mechanical clamp to force the film against a glass platen in which there are vacuum grooves placed near the edge of the film. A moderate vacuum causes large pressure forces that hold the film securely to the platen. A blast of compressed air can be used instead of a mechanical film clamp.

Even with "clear" film, as much as 50% of the illumination energy is absorbed in the film base because of the anti-halation dye used in its manufacture. A rise in temperature reduces the moisture content and causes the film to shrink, producing localized distortions which may be significant. The temperature rise of the film within the platen should be limited to a few degrees and to not more than 10°C if the film is to be measured to within a few microns. The temperature rise may be controlled by cooling the film platen with air or a liquid coolant. The thermal energy is normally removed from the illumination system by heat-absorbing glass or "cold" mirrors. In projection systems, power densities in the visible spectrum exceeding 0.1 W/in.^{2} at the film gate are typical.

The control that the operator has over the speed of the film transport can greatly affect the productivity of the machine. A slow film motion (approximately 1/10 in./sec) is necessary to be able to easily and quickly adjust the position of one film with respect to the others in the case of a multi-film transport. A medium film speed of between 1 and 5 in./sec is useful for advancing from one frame to the next. For moving long distances along the film or for rewinding, speeds from 300 to 1000 ft/min are necessary if valuable machine time is not to be wasted in this necessary but

unproductive operation. All three speed ranges have their uses; they may be discreet speeds or continuously variable from the slowest to the fastest rewind speed.

A film-frame counter is a useful operator aid for locating a particular picture on a roll of film. It saves time and thus helps keep production at a maximum. A frame counter may be an approximate device that measures film footage via a metering capstan, or can count sprocket holes or photographic marks next to each picture. An effective technique is to present a visual display leaving it up to the operator to do the final locating of the proper picture. If sprocket holes or accurately placed marks on the film are used, the counter can locate particular pictures exactly, and if desired, automatically. An automatic film advance can also use coded marks to find a particular frame, if such marks are available on the film.

The position of the viewing screen and of the machine controls with respect to the operator is most important. The type of controls and their placement make the difference between a machine that is unwieldy and tiring to operate and one that is so convenient that the operator can continue at maximum speed for hours.

When a precision stage is used for measurement, position controls--usually in the form of handwheels connected to the lead screws--are probably the fastest and most accurate means that an operator can use to set on a point. The use of a velocity control (joystick) for rapid traverse and approximate positioning of the film does save time. It relieves the operator of the tedious and annoying job of turning a lead screw for a hundred or so revolutions to traverse present-day-bubble-chamber pictures. Some measuring machines are designed with only a velocity control, usually a joystick, and this is used for setting on points as well as slewing. The

speed and accuracy of the operator is less with this method than with the position controls. When used for slewing, a joystick almost always is used to control a servo system. The motors of this system turn the lead screws. Typical speeds of rotation of precision-lapped screws (±1 micron) is about 5 rev/sec (1 mm pitch). Recirculating ball screws are in general less precise (±5 microns), but some models can be rotated in excess of 40 rev/sec.

Semiautomatic centering and tracking of bubble tracks (described for the MPI and MPII Franckensteins in Section IIIE4) is not essential but may increase overall data rates appreciably, particularly on large pictures where the tracks are long. The major advantage is that the machine automatically performs the tedious setting on the track, leaving the operator free to concentrate on measuring at maximum speed and efficiency. The accuracy obtained during "on-the-fly" measuring depends upon the speed at which the stage is moving and on the performance of the servo system. In practice, it is possible to measure with a precision of about ±2 microns at a speed of 2 mm/sec.

In addition to all the characteristics of the machines already discussed, it is often worthwhile to build into the machine features which aid the operator. These may be designed to reduce the error rate or increase the measuring speed of the machine. These aids can be achieved by logic that is internal to the measuring machine or by connecting the machine or several machines to an external device such as a small, programmable computer. (Goldschmidt-Clermont, 1964).

Interlocking and automatically sequencing the operation of the machine guarantees that the operator performs each operation in the proper order and that none is forgotten. For example, such controls might insure that the operator measures the correct number of fiducials and tracks in

the correct order, and changes the view number at the proper time. Interlocks do not usually increase the speed of operation much, but can reduce operator errors as much as 50% representing an overall data-rate improvement of about 5%. Automatic sequencing assists the operator appreciably and increases speed by about 10%. In addition, the automatic insertion of indicative data, automatic frame finding, and automatic vertex and fiducial finding may increase the speed by another 30%.

4. Conventional Measuring Machines at Berkeley

To describe or even to discuss more than a very few of the machines that are presently being used to measure bubble-chamber photographs is beyond the scope of this article. The author will discuss in detail two Franckenstein machines, measuring projectors MP-IE and MP-IID. These machines were designed and built at the Lawrence Radiation Laboratory, Berkeley.

The first Franckenstein (MP-IA) was put into service in 1957 by the Alvarez Group, analyzing hydrogen bubble-chamber pictures on a production basis. The MP-IA was designed to measure only the 35-mm film from the Berkeley 4-in., 10-in., and 15-in. hydrogen bubble chambers. The latest MP-I's (MP-IE and F) are designed to handle three rolls of film of any size up to 70-mm wide and 1000-ft long, as well as the Berkeley 46-mm and 70-mm film (all three views on one film). Six MP-I projectors with various film-handling capabilities have been built at Berkeley.

The MP-I's are semi-automatic centering and tracking projection microscopes using rear projection screens. The system design incorporates stationary optics and moving film (method 1 discussed in Section IIIE3). This machine, shown in Fig. 13 is composed of a projector,

several racks of electronics, an indicative data panel, and a card punch. The projector in the center of Fig. 14 contains the precision measuring engine, film platen, illumination and projection optics, viewing screen, operator controls, and the electromechanical-optical scanning unit which is used when autocentering. The indicative data panel at the right is used to enter fixed data to identify the event and each track. Data are output onto punched cards via the IBM 526 punch at the left of the machine.

The internal features of the projector are shown schematically in Fig. 15. The platen, projection lens, and first mirror are supported on the measuring-engine base which in turn rests on the rigid and massive base frame. A rigid structure mounted on the base frame supports the other mirrors, screen, and upper cabinet. The detecting head and reticle projector are independently mounted on the base frame. As mentioned previously, the complete illumination and optical system is stationary; only the film is moved. This is clamped in the platen which in turn is part of the top stage of the precision engine. The film to be measured is held by both mechanical clamps and by vacuum to the glass platen. The projection lamp, via suitable lenses and mirrors, illuminates the images on the platen and focuses the transmitted light into the projection lens. This lens forms an image at approximately thirty times magnification on the screen via the three mirrors. The beam-splitting mirror causes an image identical to that formed on the projection screen to be focused on the scanning disk in the optomechanical scanner or "detecting head." An illuminated reticle is projected through the beam-splitting mirror onto the screen by the reticle projector. Manual measurements are made by moving the stage, and thus the film, so that the magnified image on the projection screen coincides with the illuminated reticle at the points to be measured.

The x and y coordinates of the stage and film are determined by measuring the angular position of the two 1-mm-pitch lead screws. This is accomplished by means of rotary encoders fastened to each lead screw, giving 1000 counts (±1 micron) per revolution over the complete 100 mm by 150 mm travel of the engine. Both the x and y encoders are read electrically and the data stored instantaneously (within 10 μsec) in a buffer. The data are output from these buffers in decimal form onto punched cards. The buffer store is absolutely essential in this machine because coordinates are read out "in flight." In addition, during manual setting the buffers make it unnecessary to hold the handwheels stationary for an appreciable time during readout.

The operator's console is pictured in Fig. 14. The x and y handwheels are the two largest wheels. A joystick-type velocity control is located at the far right-hand end of the control console and is used to move quickly to the next area of interest on the projected image. The smaller knob to the left of the x and y handwheels is used to align the projected reticle to the direction of the bubble track. This alignment is not only an aid to manual setting, but, through mechanical gearing, adjusts the orientation of the electronic cross hairs and of the sine and cosine potentiometers that proportion the error signals to the servomotors that drive the lead screws when autocentering.

Film is mounted on spindles at the back of the machine and threaded through the film platen. The film transport controls are the four push buttons and the knob in the semicircular slot at the far left end of the control console. With these controls three rolls of film can be transported singly or in unison at any speed from 0.1 in./sec to 750 ft/min. The

machine is pictured with a roll of Berkeley 72-in. hydrogen bubble chamber film mounted on it. When three films are to be measured, the reel spindles to the right and left of this roll are also activated.

The remaining controls on the projector are either control push buttons or limit lights indicating that the engine is at the end of it's travel. The push buttons for manual control of the track and view numbers, and the knobs for controlling the superposition of views, are all mounted on the small panels to the right and left of the projection screen. The panel above the screen contains the track and view-number display, the film footage-counter display, and the brightness control for the projected cross hairs.

The indicative-data switches are mounted on the left half of the indicative-data panel. The array of push buttons on the right half of this panel control the automatic sequencing of track and view numbers. The control information recorded by these switches is either determined by the operator upon inspecting the event to be measured, or it may be obtained from sketch cards or library lists generated during the scanning operation.

A cathode-ray tube is mounted at the center bottom of the projection screen. The track and marker signals are displayed here as an aid to the operator in maintaining speed and precision when setting manually. It also serves as a monitor on the performance of the machine when it is in the automatic centering and tracking mode of operation. With this display, any operator can quickly and easily reproduce settings to ±1 micron. Examples of the display are shown in Fig. 16.

The track and marker signals are generated in the detecting head. An optically opaque scanning disk (Fig. 17), about 5 in. in diameter, with 24 radial transparent slits is turned by a synchronous motor at 60 rev/sec. The slits are approximately 1/5 of the average track width on

the projected image. The positions of the detecting head and of the projected reticle are adjusted mechanically until the optomechanical center of the detecting head is on the same point as the center of the reticle on the projected image. An optical mask in the detecting head causes the disk to scan only that part of the projected image that is in the immediate vicinity of the projected reticle. The light that goes through the slits is picked up by a photoelectron multiplier which generates electrical signals proportional to light flux. As each slit in turn scans across the track picture aperture, it also scans a light beam from the marker lamp. The marker light goes through the scanning disk at a radius that is smaller than that for the track picture, so that there is no mixing of the two light beams. A second photoelectron multiplier converts this scanned marker light beam into electronic signals; in effect the marker signal is an "electronic cross hair." To measure a track, the center of the rotating disk is positioned by the reticle alignment knob such that the electronic and projected cross hairs are aligned with the track being measured.

In addition to being displayed on the cathode-ray tube, the track and marker signals are also fed into electronic circuits which generate error signals that in turn control the relative speeds of the servomotors that are connected to the x and y lead screws. This circuit is activated when the machine is autocentering.

Figure 18 is a block diagram of the electronic circuits. The x and y handwheels are connected to the lead screws by synchro transmitters and receivers which are declutched from the lead screws when the machine is autocentering and tracking. Synchro declutching is necessary to eliminate degrading the servo-system performance. The joystick generates x and y signals from two internal potentiometers, the output of each being proportional

to the x and y displacement of the joystick handle.

For autocentering the track and marker signals generated in the detecting head are directed separately into the pulse shaper and time discriminator. These circuits generate an error signal proportional to the difference in time of arrival of the centers of the track and marker signals. The output of the time discriminator is applied to a sine-cosine potentiometer by a differential amplifier. The sine and cosine components of the error signal are fed to the input of the x- and y-axis servo amplifiers respectively which supply the power to the servomotors that turn the x and y lead screws. To close the servo loop, a continuous sampling (1440 pulses/sec) is made of the track images projected onto the detecting head. Tachometer feedback from the motor shaft to the servoamplifiers linearizes the servo closed-loop characteristics. The bandpass of the servo system is usually greater than 30-cps. The velocity along the track, when autocentering, is controlled by the operator via the foot pedal and is typically 2 to 3 mm/sec. The proper components of the control signal generated by the foot pedal is directed to the x and y servoamplifiers by a cosine-sine potentiometer.

The measuring speed of the MP-I's for strange particles is approximately five to six events/hour. For two-prongs the speed is more like 10 events/hour; complicated events may be as slow as three or four per hour.

A large model of Franckenstein, MP-II, has been built to measure the 46-mm film from the Berkeley 72-in. hydrogen bubble chamber. These machines, of which four have been built, are similar to the MP-I's in that they incorporate the same autocentering and tracking circuits and use the same type of rear projection screen for measuring. Figure 19 is a photograph of MP-IID. The tracks are viewed on the measuring screen

at 33X magnification, with less than 4% of the picture area being visible at one time. The measuring screen is smaller than on the MP-I's, since the event can be found on a low-power front projection screen located to the right of the operator. The image is formed on the low-power screen by long-focal-length lenses projecting via three overhead mirrors; it includes 100% of the picture at 7.5X magnification. The lenses are moved by a mechanical linkage to the engine such that the image on the projection screen remains stationary even when the engine is moved. The data switches mounted on the desk to the operator's left are used to enter the operator's number and the date. In addition there are several control and delete push buttons. A punched card containing the indicative data for the event and its approximate location on the picture is inserted into the card reader shown at the near edge of this desk.

The MP-II electronic system first reads the indicative data from the punched card and records it in binary coded decimal form on the paper-tape output (far right). It then automatically searches the roll of film for the proper picture by automatically reading the binary marks which are on the film adjacent to each stereo triplet. The searching occurs at film-transport speeds in excess of 600 ft/min. The measuring procedure is very similar to that followed on the MP-I's, except that sequencing circuits within the MP-II require that the operator measure nine fiducials (three on each of three pictures) and all the tracks associated with the vertices specified on the input control card. Each track is measured on the best stereo-view pair; a "dummy" track is entered on the unwanted view. During the measuring process, logic circuits within the machine automatically switch views and run the measuring engine to the close proximity of each ficudial and vertex to be measured. The operator does the actual precise

setting on fiducials and vertices, and records coordinate points along the proper tracks using autocentering. When the x and y coordinates of a point are recorded by means of the "record" push button, the output of the binary scalers are instantaneously stored in a buffer and then recorded on paper tape. The buffer store is again necessary because the machine reads coordinate points "in flight." The least count of the system is 2.54 microns.

The MP-II's do not use precision-lapped screws to determine x, y position, but use moire-fringe gratings and two-way binary scalers to count the fringes. The measuring engine is moved by recirculating ball screws so that it can be moved at linear speeds up to about 5 in./sec.

With autotracking, five to ten strange-particle events (typically two vertices and four to five tracks total) are measured on this machine per hour. Two-prong events can be measured at a rate of about 15 events per hour.

5. Other Types of Conventional Measuring Machines

Bubble-chamber pictures are analyzed by many laboratories throughout the world. The equipment used is either built by the laboratory personnel or is purchased from commercial concerns.[3] The simplest way of making a precision measuring machine is by using an ordinary binocular microscope and measuring engine. Rotary encoders are usually attached to the screws to make automatic the readout of the stage position. Some of these machines have zoom optics so that the event to be measured can be located more easily.

Many of the measuring machines are similar to the Franckensteins described above, namely: measurements are made on the film by digitizing the position of a precision engine; and the pictures are viewed on a rear projection screen. The engine may be moved and its position

digitized in a variety of ways. In the United States precision lead screws and rotary encoders seem to be preferred; in Europe moire-fringe digitizers are usually used. Many European machines use screws to move the measuring engine; although one English design uses hydraulic rams (Welford, 1963). Many of the Franckenstein-like machines use only a joystick to control the motion of the stage; this makes accurate setting slower than with handwheels. Some of the machines have autocentering and track following; others do not. The design of the film transport is determined, of course, by the format of the film to be measured. On many of the machines, indicative data are entered by means of a typewriter instead of switches. In spite of these differences, the machines work in a way very similar to that described for the Franckensteins. Their measuring speed varies considerably, but averages four to five events per hour.

Many bubble-chamber pictures are measured on machines less precise than those already described. These machines measure the projected image, usually on a reflecting screen. The measuring device may be a simple x, y digitizer, or it may depend upon some method of triangulation. Three basic methods frequently used (see Fig. 20) are (a) measurement of x and y, using linear encoders; (b) measurement of two angles θ_1 and θ_2, using angular encoders, where r_1 and r_2 are rigid members of constant length; (c) measurement of lengths r_1 and r_2 from origins O_1 and O_2.

The physical layout of the machines and the methods used to obtain the digitization are very varied and depend mainly upon the accuracy required. In method (a) two rigid beams are used. The digitization can be done using coarse moire-fringe digitizers on both axes or in other ways. Method (b) uses a drafting machine digitized by means of rotary encoders.

There are many ways of accomplishing method (c). The most common is to use two unstretchable wires wound around rotary encoders attached to two stationary posts at O_1 and O_2 (Fig. 20). The lengths r_1 and r_2 can then be simply related to the angles read by the two encoders. Other methods using sound waves and light rays to measure the distances have also been tried.

To make rapid measurements on the images of straight tracks (i.e., no magnetic field in the chamber), another rotary encoder can be fixed to the measuring arm at point P (Fig. 20). A template containing a straight line and a reticle is attached to this encoder. The complete measurement of one track then consists of placing the straight line along the track and recording. This gives the digitization of an arbitrary point on the track and its orientation with respect to some chosen axis.

The setting precision obtained with these simple machines is about 5 mils on the projected image. The precision on the film is dependent upon the magnification of the projector but is typically $\pm 10\mu$. Of course, distortion in the lenses and mirrors may cause the measuring precision of the machine to be less than this. This method of measuring is used where great precision is not required, primarily for heavy-liquid bubble-chamber and spark-chamber pictures. It is particularly useful for straight-track images, since only one reading is required per track.

F. Existing Data Reduction Systems

1. Operational Characteristics

Over the past five or six years data-reduction systems have been built up at many laboratories throughout the world. These vary in magnitude from university departments of about 10 people to large installations employing over 200. Table I shows statistics gathered from a representative sample of bubble-chamber groups and illustrates the enormous effort

currently being made to analyze bubble-chamber pictures.

Comparisons between the various systems are extremely difficult because of the disparity in the size of the groups and also because the apparent performance of a system (events scanned and measured, etc.) is strongly influenced by the type of experiments being performed. No comparisons are attempted here. The following points are emphasized, since they may help in the design of future systems.

On the average, one physicist or graduate student is assisted by one to two specially trained scanning technicians who scan and measure the film and also assist in bookkeeping, expediting, and other chores associated with the analysis of the data. The number of scanners is presumably limited primarily by economics. In addition to scanning technicians, most laboratories have a staff of programmers to assist the physicists with writing new programs and maintaining old ones; there are also engineers and maintenance technicians to look after the equipment.

The number and types of machines is again governed primarily by economics. However, for an efficient operation there should be a surplus of equipment or scheduling will become a problem. It is also important to have the proper ratio of scanning to measuring projectors. Experience in the Alvarez Group at Berkeley has shown that about 35% of the total scanning-technician effort is used for measuring--about 40% for jobs required the use of a scanning projector, and 25% for chores, for example, bookkeeping, expediting, computer runs, supervising, etc. In addition, physicists and graduate students should have easy access to scanning projectors if they are to work efficiently. The numbers obtained from the survey show that few groups use their measuring machines more than

100 hours/week; the average usage is about 80 hours/week. The number of scanning machines required per measuring machine is strongly influenced by the type of experiment and the speed of the measuring projector. Most groups have about two scanning projectors per measuring projector.

The measuring rates are determined by many factors, for example, the complexity and frequency of the events, the type and design of the machine used, and the size of the pictures. Consequently, it is very difficult to compare data from the various groups. In general it appears that for strange-particle events of average complexity (e. g., two vertices and four or five tracks per view) the measuring rate is five/hour or less. Automatic track following is helpful but not essential. On small pictures the increase in measuring rate produced by autotracking is not appreciable; however, for larger pictures where the tracks are long, autotracking may increase the number of events measured per hour by as much as 20%. The measuring rate can be further increased by automating the correct sequencing of the machine, insertion of indicative data, and finding and positioning the pictures. This automation can be achieved either by the use of control circuits within the machine or by attaching the measuring device to a computer. The card-controlled Franckensteins at Berkeley (described in Section IIIE) are currently averaging about eight events/hour. This measuring rate is an average for all types of events. The average rates are about half as fast for complicated events and twice as fast for simple two-prongs (one incoming and two outgoing tracks).

Scanning rates depend upon the type of experiment. At Berkeley the current rate is about 75 frames/hour. This is achieved when scanning film from the 72-in. chamber with about 10 to 15 incoming tracks/frame and recording about 30 strange-particle events/hour. Considerably less

than half the scanning effort is used for initial scanning of the film. The remaining time is used for routine rescanning and special scans (see Section IIIA). Because of limited measuring capability, most groups record only the more interesting events, and large numbers of events are deliberately ignored. The measuring power of a group strongly influences the type of experiments that can be done. The anomalous figures (Table I) for the Alvarez Group at Berkeley, where the rate of event measurements is currently higher than the rate at which events are recorded, is caused by remeasurement and measurements of events from old experiments which were scanned years ago.

In addition to the huge effort involved in scanning and measuring the pictures, each group uses an appreciable amount of computer time. This varies enormously from group to group dependent upon the availability and cost of computer time, the number of events, and the amount of analysis and bookkeeping performed on each event. The Alvarez Group at Berkeley currently uses about 100 equivalent-7090-hours per week. This amounts to about one minute per new measurement processed. However, the analysis of each event through the programs once should take only about 15 seconds. The additional time is required for reprocessing, library functions, tape manipulation, and debugging. Table II shows a breakdown of computer usage in the Alvarez Group. Only about 40% of the time is used for direct computation on the events and 10% for miscellaneous calculations (e.g., minimizing and fitting routines, Monte Carlo calculations etc.) Fifteen % of the time is used for program development. About 35% of the computer time is unproductive since it is used for formatting (PANAL and WRING), tape manipulation (MERGE-SELECT), and library procedures (LINGO or LYRIC).

Many bubble-chamber exposures are made over periods of a year or so. Such experiments currently involve recording and (if measuring capability permits) measurement of 50,000 to 300,000 events. Analysis of such an experiment is usually divided into subexperiments pertaining to different physics problems. These subexperiments may contain as few as 100 events, or perhaps 50,000. Analysis is most active during the exposure and for one to two years thereafter, although some experiments may still be active five years after the exposure started. In a large bubble-chamber group several experiments are analyzed concurrently.

2. Cost of Operation

Analysis of bubble-chamber data is very expensive. This is illustrated in Table III which shows approximate costs for data analysis for the Alvarez Group, Berkeley. Since this group is one of the largest in the world, it is not a very representative example; however, it does illustrate the large expenditure to be expected for the analysis of bubble-chamber pictures. Two interesting facts emerge from this table. First, the capital investment in equipment is similar to the cost of operating and maintaining the equipment for one year. Consequently, depreciation of this equipment, even if calculated on a four-year basis (equipment usually lasts longer), is quite small compared with all other costs. Second, if the cost of computer time was calculated at the commercial rate (> $300/hr) it would be much greater than the cost of scanning personnel. However, the low recharge rate and the accessibility of the computers at Berkeley does encourage us to use the computers more extensively. Costs at Berkeley are higher than at many other places because of the high overhead on salaries (about 100%) charged to the physics groups.

Costs given in the survey of other groups are very hard to interpret. In Europe, salaries are very much lower than in the U. S. This is also reflected in a lower cost of equipment. The price of equipment varies considerably. A measuring projector similar to a MP-I-type Franckenstein can be bought for between $30,000 and $100,000 depending upon the complexity of the machine. Machines that measure the projected image are cheaper--usually $10,000 to $30,000. A one-eyed scanning projector can be obtained for as little as $300; however, a three-view projector usually costs about $15,000.

IV. SPARK CHAMBER DATA PROCESSING

A. Data Analysis and Experiment Design

As pointed out elsewhere, one of the advantages of using spark chambers is the freedom allowed to the physicist to adapt the physical configuration of his apparatus to the physics of the given experiment. This advantage is not without cost, however. Since no two spark-chamber experiments are the same, a general approach to data reduction is very difficult. In fact, some thought should be given to how the data from an experiment is to be analyzed at the time the experiment is designed, in order to avoid waste of time, effort, and money invested in obtaining the data. The chambers and triggering system must be designed with an eye to simple and rapid data reduction, as well as the physics that is to be done. In general, the design criteria dictated by the data analysis will differ depending on the analysis equipment available and whether automatic equipment is to be used. The latter is treated in Chapter IX. What follows in the rest of this section are general remarks and various procedures and techniques

that may be useful in the design of a spark-chamber experiment.

1. Arrangement of the Chambers

Proper physical placement of the spark chambers may eventually simplify the scanning, while not affecting the physics. For example, in many experiments coplanarity of several tracks is an important criterion for rejecting background. In such an experiment it may be possible to arrange the chambers in such a way that one of the stereo views shows an "edge on" projection of the event. Then coplanarity becomes a simple scanning criterion (Cook et al., 1963). Another possible example is an experiment where the opening angle between two particles is of interest. The chambers should then be arranged in such a way as to allow a film format such that a scanner may easily check the appropriate angle. Such considerations are particularly important for experiments where there is a large background that can not be rejected by the triggering system and must be done by the scanning.

2. Fiducial Marks

Fiducials are placed on the various chambers in the experiment to relate the positions of the chambers and correct for any optical distortion that may exist in the system. This latter point is of singular importance. Because of the temporary nature of a spark-chamber setup, the tendency is to rather haywire the optical system. Thus there may be considerable optical distortion caused by warped mirrors. This distortion and indeed the relative position of the various chambers in the array may change during the course of the experiment. The placement of the fiducials can play a crucial role in the analysis of the experiment.

A very simple system is to place a grid on each chamber and to reference all measurements to the nearest grid line. This system can

eliminate in a direct way all optical effects since measurements are then made in real space. Unfortunately this system is only useful for experiments involving relatively few events. If the measuring is done with essentially no automation (for example, a projector and rulers) this method is straightforward but too slow for large numbers of events because of the time taken to record the measurements. On the other hand, if a digitized measuring device that automatically records the measurements is used (see Section IVB3), then the procedure of measuring each track with respect to a local fiducial at least doubles the number of measurements made for each event. To speed up event analysis, one measures only a few fiducials on each picture, and the entire set only from selected pictures taken at different times during the experiment. Since the entire grid is needed only occasionally, it may be worthwhile arranging two sets of fiducials. One set is recorded on each picture, which provides only a basic set. The second set then consists of a complete grid to check the optical distortion and geometry of the chambers occasionally during the experiment. More concerning optical distortion is contained in the section on "Optics and Film Format."

3. Stereo Technique

For parallel-plate spark chambers little difficulty is encountered in taking stereo pictures. In some cases 90-deg stereo is possible when two adjacent edges of the chamber are accessible. When only opposite edges are accessible, a tilted mirror behind the chamber is often used (Fig. 21). The depth of the spark in the chamber is then given by $Z = Z_0 + y \sin\alpha + d/\sin 2\alpha$ where d is the displacement between the image and the spark as seen by a camera at infinity (this is the case when a spherical field lens is used; see Section C). This is equivalent to a small-angle stereo using a second camera.

An adaptation of this system can be used for cylindrical spark chambers (Beall et al., 1963). The mirror should be in the form of a helix. The problems of fabricating a helical mirror are overcome by making an equivalent mirror from a number of flat mirrors in the form of a turbine blade. (Fig. 22).

Another technique has been used for cylindrical chambers that are not complete cylinders. This system is illustrated in Fig. 23 for a 180-deg chamber. One view is taken parallel to the axis of the cylinder. If the chamber plates are made from or coated with some highly reflecting material (such as polished aluminum) the light from the spark is multiply reflected around the cylinder and can be brought to the camera by a subtly placed mirror. This second view gives a direct measurement of the spark position along the axis of the cylinder. It should be noted however, that in this view a straight track appears as a section of a hyberbola.

4. Optics and Film Format

The effect of bad optics on data reduction has already been mentioned. The main point that should be kept in mind during the design, setup, and operation of a spark-chamber experiment is that although almost any optical distortion is subject to correction, it will have to be done ! Since any complicated computer programs to correct for sloppiness in the optics will probably be useless for the next experiment, time and money is better invested in avoiding the correction as much as possible. Supports for mirrors should be carefully designed, and everything possible done to make the mirrors flat and above all avoid time-varying warpage. Remember that glass in large sheets is quite flexible.

For nonautomatic film scanning, it is convenient to keep the entire picture on one film. The arrangement of the chambers on the film

need not be the same as that in real space. However, wherever possible one should arrange them so as to make scanning as easy as possible. A week spent adjusting and changing mirrors may save six months of scanning and measuring time.

B. Scanning and Measuring

If the scanning of a spark-chamber experiment differs at all from a bubble-chamber problem it probably tends to be simpler. The spark-chamber pictures are in general much simpler, and the scanner is asked to look for a rather restricted topological pattern which is quite easy to recognize. Typical examples of the scanning criteria that might be used are: Do certain chambers have one or two tracks? If there is a track in one chamber is there a corresponding track in some other chamber? Are there tracks in one chamber that are roughly an extrapolation of tracks in another chamber? Such criteria are easy to apply and, therefore, usually one can very rapidly scan the film to find pictures that must be measured for further analysis. Once the picture to be measured has been found, the problems of the spark chamber are somewhat different from those of the bubble chamber.

1. Spark Chambers without Magnetic Field

For spark chambers without a magnetic field track measuring can be considerably simplified. Since many chambers used in an experiment are usually of this type, much benefit can be derived by reducing the number of measurements required. This is accomplished by using some system of measurement which measures all of the sparks that make up an individual track simultaneously. The usual system is for the scanner to lay a straight edge or fiducial line along all of the sparks that constitute a track and then make the "best fit" by eye to the sparks. If one point on this line, say x, y,

is recorded along with the direction of the line, these three numbers serve to parametrize the track. This technique for measuring the tracks is enormously faster than recording coordinates of each spark and later fitting a straight line to these measurements. The problem that arises is with the "best fit" to these sparks. Indeed, this problem is the most plaguing in spark-chamber data analysis. What part of a spark should be used to best measure the position of the particle passage through the chamber? This has been subject to a great deal of debate, and some experimental information exists. The answer to the problem is never clear and may vary from time to time within a given chamber as the operating conditions of the chamber change. If the particle passes within about 10 or 20 deg of the normal to the spark-chamber plate, little difficulty is encountered. In this case the "best fit" by eye probably gives as good a result as a more detailed computer fit to coordinates of each spark. On the other hand, if the direction of the track makes an angle with respect to the normal to the plates greater than about 20 deg, a careful measurement of each spark and a computer fit to these sparks is probably unwarranted, since under these circumstances it is never clear what part of the spark should be used. For experiments where the ultimate in precision is required and the particles may be traversing the gaps at rather large angles, the only solution is to make series of experimental tests of the chamber under various operating conditions. Then the operating conditions of the chamber (i.e., gas pressure, gas purity, clearing fields, operating voltage) must be carefully controlled during the experiment to insure that the characteristics of the chamber are the same as they were when the chamber was calibrated.

2. Spark Chambers in a Magnetic Field

For chambers immersed in magnetic fields the problem of measuring becomes very much more akin to that of the bubble chamber. In this case, the best information comes from a measurement of the coordinates of each spark and then a fit to these measurements to determine the direction and momentum of the particle. In the case of a chamber operating in a magnetic field, however, the problem of what part of the spark to use is even more serious than in the chamber without a magnetic field. Between the time of the passage of the particle through the spark chamber and the time the voltage is applied to the plates the electrons tend to drift under the action of the clearing field of the chamber. With the crossed electric and magnetic field, the electrons then move in a direction parallel to the spark-chamber plates. Thus when the sparks are formed they may be displaced from the original track of the particle. Since in most spark-chamber configurations the clearing field is in an opposite direction in adjacent spark chamber gaps, the drift of the electrons in the magnetic field is also in opposite directions in adjacent gaps. Therefore, one sees a staggering of the tracks in alternate gaps. Under these conditions, the best one can probably do is to average adjacent pairs of sparks to determine the best location for the original particle position. Such a system works as long as the particle is traveling more or less normal to the plate. As the particle trajectory turns in the magnetic field and becomes parallel to the plate one usually finds several sparks in a gap from a single particle passage. These multiple sparks make impossible accurate determination of the position of the particle passage. Fortunately, careful consideration of this problem during the design of the spark-chamber experiment can make an accurate measurement at this point unnecessary.

3. Hardware for Spark-Chamber Data Analysis

Hardware for measuring and scanning spark-chamber pictures has been produced by a number of groups, and a partial list of references appears in the bibliography for this chapter (see Hardware, Spark-Chamber Scanning). The simplest hardware that one can envision is an ordinary microfilm reader to serve as a projector and a rule and a protractor for the measuring. For experiments involving only a few thousand pictures this is quite sufficient and usually accurate enough. For experiments involving tens or hundreds of thousands of pictures one needs a more automated device than this. The automatic recording of the coordinate information is particularly important. A number of systems using automatic digitization for spark-chamber measuring projectors have been constructed by different groups. Even for chambers in a magnetic field, these devices are usually simpler than the track-following Franckenstein-type measuring projectors used on bubble-chamber pictures, since the track-following feature is of no use for the spark-chamber photograph. For chambers without a magnetic field where one would prefer to record three parameters for an entire track rather than individual spark locations, one needs to add to the usual x, y coordinates another parameter giving the direction of the track. One method is to use an ordinary drafting machine on the scanning table with each of the three angles at the bearings of the drafting machine digitized. Another system is to use a Franckenstein-type measuring projector without the track-following feature. A rotating fiducial line is added to the measuring projector to digitize the direction of the track. The position of the stage and the angle of the line are moved until the line lies along the track, and then the x, y position of the stage and the direction of the line are automatically recorded.

C. Spatial Reconstruction

Spatial reconstruction for spark-chamber tracks is much simpler than for bubble chambers because it is relatively easy to identify corresponding spark images. Even when more than one track traverses the chamber, the corresponding spark images can usually be identified by some characteristic feature. Because of this, spatial reconstruction for a spark-chamber experiment is usually a simple problem in geometry. It should be remembered, however, that a spatial-reconstruction program for one experiment is of little or no use for another experiment. Consequently careful consideration should be given to the spatial-reconstruction problem during the design of the experiment. For a spark chamber of any reasonable size, the collimation of the light by the spark-chamber plates requires that the optics of the spark-chamber experiment be arranged in such a way that the light traveling down the gap of the spark chamber can reach the camera lens. Several techniques are commonly used to solve this problem. A spherical field lens at the chamber with the camera lens at the focal point of the field lens (see Fig. 24) forces light from all spark-chamber gaps to reach the camera. Such a lens actually simplifies the data reduction, because the image on the film is then a simple projection of the spark positions on the plane of the field lens. So, coordinates measured in the film space are proportional to the coordinates on this surface. A second technique for solving the problem of "seeing" down the gaps of the spark chamber is to use a cylindrical field lens. Since for a parallel-plate chambers deflection of the light leaving the spark-chamber gap need be only in one plane, a cylindrical field lens serves the purpose of allowing the camera to record sparks deep in the chamber. Spatial reconstruction now involves a coupling between the two stereo views of the spark chamber.

For this reason one should avoid using a cylindrical field lens rather than a spherical lens.

A third solution to the problem of "seeing" down the gap can sometimes be used. If the spark chamber can be constructed of independent gaps, each gap can be set at a slight angle with respect to the others. Thus, all of the planes of the gaps can be made to intersect in a line through the lens of the camera. This can be a useful scheme for very large chambers where it is felt that construction of an extremely large spherical lens is unwarranted. However, at best this scheme is poor from the standpoint of data analysis. First, the tilting of the gaps in a practical case can limit one to a small stereo angle. Determination of depth in the chamber is usually rather poor. In addition, both coordinates measured on the film for this system only give directions from the camera to the spark. Thus, the two views are more strongly coupled than with the cylindrical lens, and spatial-reconstruction equations are then more complicated.

V. ACKNOWLEDGMENTS

We would like to thank many people for their help and comments. In particular, William E. Humphrey, Yves Goldschmidt-Clermont, Samuel Penny, David Rahm, Frank T. Solmitz; and all those people who supplied the data presented in Table I. This work was done under the auspices of the U. S. Atomic Energy Commission.

VI. APPENDIX: TRACK IDENTIFICATION AND SCANNING-TABLE MEASUREMENTS IN BUBBLE-CHAMBER ANALYSIS

A. Bubble Density

The bubble density can be used very conveniently to identify tracks in the chamber. The number of bubbles per centimeter along a track, is determined by the operating conditions of the bubble chamber (i.e., temperature and pressure) and the velocity of the particle. It is found experimentally that the relation is approximately

$$\text{bubble density} = D = Az^2/\beta^2,$$

where A is dependent upon the chamber conditions only, β is the velocity of the particle in units of c, and z is its charge in units of e. For unit-charged particles the value of $1/\beta^2$ gives the "relative density" (d) of the particle, i.e., the density relative to the density for the particle when $\beta = 1$. Experimentally this relation seems good for $0.5 < \beta < 0.8$ for heavy liquids and up to $\beta \sim 0.97$ for hydrogen (Biswas et al., 1963; Fabian et al., 1963; and Hahn et al., 1961). For scanning purposes, curves of $1/\beta^2$ vs momentum are very useful for identifying particles with densities from 1.5 to 5.0. If the particle is more heavily ionizing than this, the track usually becomes solid; if it is less ionized, it is hard to distinguish by eye from minimum-ionizing tracks. Of course, since the number of bubbles per centimeter depends upon the sensitivity of the chamber, it is essential to have a track of known ionization in the picture for comparison. Also care has to be exercised since the sensitivity may vary over the volume of the chamber, causing tracks with the same value of β to have different track densities in different parts of the chamber. To use this method during scanning, the curvature of the track is measured with a circular template and the density estimated by eye. Estimation of bubble density

is difficult for dipping tracks because the track image is foreshortened and the track appears more dense than a flat track with the same β.

This method of track identification is very useful for distinguishing π^+ from protons in the momentum region 0.1 to 1 BeV/c, thus making identification of K^0 and Λ decays comparatively simple in many cases. The identification $\pi^\pm$ from $K^\pm$ is harder, but can be made by ionization from 100 to 600 MeV/c. Distinguishing $\pi^\pm$ from $\mu^\pm$ is usually impossible at any momentum because the masses are so similar. An electron is easily identified if its momentum is less than about 100 MeV/c, since it is the only particle that produces a minimum-ionizing track at such a low momentum.

Accurate bubble-density information can be obtained by measuring gap lengths in the track (Barkas, 1961). Then the distribution of distances between bubble centers is $N(x) = N_0 e^{-x/g}$, where N_0 is the total number of gaps on a track, and g is the mean gap length (MGL) and is proportional to β^2. Actually, distances between the edges of bubbles are measured. To use this method successfully, one must control the bubble-chamber conditions carefully, since the limits of β for which bubble-density measurements are useful depend upon chamber conditions. In addition, the sensitivity of the chamber must be fairly uniform over its volume.

B. Range

Range measurements can only be used for identifying low-momentum tracks, since fast tracks leave the chamber. The momentum interval in which this method is useful depends upon the size of the chamber and the chamber liquid and operating conditions. To give some feeling for the sizes involved, range-momentum curves for hydrogen are shown in Fig. A1. In propane and xenon the ranges are about $0.3R_H$ and $0.1R_H$ respectively,

where R_H denotes the range in hydrogen. To utilize this method efficiently, when there is a magnetic field in the bubble chamber, it is very handy to have a set of templates for flat stopping μ, π, K, and p tracks of both charges. A set is required for each value of the magnetic field used in the experiment. Since the magnification varies with depth in the chamber, the templates are usually drawn with the right magnification of tracks in the center of the chamber when projected onto the scanning table. Of course, these templates will not fit a dipping track too well. However, after some experience, a scanner can become quite proficient at recognizing the identity of the particle which made the stopping track, and therefore will not need templates.

C. δ-Rays

A δ-ray electron results from the elastic collision between an incident particle and a stationary electron in the bubble-chamber medium. The energy and number of these electrons can be used to identify the incident particle (Crawford, 1957).

Consider an electron mass m_e struck by a particle of mass m. Then the kinetic energy (K_e) of the electron is given by

$$K_e = 2m_e \bar{\gamma}^2 \bar{\beta}^2 \cos^2\theta_e (1 + \bar{\gamma}^2 \bar{\beta}^2 \sin^2\theta_e)^{-1} \qquad (1)$$

where θ_e is the laboratory angle of the electron, and $\bar{\gamma}$ and $\bar{\beta}$ refer to the center-of-mass system. For $m \gg m_e$, we have $\bar{\gamma}\bar{\beta} \approx \gamma\beta$ i.e., the observed values for the incident particle in the laboratory system. Now the mass of the particle is

$$m = p/\gamma\beta \approx p/\bar{\gamma}\bar{\beta}, \qquad (2)$$

where p is the momentum of the incident particle, which can be determined from a curvature measurement. Hence if we determine $\bar{\gamma}\bar{\beta}$ from Eq. (1), we can calculate m from Eq. (2). To find $\bar{\gamma}\bar{\beta}$ we can measure the angle θ_e

and obtain the energy of the electron by range or curvature measurement, or by counting the number of turns made by the electron spiral. However, in practice this method is difficult to use. Measurement of θ_e is usually very inaccurate because the beginning of the δ-ray is obscured by the incident track, and because of multiple scattering of the electron.

Nevertheless, δ-ray counts are very useful in determining contamination in a beam of particles incident on the chamber (see Section IIIA3). This method is based upon a count of the numbers of high-energy δ-rays produced by beam tracks.

We first utilize the fact that the maximum energy in MeV of a δ-ray produced by a particle of momentum p and mass m is

$$K_{e\,max} = 2 m_e \bar{\gamma}^2 \bar{\beta}^2 \simeq 2 m_e \gamma^2 \beta^2 = 2 m_e \left(\frac{p}{m}\right)^2. \qquad (3)$$

Consequently we know that if we have, for example, a separated K beam of momentum p composed of a mixture of K^-, π^-, and μ^-, then the K's cannot make δ-rays of energy greater than $K_{e\,max} = 2 m_e \left(\frac{p}{m_k}\right)^2$. Therefore, if we observe δ-rays with energy greater than $K_{e\,max}$, we know these must have been made by π^-, μ^-, or e^-.

Secondly, the cross section for producing δ-rays greater than some energy K_{min} is given by

$$\sigma(T > T_{min}) = \frac{\pi r_0^2}{(\gamma\beta^2)^2} Z^2 \left(\frac{1}{T_{min}} - 1 - \beta^2 \ell n \frac{1}{T_{min}} \right), \qquad (4)$$

where Z is the charge of the bubble-chamber liquid, $T = K_e/K_{e\,max}$, and $r_0 = e^2/m_e = 2.8 \times 10^{-13}$ cm.

Then for $\bar{\gamma}\bar{\beta} \simeq \gamma\beta$ (i.e., $\gamma\beta$ less than 30 for pions, 100 for kaons, and 180 for protons), we have

$$\sigma(K_e > K_{e\,min}) = \left(\frac{\pi r_0^2}{\beta^2}\right) Z^2 \left(\frac{2m_e}{K_{e\,min}}\right)\left\{1 - \frac{K_{min}}{2m_e\gamma^2\beta^2}\left[1 + \beta^2 \ell n \frac{(2m_e\gamma^2\beta^2)}{K_{e\,min}}\right]\right\}. \quad (5)$$

For $\gamma\beta \gtrsim 1.5$, a good approximation for the cross section in barns is

$$\sigma(K_e > K_{e\,min}) = \frac{\pi r_0^2}{\beta^2} Z^2 \frac{2m_e}{K_{e\,min}} \quad (6)$$

$$= \frac{0.25}{\beta^2 K_{e\,min}} Z^2,$$

where $K_{e\,min}$ is in MeV.

For electron contamination in the beam the formula for $\sigma(T > T_{min})$ should be modified (Nordin, 1958) to

$$\sigma(T > T_{min}) = \frac{4\pi r_0^2}{\gamma}\left[\frac{1}{T_{min}} - \frac{1}{(1-T_{min})} + \frac{1}{2} - T_{min}\right]. \quad (7)$$

From Eqs. (3), (6), and (7), we see that for a particular momentum, heavy particles produce a large number of low momentum δ-rays, whereas light particles produce a smaller number of δ-rays, but these can have much higher momentum. Hence, by observing the number of δ-rays with an energy greater than that possible from K mesons [i.e., $2\,m_e(p/m_k)^2$], we can calculate the contamination of light particles in the K beam.

D. Depth in the Chamber and Dip Angle

The depth of a point on a track can be found easily provided the film planes are all parallel to each other. We will define the depth (z) as being the distance of the point from a fiducial (F) on the inside of the glass window nearest to the camera in a direction parallel to the lens axes. If we

superimpose the three images of the point A at depth z in the chamber, the images of the fiducial mark F will be separated by a distance Δf on the scanning table (as shown in Fig. A2a). Then the depth z is

$$z = \frac{\Delta f \, Kn}{M_f} ,$$

where K, the stereo ratio, is equal to $[L' + (z/n)]/d$, M_f is the magnification of the image on the scanning table at the fiducial plane of the bubble chamber with respect to the original object size, n is the refractive index of the bubble-chamber liquid, L' is the effective optical distance from the camera lens to the fiducial plane, and d is the separation of the camera lenses. Since K varies only slowly, $z \propto \Delta f$ can be used for many purposes. Note that if the fiducial plane is parallel to the film plane, all fiducials will be superimposed at the same time.

To find the dip angle (λ) of a track, consider the two images of the track segment AB, $A' B_1$, and $A' B_2$ on views 1 and 2, respectively, superimposed at A (Fig. A2a). To a good approximation (first-order optics) $B_1 B_2$ is parallel to the stereo axis of views 1 and 2. Then we have

$$\tan\lambda = nK\Delta/S,$$

where Δ is the distance $B_1 B_2$, and S is the plane-projected arc length of AB. Note that S is not the average of lengths $A' B_1$ and $A' B_2$; it is actually the projected arc length which would be observed if the camera lens happened to be directly over A. For small dip angles, using either $A' B_1$ or $A' B_2$ is sufficiently accurate. However for large dip angles, we can use the following method for finding S (Lynch, 1959). When the two images of track segment AB from views 1 and 2 are superimposed at A' (Fig. A2a), the points B_1 and B_2 are distance Δ apart, the direction $B_1 B_2$ being parallel to the stereo axis for lenses 1 and 2. In addition, if there is a third view,

when this is projected and point A superimposed at A', the points $B_1B_2B_3$ will form a mapping of the camera lens axes C_1, C_2, C_3 (Fig. A2b). Consequently, if the track segment AB is in the region of the chamber P with respect to C_1, C_2, and C_3, then the required arc length is from A to point P', where P' $B_1B_2B_3$ form a mapping of $PC_1C_2C_3$. If the tracks are curved, it is usually rather hard to estimate the right curvature of arc A' P', but this will only cause a small error in measuring S.

E. Momentum

If a uniform magnetic field is applied to the bubble chamber and the particle loses no momentum, its trajectory will be a helix of radius R with its axis parallel to the magnetic lines of force. For the momentum P in MeV/c we have

$$P = \frac{0.3\,HR}{\cos\alpha} ,$$

where H is the magnetic field in kilogauss, R is the radius in centimeters, and α is the pitch angle of the helix. If the magnetic field is parallel to the camera axes, α is equal to the dip angle (λ).

For scanning purposes this relation is sufficiently accurate to find the momentum, even though the magnetic field is not usually uniform. The scanners are equipped with circular templates to measure the radius ρ on the scanning table. Usually ρ can be found to a few per cent; the main inaccuracy in P is in the estimation of the dip angle (λ). Since it is impossible to reconstruct the correct arc AP' (Fig. A2b), the best procedure to reduce the effects of conical projection is to measure both the projected arc length (S_n) and the radius of curvature (ρ_n) on view n, where n is the lens that has its axis nearest to the track.

Then we can write

$$P = \frac{0.3HR_n}{\cos(\tan^{-1} K\Delta/S_n)} = \frac{C\,\rho_n}{\cos(\tan^{-1} K\Delta/S_n)} ,$$

where C is approximately constant and can be calculated from the magnification of the scanning projector.

F. Origins of Neutral Particles that Decay to Produce V's

When an experiment involving V's is scanned, great difficulty is often experienced in associating the V's with their appropriate production vertex. A quick method for doing this is shown in Fig. A3 which represents one view of the V projected on the scanning table. The V is formed by the decay of a neutral at A into two particles of momentum P_1 and P_2 at angles θ_1 and θ_2 to the direction of the neutral. Then if we extrapolate (if necessary) the two circles to intersect at B, the origin of the neutral will be somewhere along the line AB.

The proof of this is as follows: it assumes that the camera is directly over the vertex of the V with its axis parallel to the lines of magnetic field and perpendicular to the surface of the scanning table; inhomogeneties in the magnetic field and any momentum loss of the particles are neglected.

The components of the momentum in the surface of the scanning table are

$$P'_1 = C\,\rho_1 \text{ and } P'_2 = C\,\rho_2$$

where ρ_1 and ρ_2 are the radii of curvature of the two tracks on the scanning table. Conservation of transverse momentum gives

$$P'_1 \sin\theta_1 = P'_2 \sin\theta_2$$

or

$$\rho_1 \sin\theta_1 = \rho_2 \sin\theta_2 .$$

This defines the direction of the neutral particle on the surface of the scanning table.

Now, by the construction shown in Fig. A3, we have

$$\text{chord AB} = 2\,\rho_1 \sin\theta_1 = 2\rho_2 \sin\theta_2.$$

Consequently, the neutral direction is along BA. To reduce inaccuracies due to conical projection, the construction should be made on the view whose lens axis is nearest to the V. Of course, since this method depends upon conservation of transverse momentum, it is only applicable for two-body decays of the neutral.

G. Coplanarity

To find out if three tracks are coplanar in the bubble chamber, the simple construction shown in Fig. A4 can be made. Consider the projected images of the two-prong event at A. The images of the arbitrarily chosen points B and C are B_1 and B_2 and C_1 and C_2. Then C_1, C_2, B_1, B_2, and A_1A_2 are parallel to each other and to the stereo axis. The extrapolated image of track 1 intersects B_1C_1 and B_2C_2 at D_1 and D_2, respectively. Then if track 1 is coplanar with tracks 2 and 3, the line D_1D_2 will be parallel to A_1A_2, etc., because D is a real point in space in the plane of 1, 2, and 3. Also we will have

$$\frac{C_1D_1}{D_1B_1} = \frac{C_2D_2}{D_2B_2}.$$

For the special case where track 1 is horizontal in the chamber (i.e., in a plane perpendicular to the camera-lens area) and A_1A_2 are superposed at A, then D_1D_2 will be superposed also at D; consequently AD, B_1C_1, and B_2C_2 will be concurrent at D. This gives a very quick way of finding out if two outgoing tracks are coplanar with an incident beam track, which is usually horizontal. For curved tracks the tangents should be used.

VII. REFERENCES

Adair, R. K. (1955), Phys. Rev. 100, 1540.

Adair, R. K. and Fowler, E. C. (1963), Strange Particles, Interscience Tracts on Physics and Astronomy No. 15 (Interscience, New York).

Alston, M. H., Berge, J. P., Braley, J. E., Campbell, G. H., Harvey, R. J., Hutchinson, M., and Schneider, T. C. (1961), Alvarez Group Memo 358, Lawrence Radiation Laboratory, Berkeley (unpublished).

Alston, M. H., Braley, J. E., Stedman, J., Stevenson, M. L., and White, P. (1963), Alvarez Group Memo 432, Lawrence Radiation Laboratory, Berkeley (unpublished).

Alston, M. H., Braley, J. E., and White, P. (1963), Rev. Sci. Instr. 34, 64.

Alston, M. H. and Penny, S. J. (1964), Alvarez Group Memo P-106, Lawrence Radition Laboratory, Berkeley (unpublished).

Anderson, J. and Laney, H., (1964), Alvarez Group Physics Memo 527, Lawrence Radiation Laboratory, Berkeley (unpublished).

Barkas, W. H. (1961), Phys. Rev. 124, 897.

Beall, E. F., Holley, W., Keefe, D., Kerth, L. T., Thresher, J. J., Wang, C. L., and Wenzel, W. A. (1963) Nucl. Instr. Methods 20, 205.

Berge, J. P. (1959), Alvarez Group Memo 86, Lawrence Radiation Laboratory, Berkeley (unpublished).

Berge, J. P., Solmitz, F. T., and Taft, H. (1961), Rev. Sci. Instr. 32, 538.

Bethe, H. A. (1953), Phys. Rev. 89, 1256.

Biswas, N. N., Derado, I., Gottstein, K., Kenney, V. P., Lucas, D., Lutjens, G., and Schmitz, N. (1963), Nucl. Instr. Methods 20, 135.

Bock, R. (1962), GRIND Manual DD/Exp/62/10, CERN, Geneva (unpublished).

Burren, J. W. and Sparrow, J. (1963) NIRL/R/14, Rutherford High Energy Laboratory, England.

Byers, N. and Fenster, S. (1963) Phys. Rev. Letters 11, 52.

Capps, R. H. (1961) Phys. Rev. 122, 929.

Champomier, L. (1964), Lawrence Radiation Laboratory Report UCRL-11222 (unpublished).

Chew, G. F. and Low, F. E. (1959) Phys. Rev. 113, 1640.

Cook, V., Keefe, D., Kerth, L. T., Murphy, D. G., Wenzel, W. A., and Zipf, T. (1963) Phys. Rev. 129, 2743.

Crawford, F. (1957) Engineering Note M29, UCID-241, Lawrence Radiation Laboratory, Berkeley (unpublished).

Dahl, O. (1963), Alvarez Group Memo P-49, Lawrence Radiation Laboratory, Berkeley (unpublished).

Dahl, O. and Kalbfleisch, G. (1963), Alvarez Group Memo P-54, Lawrence Radiation Laboratory, Berkeley (unpublished).

Dalitz, R. H. (1963), Ann. Rev. Nucl. Sci. 13, 339

Fabian, B. N., Place, R. L., Riley, W. A., Sims, W. H., and Kenney, V. P. (1963), Rev. Sci. Instr. 34, 484.

Feinberg, G. and Lederman, L. M. (1963), Ann. Rev. Nucl. Sci. 13, 431.

Ferro-Luzzi, M., Solmitz, F. T., and Stevenson, M. L. (1962) Proceedings of the 1962 International Conference on High Energy Physics at CERN, (CERN, Geneva) 376.

Gatto, R. and Stapp, H. P. (1961) Phys. Rev. 121, 1553.

Gluckstein, R. L. (1963), Nucl. Instr. Methods 24, 381.

Guild, J. (1960), Diffraction Gratings as Measuring Scales (Oxford University Press, New York).

Goldschmidt-Clermont, Y. (1964), rapporteur's talk given at the International Conference on High-Energy Physics, Dubna (to be published).

Hahn, B., Hugentoller, E., Steinrisser, F. (1961), Proceedings of the International Conference on Instrumentation for High Energy Physics (Interscience,New York) p. 143.

Hardware, spark-chamber scanning:

(1) Burleson, G. R., Deshong, J. A., Hoang, T. F., Kalmus, P. I. P., Kushowski, R. L., Niemela, L. Q., Roberts, A., Romanowski, T. A., Warshaw, S. D., Yurka, G. E. (1963), Nucl. Instr. Methods 20, 448.

(2) Hodges, J. C., Keefe, D., Kerth, L. T., Thresher, J. J. and Wenzel, W. A. (1962) Lawrence Radiation Laboratory Report UCRL-10251.

(3) Macleod, G. R. (1963), Nucl. Instr. Methods 20, 367.

Harvey, R. J. (1962), Alvarez Group Memo 404, Lawrence Radiation Laboratory, Berkeley (unpublished).

Humphrey, W. E., (1959) Alvarez Group Memos 111 and 115, Lawrence Radiation Laboratory, Berkeley (unpublished).

Humphrey, W. E. (1962) Alvarez Group Memo P-6, Lawrence Radiation Laboratory, Berkeley (unpublished).

International Conference on Fundamental Aspects of Weak Interactions, Proceedings (1963), BNL 837 (C-39) (Brookhaven National Laboratory, Upton, Long Island).

Informal Meeting on Track Data Processing, CERN, Geneva, Proceedings (1962), (CERN, Geneva).

International Meeting on Instruments for the Evaluation of Photographs, Proceedings (1958) CERN Report 58-24.

International Conference on High Energy Accelerators and Instrumentation, Proceedings (1959), (CERN, Geneva) pp. 521-557.

International Conference on Instrumentation for High-Energy Physics, Proceedings (Lawrence Radiation Laboratory, Berkeley), pp. 223-265.

Instrumentation for High Energy Physics (1963), Nucl. Instr. Methods 20, 367.

Johnson, D. (1961), Alvarez Group Memo 271, Lawrence Radiation Laboratory, Berkeley (unpublished).

Johnson, D. (1962), Alvarez Group Memo P-5, Lawrence Radiation Laboratory, Berkeley (unpublished).

Lynch, G. (1959) Alvarez Group Memo 135, Lawrence Radiation Laboratory, Berkeley (unpublished).

Lynch, G. (1963) Alvarez Group Memo P-24, Lawrence Radiation Laboratory, Berkeley (unpublished).

Lynch, G., Safier, F., and Noony, G., (1962) Lawrence Radiation Laboratory Report UCRL-10335 (unpublished).

Moorhead, A. (1960), CERN Report 60-33 (unpublished).

Nordin, P. (1959), Lawrence Radiation Laboratory Engineering Note LA-14, UCID-147 (unpublished).

Penny, S. (1962), Alvarez Group Memo P-8, Lawrence Radiation Laboratory (unpublished).

Puppi, G. (1963), Ann. Rev. Nucl. Sci. 13, 287.

Rosenfeld, A. H., Editor (1961), Lawrence Radiation Laboratory Report UCRL-9099 (unpublished).

Rosenfeld, A. H. (1963), Nucl. Instr. Methods 20, 422.

Rosenfeld, A. H. and Snyder, J. N. (1962), Rev. Sci. Instr. 33, 181.

Rosenfeld, A. H. (1963), "Strongly Interacting Particles and Resonances," in Proceedings of the Sienna International Conference on Elementary Particles (Societa Italiana di Fisica, Bologna).

Rosenfeld, A. H. and Humphrey, W. E. (1963), Ann. Rev. Nucl. Sci. 13, 103.

Solmitz, F. (1960), "Helix Fit to Track Images," Ecole Polytechnique, Paris (unpublished).

Solmitz, F. T. (1964), Ann. Rev. Nucl. Sci. 14, 375.

Thorndike, A. T. (1958), BNL Bubble Chamber Group Memo F-3, Brookhaven National Laboratory (unpublished).

Treiman, S. B. and Yang, C. N. (1962), Phys. Rev. Letters 8, 140.

Welford, W. T. (1963), Appl. Opt. 2, 981.

White, H. S. (1961), Lawrence Radiation Laboratory Report UCRL-9475, (unpublished).

White, H. S., Editor (1961), UCID-1340, Lawrence Radiation Laboratory, Berkeley (unpublished).

White, H. S., Buckman, S., Hall, D. E., Hurwitz, E., Meissner, L. B., Smith, J. C., and Stannard, F. R. (1960), Lawrence Radiation Laboratory Report UCRL-9457 (unpublished).

Wojcicki, S. (1964), Phys. Rev. 135, B484.

Zarian, H. (1962) Alvarez Group Memo 214, Lawrence Radiation Laboratory, Berkeley (unpublished).

VIII. FOOTNOTES

1. This is a plot used by the Navy for navigation and depicts the lines of longitude and latitude projected onto the polar plane passing through Greenwich. A track is represented by a point plotted at its azimuthal (latitude) and dip (longitude) angles. Spatial angles are obtained by measurement along the great cicle joining the points. Coplanarity is exhibited by points lying on the same great circle.

2. International Business Machines, San Jose, California, and Itek Corporation, Lexington, Massachusetts.

3. Sources in the United States include Itek Corporation, Lexington, Massachusetts; Nuclear Research Instruments, Berkeley, California; Micrometric Corporation, Berkeley, California; Recordak Corporation (Eastman Kodak), New York, N. Y.; and Vanguard Instrument Corporation, Roosevelt, Long Island, N. Y. In Europe, sources include Beds and Herts, Drawing Services Limited, Luton, Beds, England; Ferranti Ltd., Edinburgh, Scotland; Koristka, Milano, Italy; Prevost, Milano, Italy; Sogenigue, Ltd., Newport Pagnell, Bucks, England; and Societe d' Optique et Mecanique, Paris, France.

Table I. Survey of a Sample of Bubble Chamber Groups

Group	BNL	CERN	University of Chicago	Columbia University	Florida State University	University of Wisconsin	University of Maryland	University of Padova	Rutherford Laboratory	University of Turin	UCLA	LRL Berkeley (Alvarez)	LRL Berkeley (Powell-Birge) (Trilling-Goldhaber)	Yale
People														
Physicists	20	54	4	5	2	11	9	15	6	10	4	21	13	7
Grad. students[a]	0	4-1/2	4	7	6	32	8	4	0	5	5	21	17	6
Programmers	6	3	2	2	1/2	5	1	4	5	0	1/2	20	6	1
Engineers	2	4	1	1/2	0	0	0	5	1	0	0	4	2	0
Scanners (FTE)	21	69	26	16	2-1/2	66	10	20	4	12	4	65	45	20
Maintenance Technicians	12	6	1	2	1/10	5-1/2	2	3	1	--	1	18	6	2
Machines														
Scanning projector	14	7	12	4	2	20	15	10	5	4	--	14	11	4
Measuring projector	6	12	2	3	1	8	6	6	2	2	3	9[c]	6	3
Performance (rates/year)														
Pictures scanned ($\times 10^6$)	--	2	--	1	--	2	--	--	--	--	--	1	1	--
Events recorded ($\times 10^3$)	40	--	150	25	50	400	30	100	100	--	--	220	125	100
Events[b] measurements ($\times 10^3$)	40	52	100	20	15	150	10	20	10	4	4	300[d]	75[e]	50

Table I. continued

a. Part time.

b. Includes remeasurements.

c. Includes four MP-II Franckensteins (described in this chapter) and five SMP's (described in Chapter IX).

d. Includes SMP measurements.

e. Does not include measurements made by FSD (flying spot digitizer) described in Chapter IX.

Table II. Computer Usage for Alvarez Group, Berkeley

Program	Approximate utilization (% or hr/wk) (7090)[a]	Time per new measurement (7090[b] secs)	Time for 1 pass per meas. (7090 sec)
PANAL (Prepackage formatting)	5	3	3
PACKAGE (Track reconstruction and kinematics)	20	12	7
WRING (Postpackage formatting)	5	3	1
EXAMIN, AFREET, DST-EXAM (Interpretation of events and physics calculations)	15	9	3
SUMX (Histograms, plots, etc.)	5	3	< 1
Merge-Select (Tape manipulation)	10	6	--
LINGO, LYRIC (Library)	15	9	--
Miscellaneous (Minimizing, Monte Carlo, phase space, etc.)	10	6	--
Programming (Debug, etc.)	15	9	--
Totals	100 hr/wk	60 sec per meas.	15 sec per meas.

a. Total time used per week is 100 hours of 7090 equivalent time. The computers actually used are two 7094's and a 7044.

b. Assuming 6000 new event measurements are added per week.

Table III. Cost of Data Analysis for Alvarez Group, Berkeley

Item	Approximate cost/yr (k$)	Approximate cost/event measurement ($) [e]	Approximate cost/useful event ($) [f]
Direct costs			
Salaries for Scanning Technicians and key-punch Operators (68 FTE at 10 k$)[a]	680		
Maintenance (including salaries for maintenance technicians and engineers)[a]	325		
Computation (100 hr/wk at 85/hr)[b]	425		
Computer for SMP (rent)	100		
Salaries for programmers[a] (20 at 20 k$)	400		
Subtotal	1930	6.45	9.65
Depreciation of equipment			
	Capital cost[c] (k$)	Depreciation[d] per year (k$)	
4 MP-II Franckensteins at 150 k$ each	600	150	
14 scanning projectors at 15 k$ each	210	50	
5 SMP's at 40 k$ each	200	50	
Subtotal	1010	250	0.85 1.25
Total	1010	2180	7.30g 10.90

Table III continued

a. Salaries includes overhead at about 100%.

b. Recharge rate to physics groups; commercial rate is about $300 to $500/hr.

c. Capital cost of equipment does not include development.

d. Depreciation calculated over a four-year period (i.e., 25% of capital cost per year).

e. The current rate is 300,000 event measurements/year.

f. The useful number of events is taken to be 200,000/yr. The difference between the cost per event measurement and that per useful event is due to remeasurements and events that are unacceptable for some reason (e.g., outside fiducial volume).

g. Does not include salaries for physicists and graduate students because much of their time is spend teaching, planning, and setting up experiments, etc. The time spent by physicists and graduate students on data analysis will add 1.00 to 1.50$ to the cost of an event measurement.

FIGURE LEGENDS

Fig. 1. Angular distribution in the center of mass of the reaction $K^- + p \rightarrow \bar{K}^0 + n$ at 1.22 GeV/c incident K^- momentum (1895-MeV c.m. energy). The dashed histogram represents the angular distribution of the events for which the $\bar{K}^0$ was greater than 5 mm (500 events). The curve is a fit to the data up to the sixth power of $\cos\theta$ (Ferro-Luzzi et al., 1962).

Fig. 2. Dalitz plot for the reaction $K^- + p \rightarrow \bar{K}^0 + p + \pi^-$ for the events defined by $1.45\ \text{BeV}/c < P_{K^-} < 1.55\ \text{BeV}/c$. The envelopes correspond to incoming momenta of 1.45 and 1.55 BeV/c (Wojcicki, 1964). This plot shows the existence of a K^* (K-π resonance) with a mass of 890 MeV ($M^2 = 0.79\ \text{BeV}^2$).

Fig. 3. A typical picture from the 72-in. hydrogen bubble chamber at Berkeley and the corresponding entries on a scan sheet. Three events are recorded: (1) A type 32 (2-prong and associated V), (2) type 22 (2-prong), (3) type 82 (a Σ^+ production and decay).

Fig. 4. Normal flow of data through the Alvarez group data-analysis system (not including the library system). PANAL and WRING are essentially library routines, since they only condense and reorganize data.

Fig. 5. Flow diagram of the PACKAGE program. The PANG part of the program performs stereo reconstruction of each track; KICK makes a kinematic analysis at each vertex in an event. The PANG and KICK event types are rewritten for each experiment, but the remainder of the program is unchanged.

Fig. 6. Flow diagram for the library system, LINGO, and other programs of the Alvarez group. The division between the library functions and the rest of the system is indicated by the dotted line (Rosenfeld, 1963).

Fig. 7. FOG-CLOUDY-FAIR system used for Franckenstein measurements (White 1960).

Fig. 8. Overall flow diagram for the QUEST program. The left-hand part of the diagram represents PACKAGE, and the right-hand part is routines that have been written to control the progress of the event through the processing (Alston et al., 1963).

Fig. 9. Scanning Projector 4A designed and built at the Lawrence Radiation Laboratory at Berkeley and used by the Alvarez Physics Group for scanning film from the 72-in. hydrogen bubble chamber.

Fig. 10. Scanning Projector 5A designed and built at the Lawrence Radiation Laboratory at Berkeley and used by the Trilling-Goldhaber, Powell-Birge, and Segrè-Chamberlain Physics Groups for scanning bubble-chamber film from many laboratories.

Fig. 11. Scanning tables designed and built at the Brookhaven National Laboratory.

Fig. 12. Scanning table used at the CERN laboratory in Geneva for scanning film from the CERN 80-cm hydrogen bubble chamber.

Fig. 13. Overall view of the Franckenstein measuring projector IE, designed and built at the Lawrence Radiation Laboratory at Berkeley, shown with film from the Berkeley 72-in. hydrogen bubble chamber (all three views on one film) mounted on the center-reel drive of the three-roll film transport.

Fig. 14. Control console of measuring projector IE. The indicative data panel is mounted on the desk to the right. Data are output by the card punch on the left.

Fig. 15. Optomechanical schematics of the Franckenstein measuring projector IE.

Fig. 16. Typical track and marker signals as displayed on the cathode-ray-tube monitor mounted at the lower edge of the projection screen of Franckenstein measuring projector IE.

Fig. 17. Schematic representation of the scanning disk that generates the track and marker signals. This disk is part of the detecting head (see Fig. 15).

Fig. 18. Electronic schematic diagram of the operator controls and automatic centering and tracking circuits of the Franckenstein measuring projector IE.

Fig. 19. Franckenstein measuring projector IID, designed and built at the Lawrence Radiation Laboratory at Berkeley. Machines of this type are used by the Alvarez Physics Group for measuring film from the 72-in. hydrogen bubble chamber.

Fig. 20. Schematic diagrams of image-plane digitizers. (a) Scheme for measuring coordinates of a point (P) in x and y using linear encoders. (b) Scheme for measuring coordinates of a point (P) by measuring two angles (θ_1, θ_2). The two lengths (r_1, r_2) are constant. (c) Scheme for measuring coordinates of a point (P) by measuring distances (r_1, r_2) from each of two origins (O_1, O_2).

Fig. 21. Schematic representation of the use of a mirror behind a parallel-plate spark chamber to achieve small-angle stereo.

Fig. 22. Photograph of a cylindrical chamber with a segmented mirror for stereo recording. The mirror is at the left.

Fig. 23. An illustration of the technique of multiple reflections for recording the depth of sparks in semicylindrical spark chambers.

Fig. 24. A spherical field lens used to optically place the camera at infinity.

Fig. A1. Range-momentum curves for liquid hydrogen. Liquid hydrogen conditions: $T = 27.6 \pm 0.1\ ^{\circ}K$; $P = 48.5 \pm 5$ psia; $p = (5.86 \pm 0.6) \times 10^{-2}\ g/cm^3$. (Curves by Glenwood Clark and William Diehl, Lawrence Radiation Laboratory Report UCRL-2426 (rev) Vol. II, 1957.

Fig. A2. (a) Diagram of the three images of a track AB projected onto a scanning table such that the three images are superimposed at A'. F_1, F_2, F_3 are the images of a fiducial on the top glass of the chambers. (b) Plan view showing the relative positions of the camera axes C_1, C_2, and C_3 and the point B in the chamber.

Fig. A3. Construction for determining the possible origin of V's.

Fig. A4. Construction for finding if three tracks are coplanar.

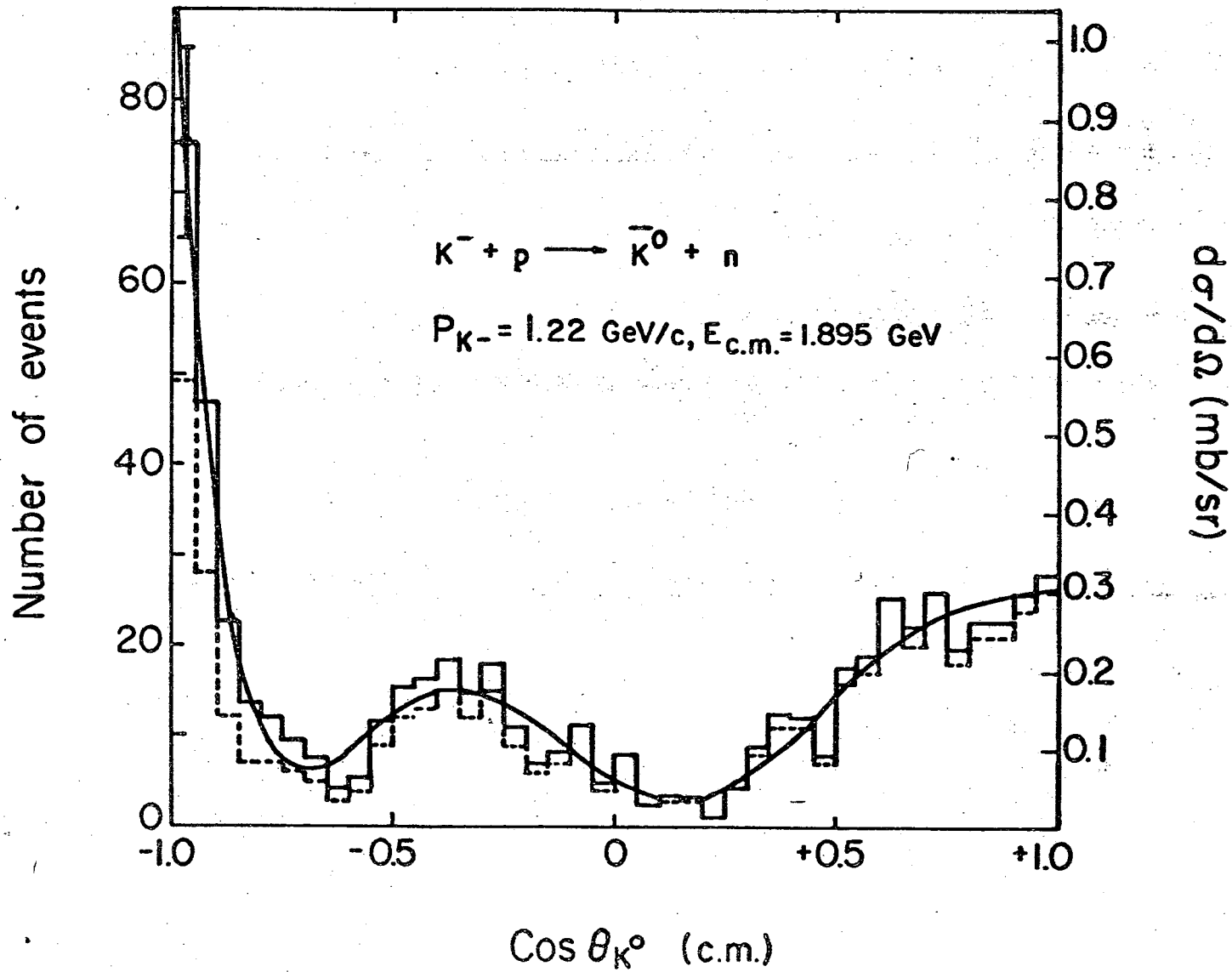

MU-26917

Fig. 1

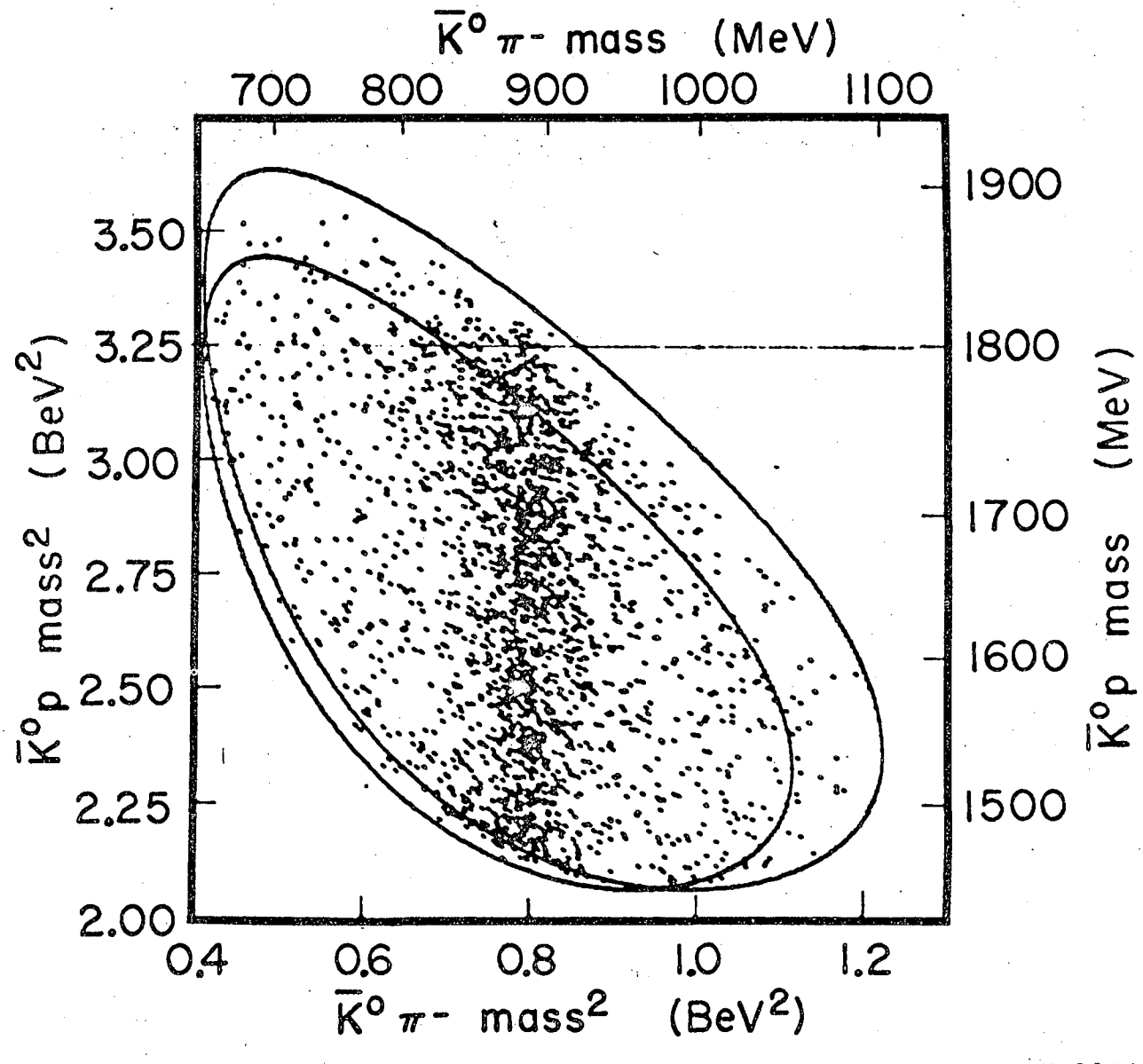
$\bar{K}^0\pi^-$ mass (MeV)
700
800
900
1000
1100
3.50
3.25
3.00
2.75
2.50
2.25
2.00
$\bar{K}^0p$ mass^2 (BeV^2)
1900
1800
1700
1600
1500
$\bar{K}^0p$ mass (MeV)
0.4
0.6
0.8
1.0
1.2
$\bar{K}^0\pi^-$ mass^2 (BeV^2)
MU-32464

Fig. 2

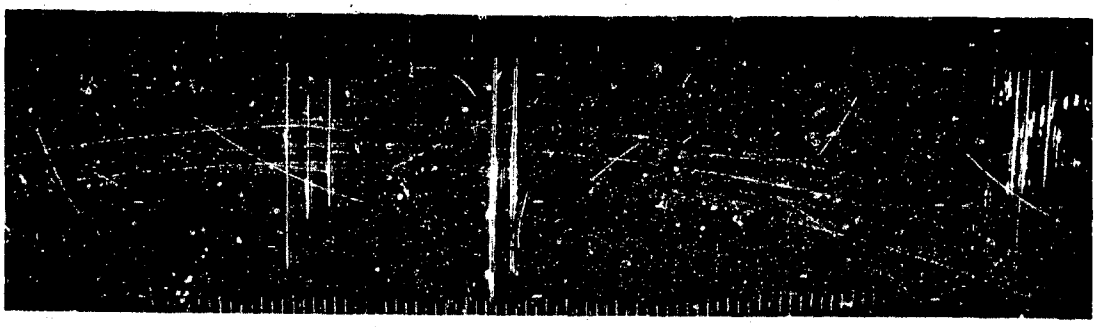

SCAN SHEET

Roll #	Frame #	Scan #	Beam Track	Exp. #	Interpretation	Year	Vertices	Month	Primary Event Type	1st Vertex X	1st Vertex Y	1st Vertex P_1	1st Vertex P_2	Day		2nd Vertex X	2nd Vertex Y	2nd Vertex P_1	2nd Vertex P_2	Scanner		3rd Vertex X	3rd Vertex Y	3rd Vertex P_1	3rd Vertex P_2
1 2 3 4	5 6 7	8	9 10	11 12	13 14 15		16	17 18	19 20 21	22	23 24	25	26	27 28	29 30 31	32	33 34	35	36	37 38 39	40 41 42	43	44 45	46	47
3358		1		07	165			01						04						046					
	496		01				2		032	D	10					D	135								
			02				1		022	E	14														
			03				2		082	E	24					E	24								

ZN-4669

Fig. 3.

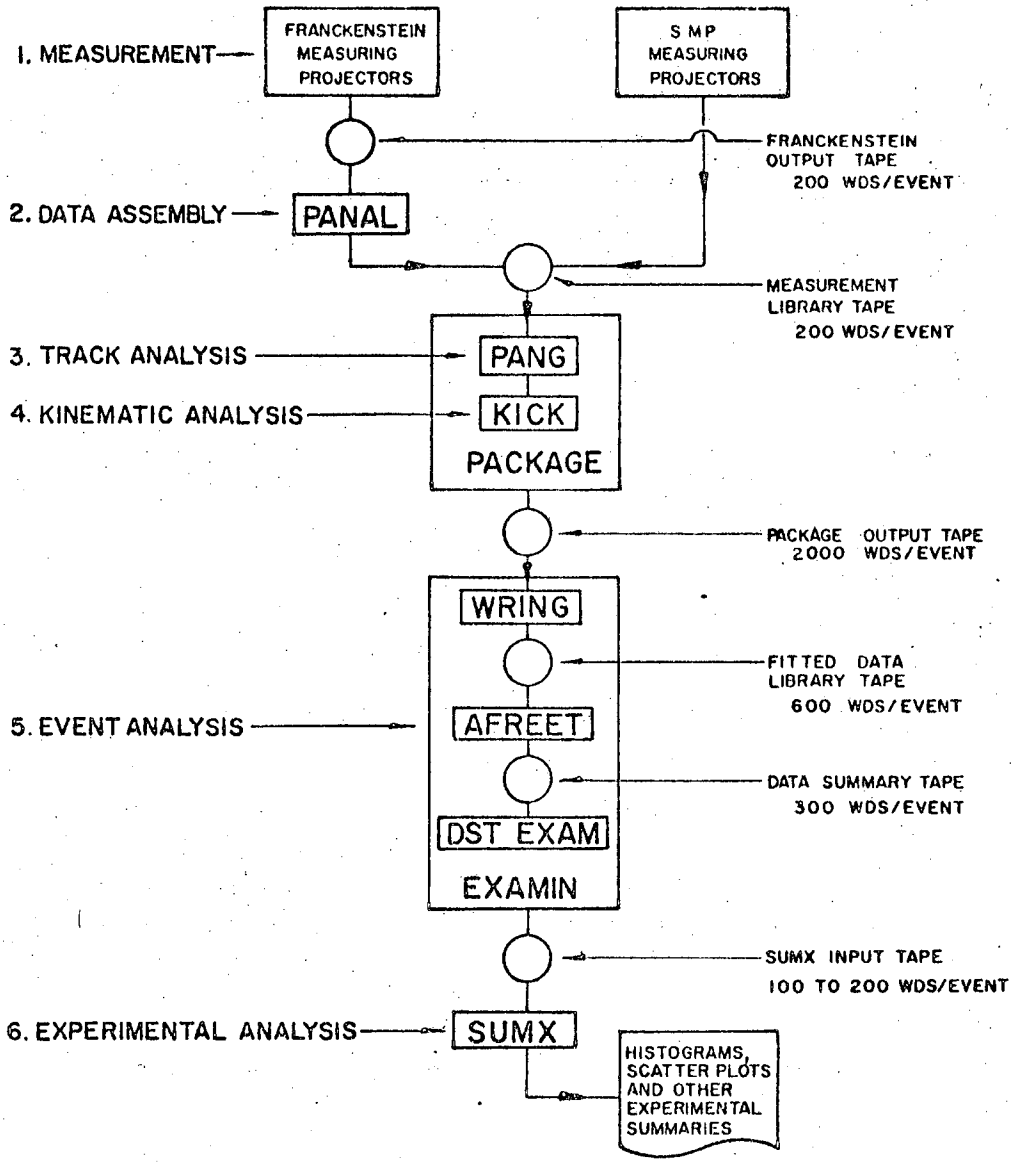

MUB-5152

Fig. 4

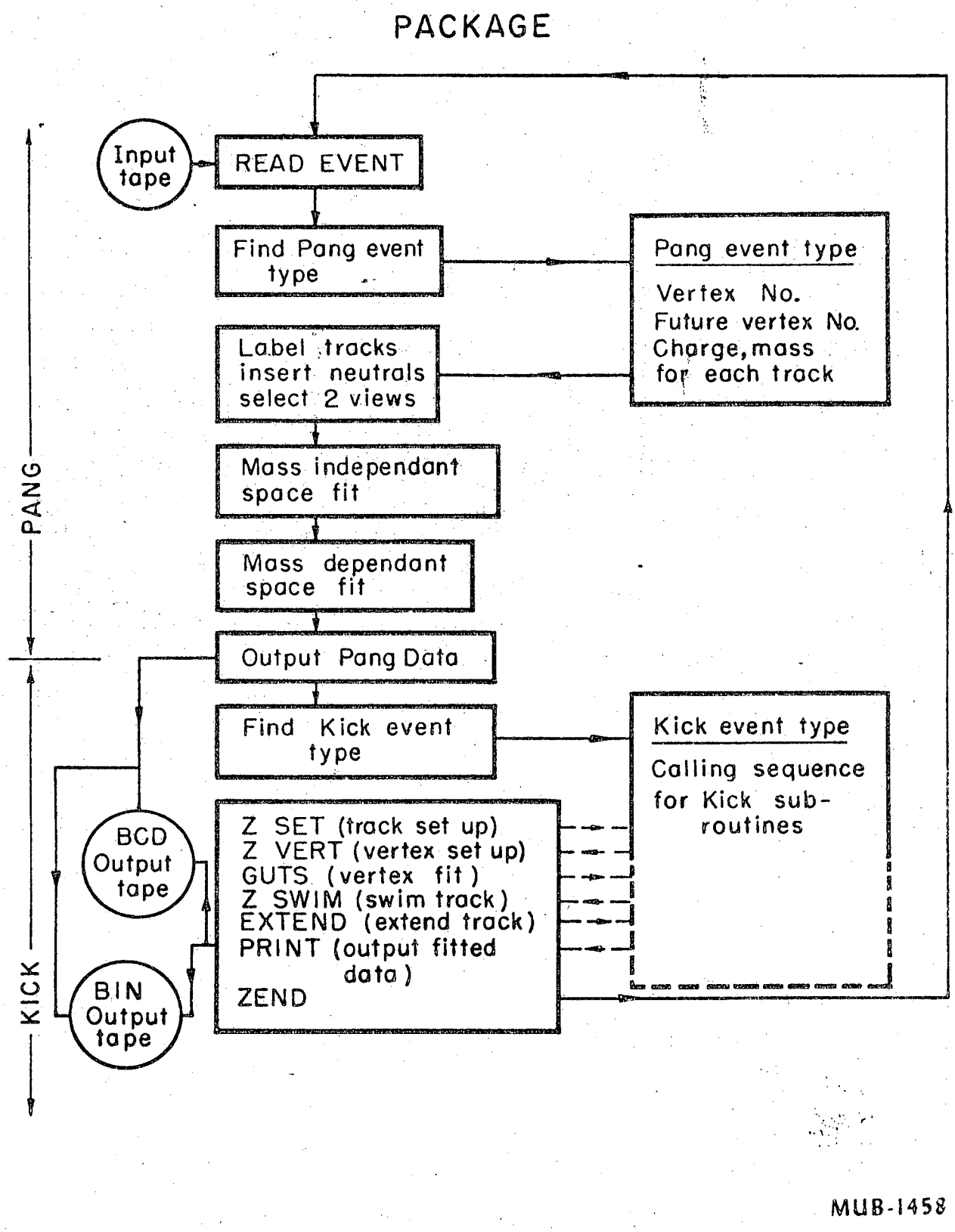
PACKAGE
Input tape
READ EVENT
Find Pang event type
Pang event type
Vertex No.
Future vertex No.
Charge, mass for each track
Label tracks insert neutrals select 2 views
Mass independant space fit
Mass dependant space fit
Output Pang Data
Find Kick event type
Kick event type
Calling sequence for Kick sub-routines
BCD Output tape
BIN Output tape
Z SET (track set up)
Z VERT (vertex set up)
GUTS (vertex fit)
Z SWIM (swim track)
EXTEND (extend track)
PRINT (output fitted data)
ZEND
PANG
KICK
MUB-1458

Fig. 5

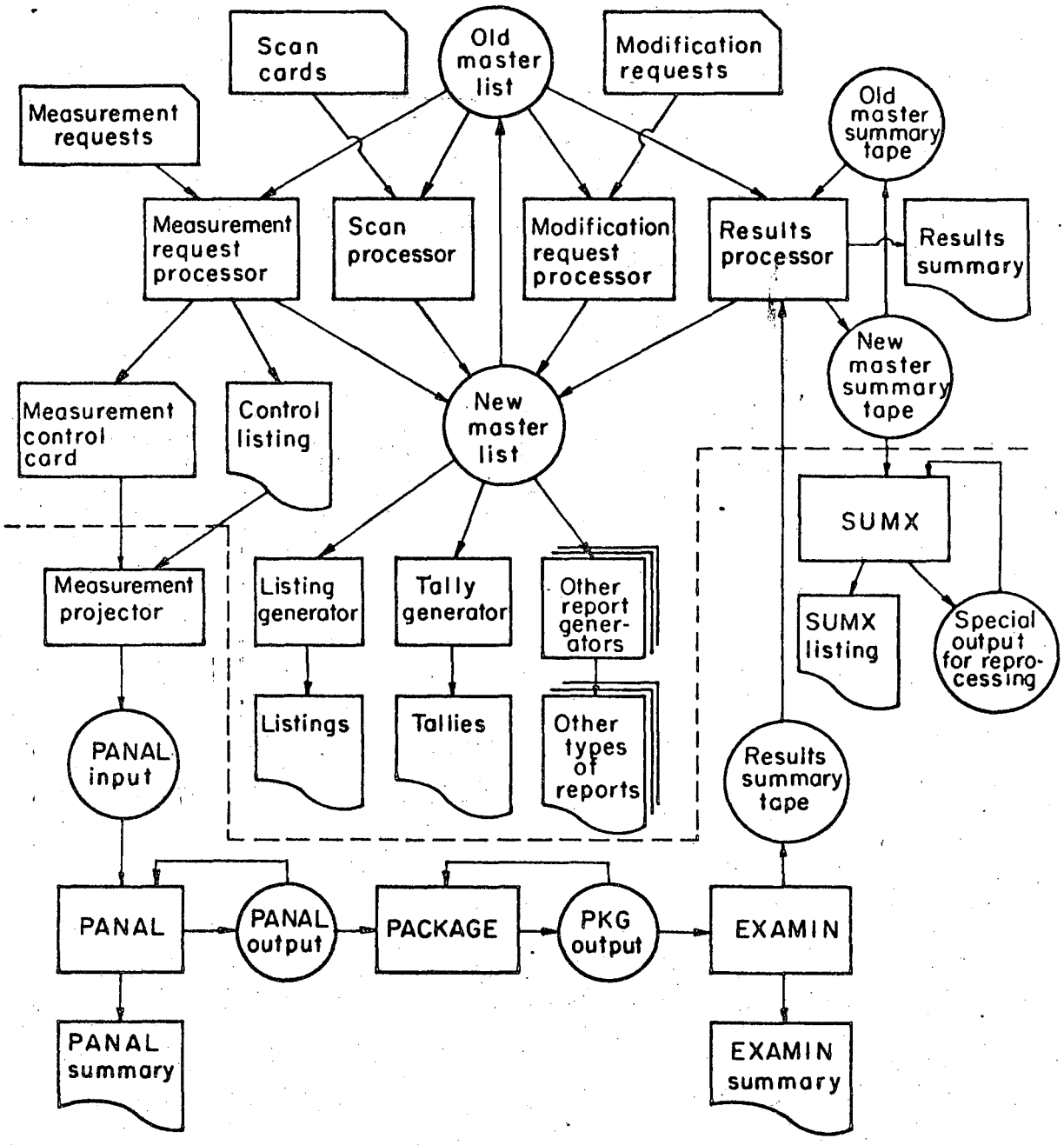
Scan cards
Old master list
Modification requests
Measurement requests
Old master summary tape
Measurement request processor
Scan processor
Modification request processor
Results processor
Results summary
New master summary tape
Measurement control card
Control listing
New master list
SUMX
Measurement projector
Listing generator
Tally generator
Other report generators
SUMX listing
Special output for reprocessing
PANAL input
Listings
Tallies
Other types of reports
Results summary tape
PANAL
PANAL output
PACKAGE
PKG output
EXAMIN
PANAL summary
EXAMIN summary
MU-27262

Fig. 6

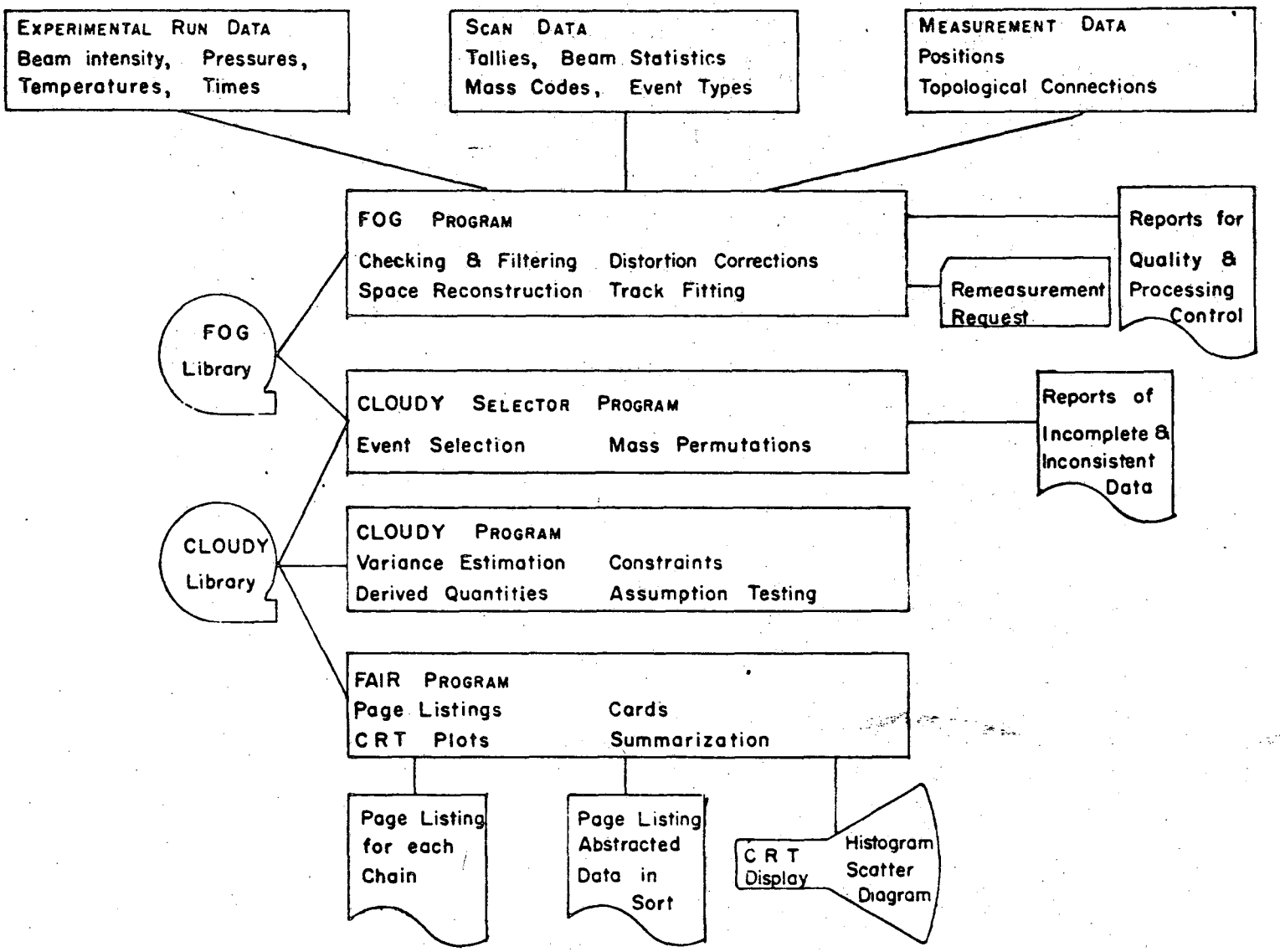

MU-21159

Fig. 7

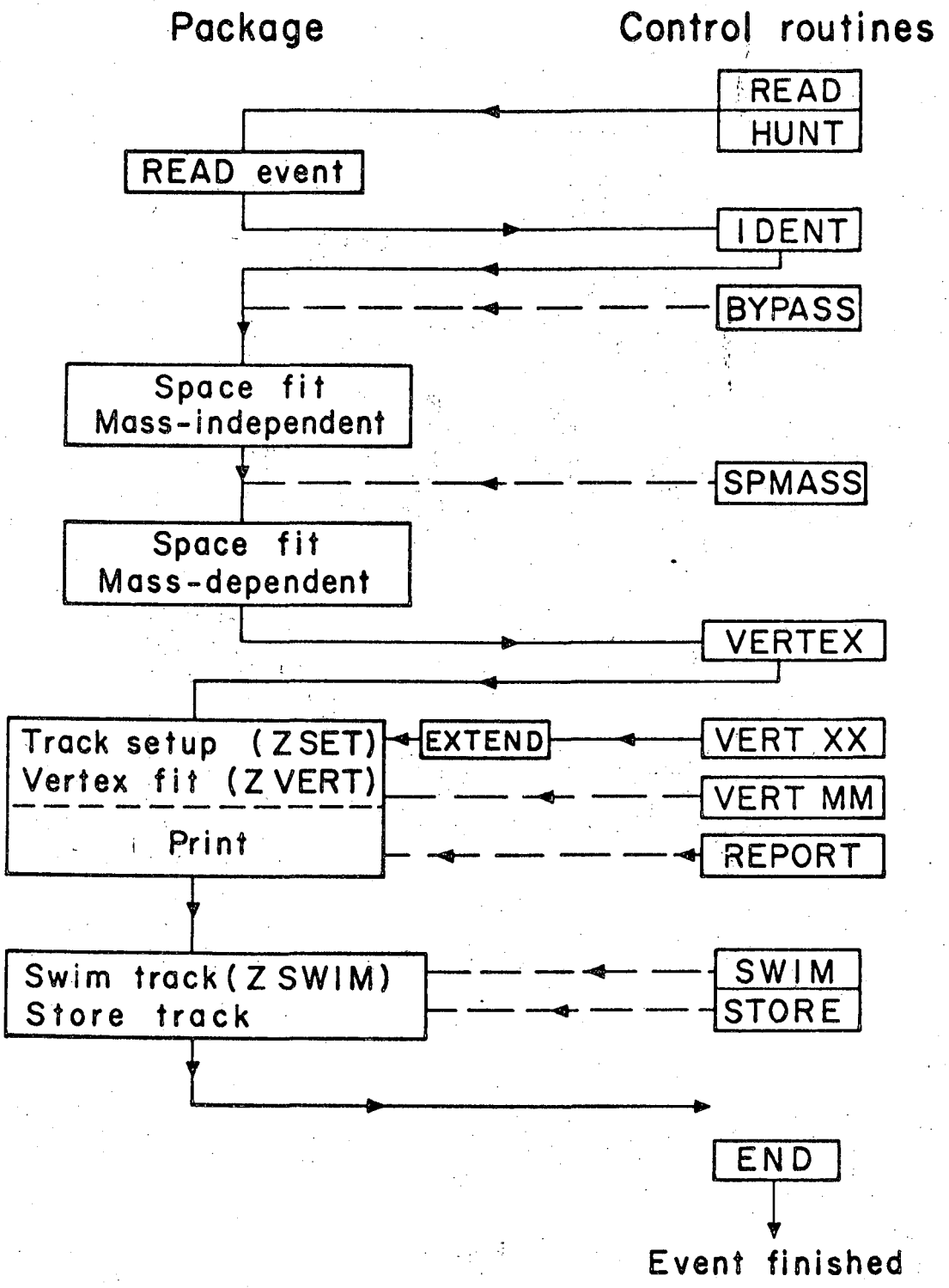
Package
Control routines
READ
HUNT
READ event
IDENT
BYPASS
Space fit
Mass-independent
SPMASS
Space fit
Mass-dependent
VERTEX
Track setup (ZSET)
Vertex fit (ZVERT)
Print
EXTEND
VERT XX
VERT MM
REPORT
Swim track (ZSWIM)
Store track
SWIM
STORE
END
Event finished
MU-27949

Fig. 8

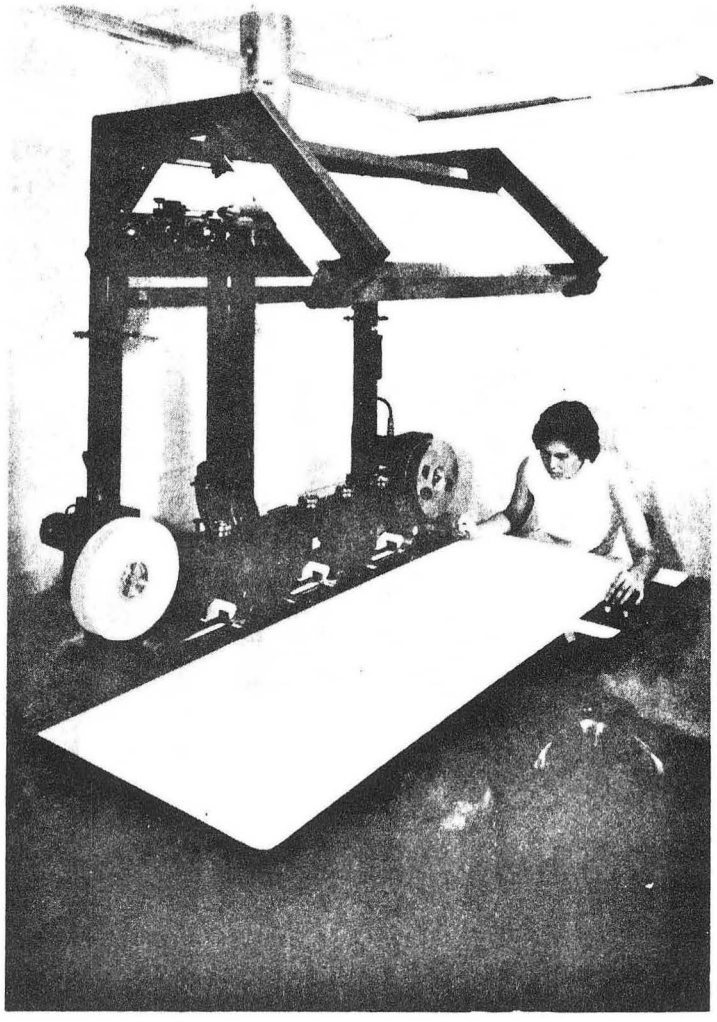

ZN-4670

Fig. 9

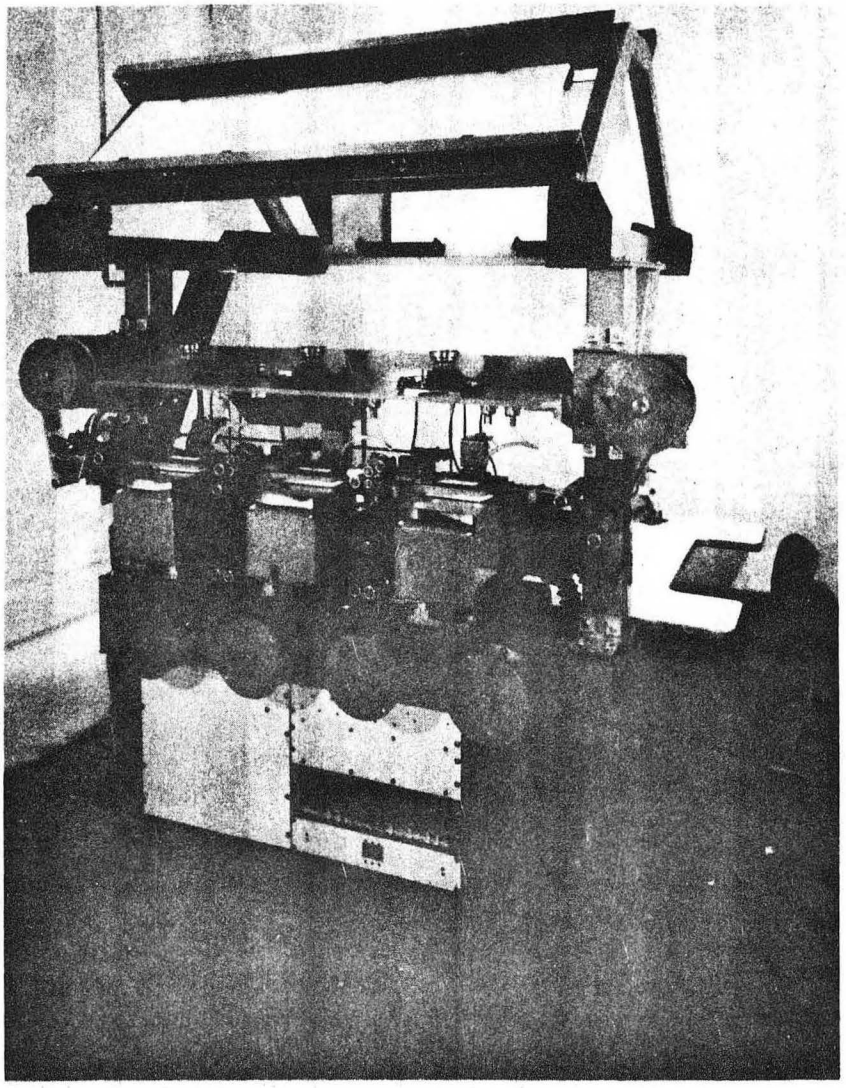

ZN-4674

Fig. 10

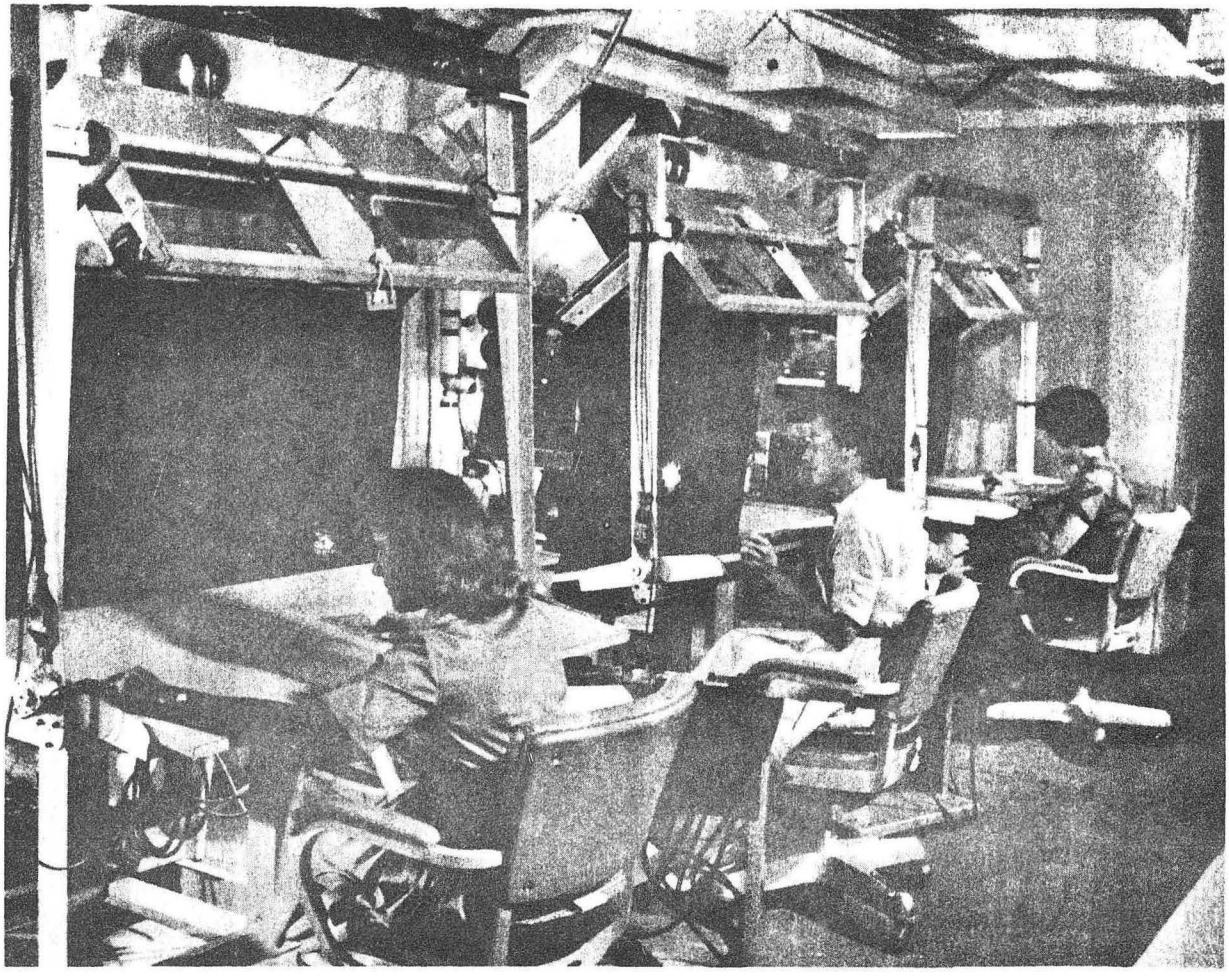

ZN-4675

Fig. 11

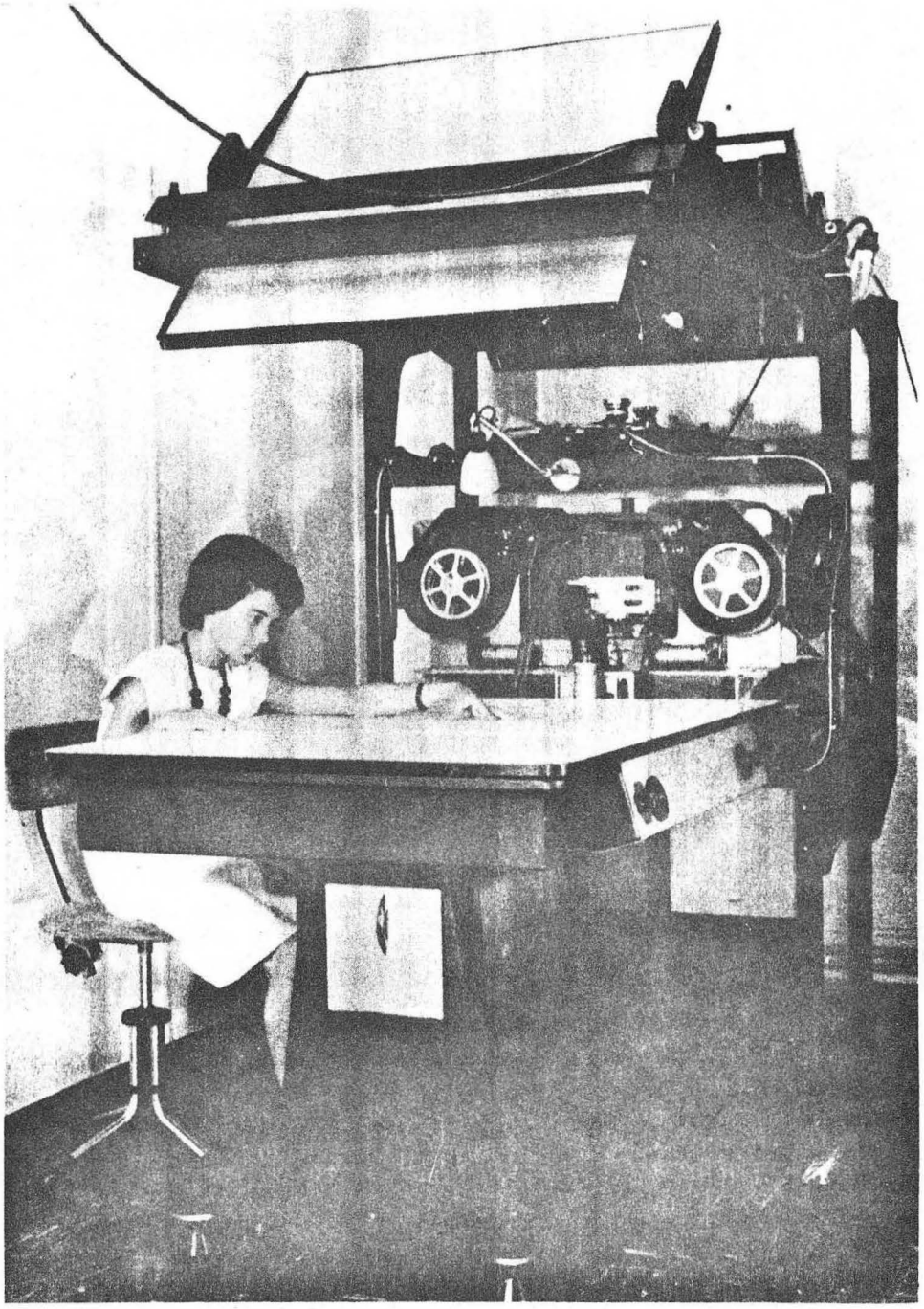

ZN-4676

Fig. 12

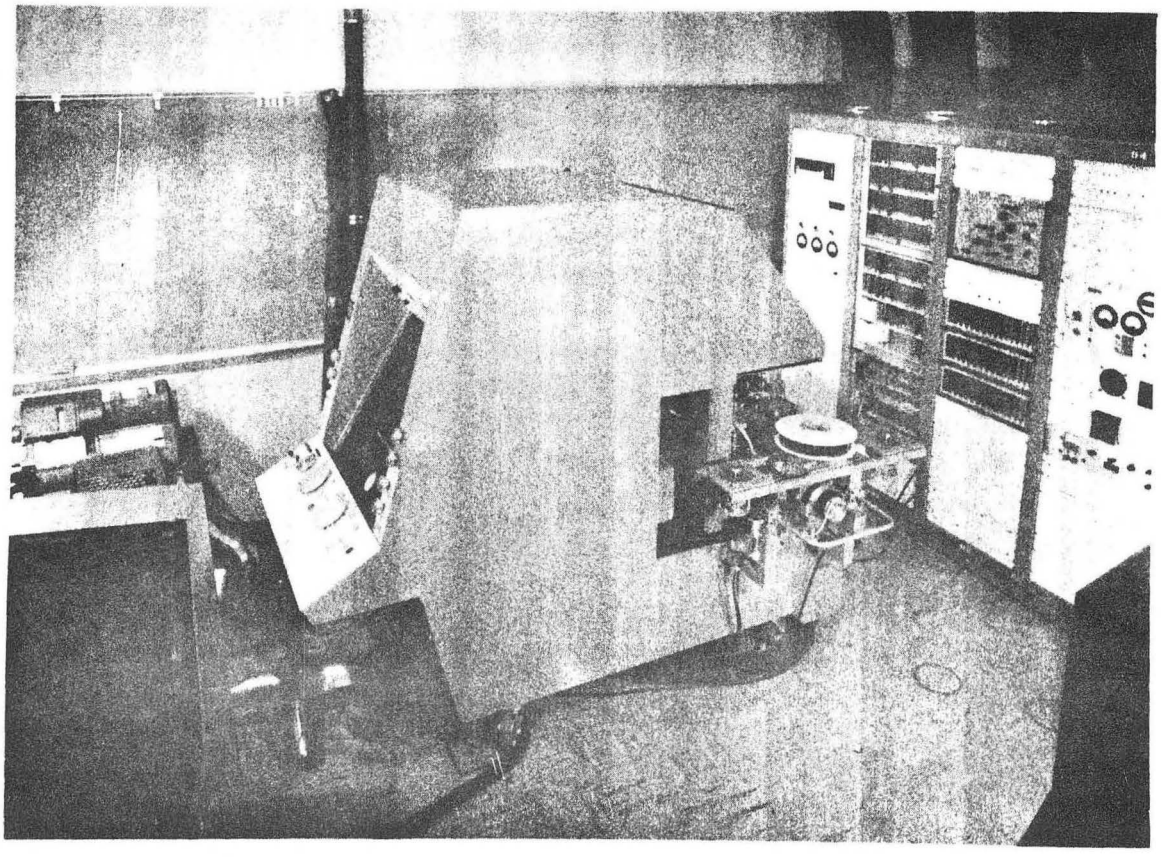

ZN-4671

Fig. 13

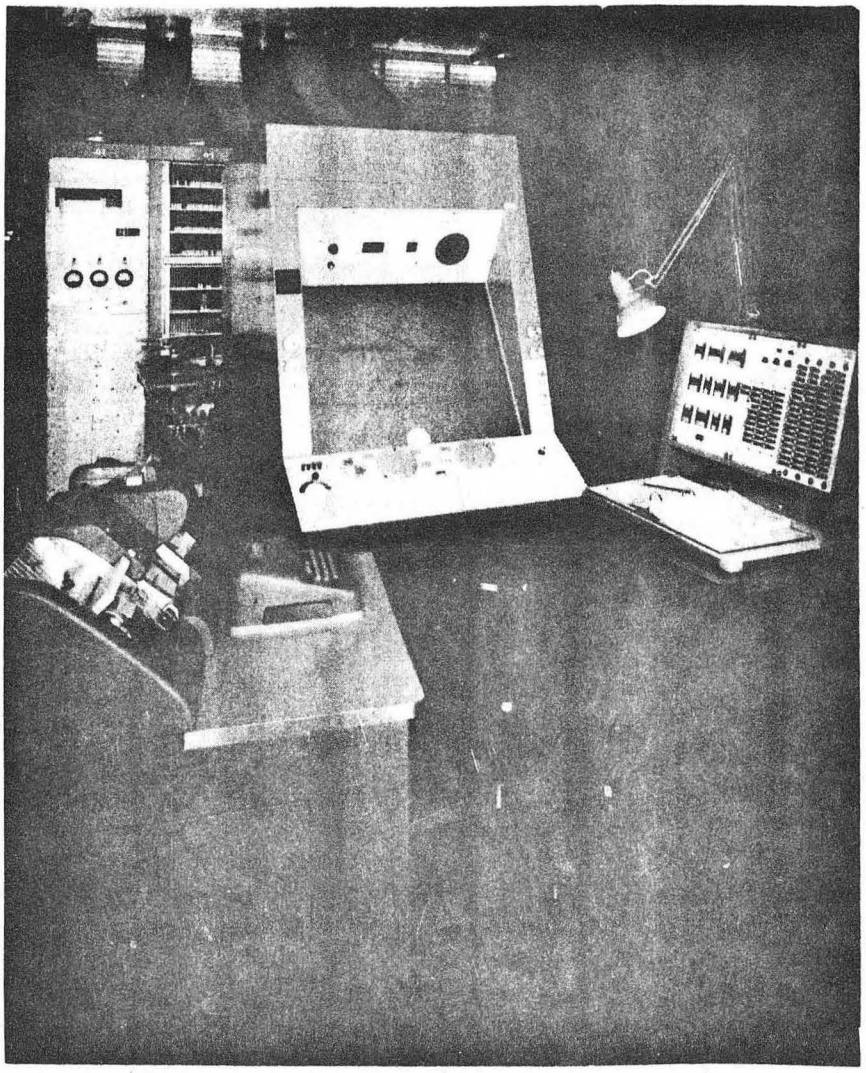

ZN-4672

Fig. 14

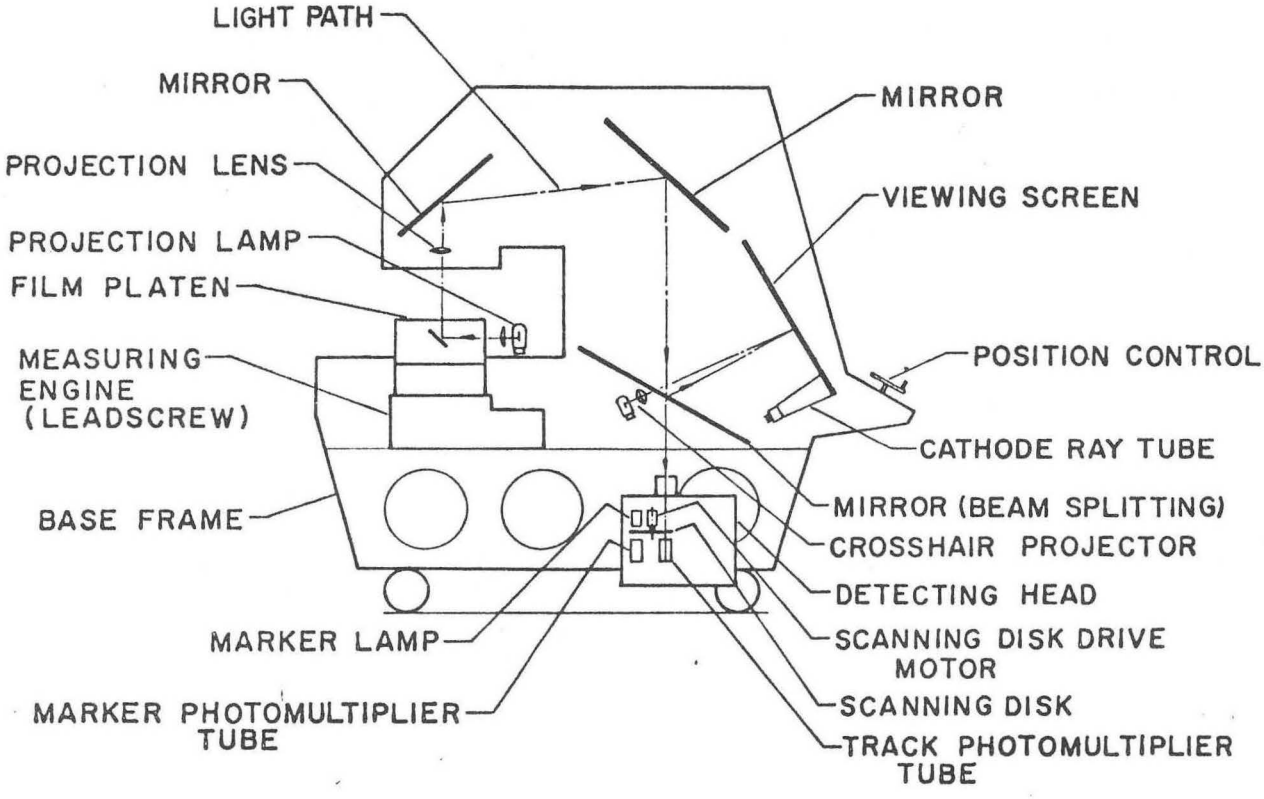
LIGHT PATH
MIRROR
PROJECTION LENS
PROJECTION LAMP
FILM PLATEN
MEASURING ENGINE (LEADSCREW)
BASE FRAME
MARKER LAMP
MARKER PHOTOMULTIPLIER TUBE
MIRROR
VIEWING SCREEN
POSITION CONTROL
CATHODE RAY TUBE
MIRROR (BEAM SPLITTING)
CROSSHAIR PROJECTOR
DETECTING HEAD
SCANNING DISK DRIVE MOTOR
SCANNING DISK
TRACK PHOTOMULTIPLIER TUBE
MUB-5153

Fig. 15

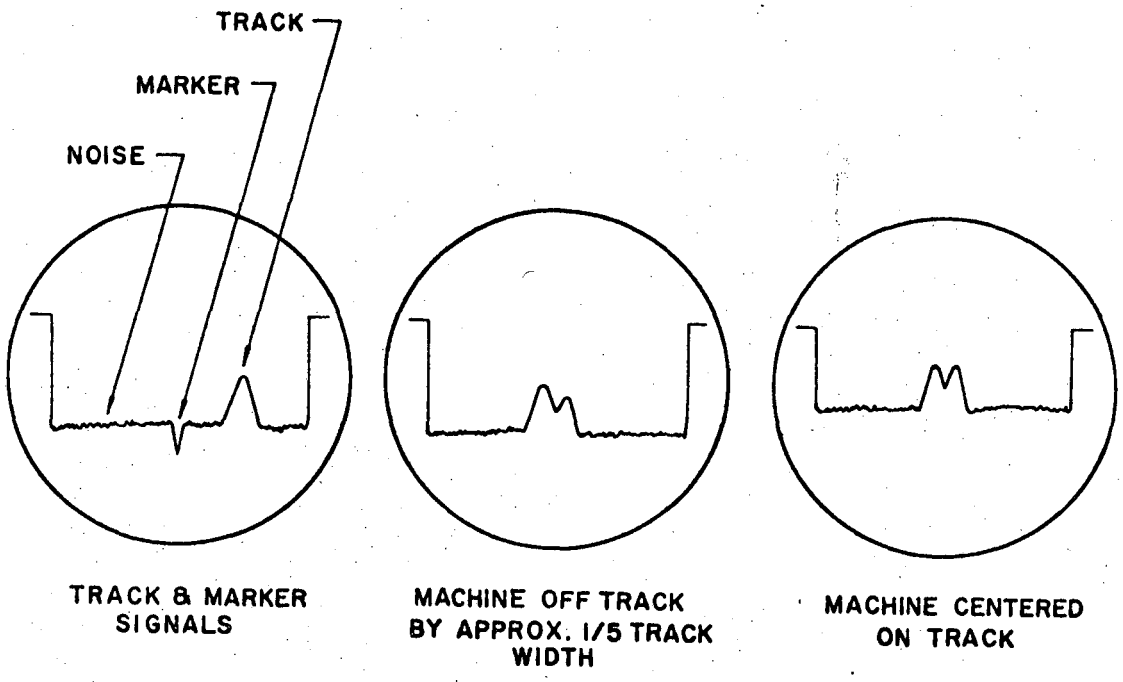
TRACK
MARKER
NOISE
TRACK & MARKER SIGNALS
MACHINE OFF TRACK BY APPROX. 1/5 TRACK WIDTH
MACHINE CENTERED ON TRACK
MUB-5154

Fig. 16

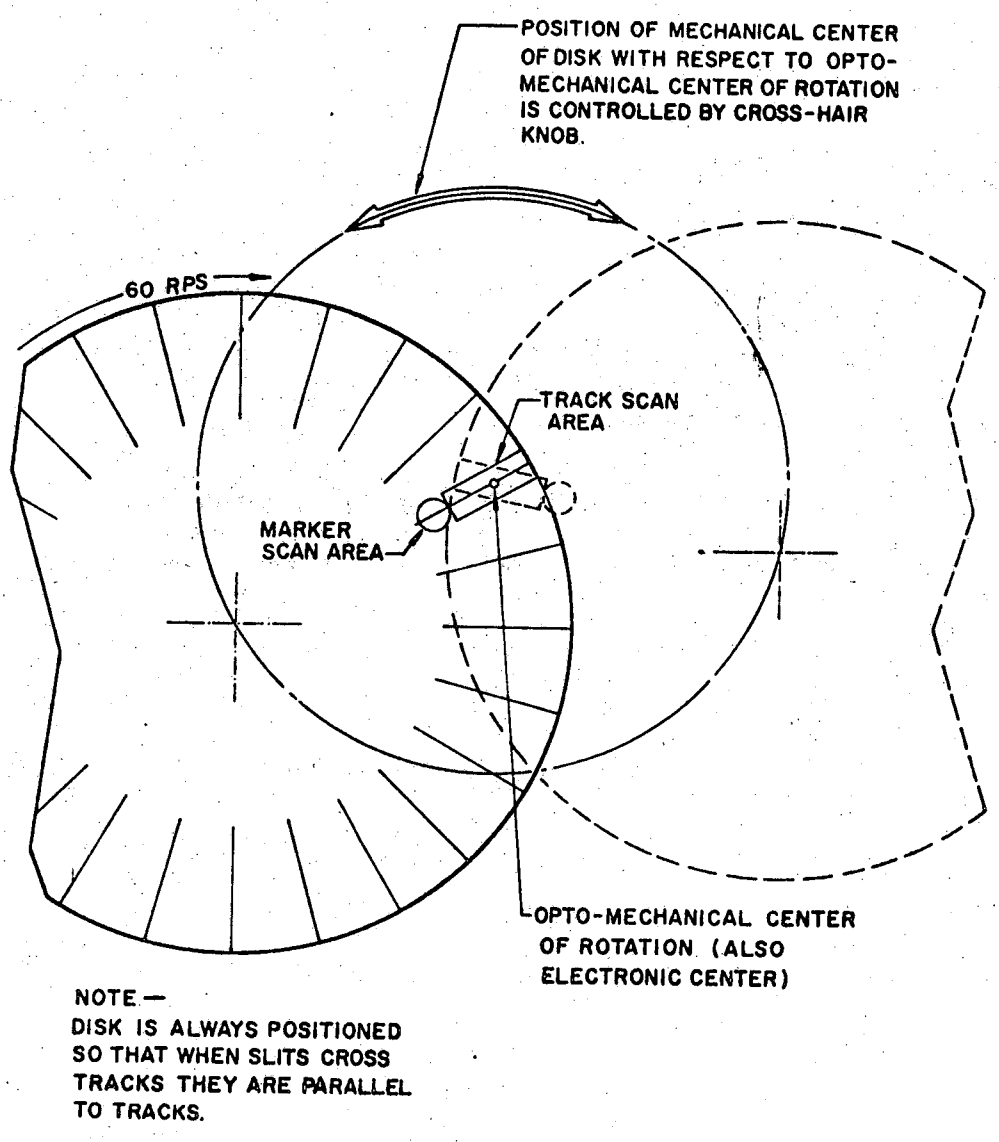
POSITION OF MECHANICAL CENTER OF DISK WITH RESPECT TO OPTO-MECHANICAL CENTER OF ROTATION IS CONTROLLED BY CROSS-HAIR KNOB.
60 RPS
TRACK SCAN AREA
MARKER SCAN AREA
OPTO-MECHANICAL CENTER OF ROTATION (ALSO ELECTRONIC CENTER)
NOTE—
DISK IS ALWAYS POSITIONED SO THAT WHEN SLITS CROSS TRACKS THEY ARE PARALLEL TO TRACKS.
MUB-5155

Fig. 17

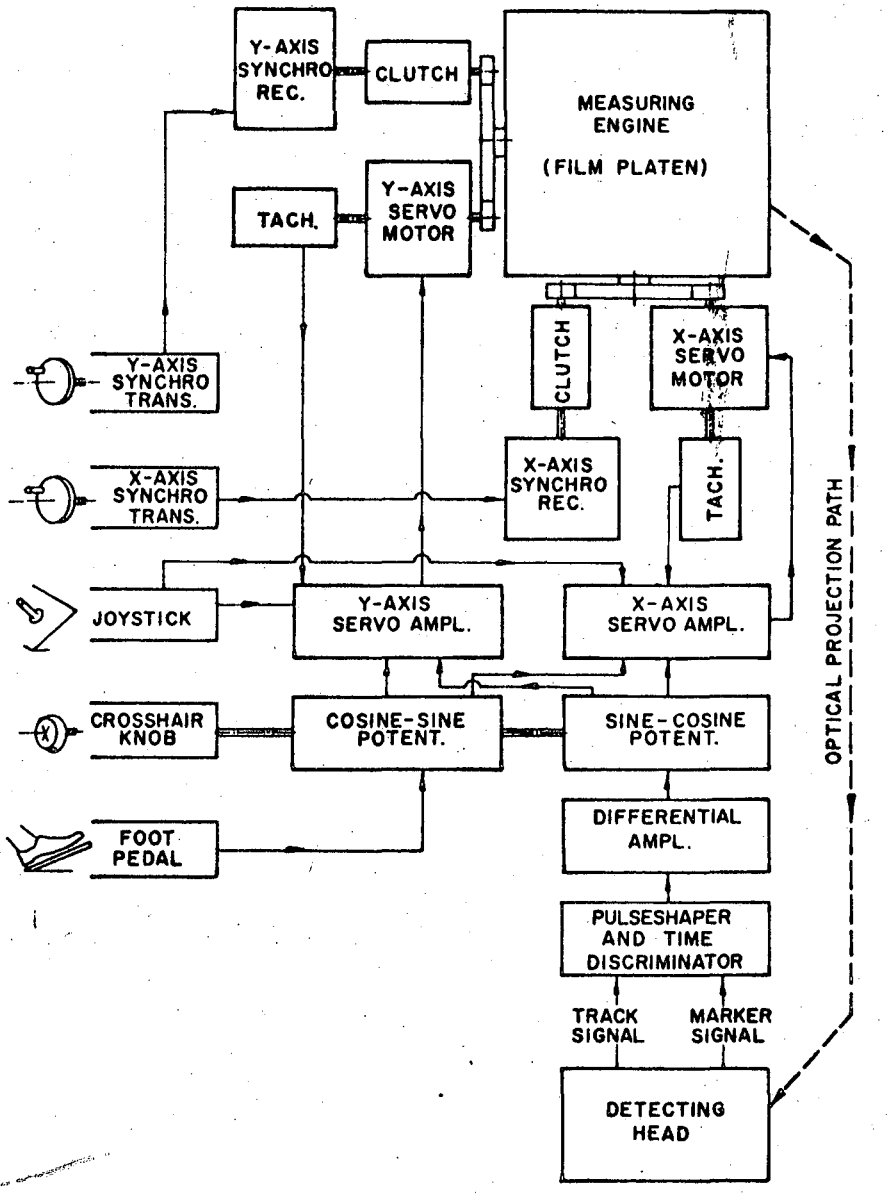
Y-AXIS SYNCHRO REC.
CLUTCH
MEASURING ENGINE
(FILM PLATEN)
TACH.
Y-AXIS SERVO MOTOR
CLUTCH
X-AXIS SERVO MOTOR
Y-AXIS SYNCHRO TRANS.
X-AXIS SYNCHRO TRANS.
X-AXIS SYNCHRO REC.
TACH.
JOYSTICK
Y-AXIS SERVO AMPL.
X-AXIS SERVO AMPL.
CROSSHAIR KNOB
COSINE-SINE POTENT.
SINE-COSINE POTENT.
DIFFERENTIAL AMPL.
FOOT PEDAL
PULSESHAPER AND TIME DISCRIMINATOR
TRACK SIGNAL
MARKER SIGNAL
DETECTING HEAD
OPTICAL PROJECTION PATH
MUB-5156

Fig. 18

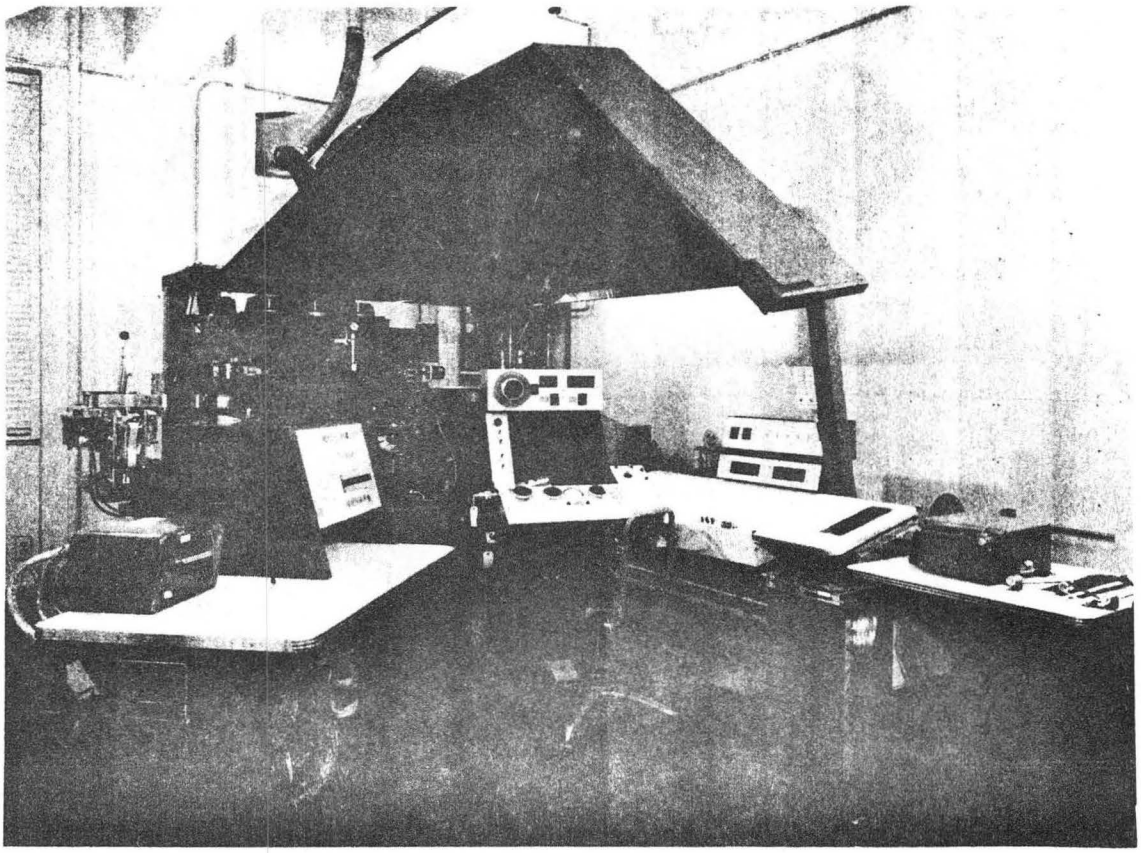

ZN-4673

Fig. 19

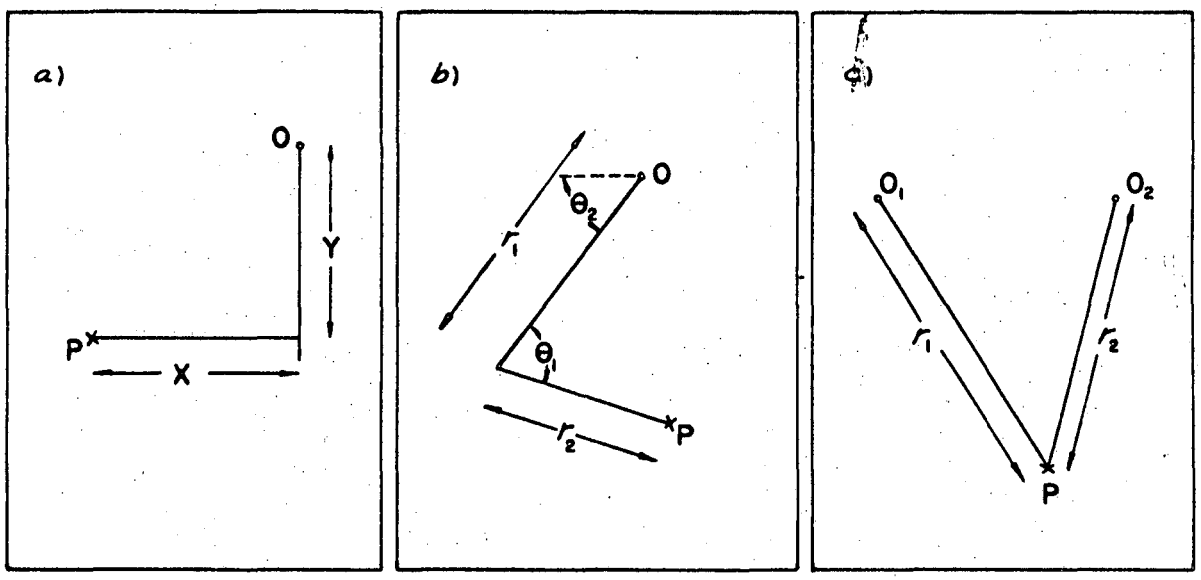

MUB-5157

Fig. 20

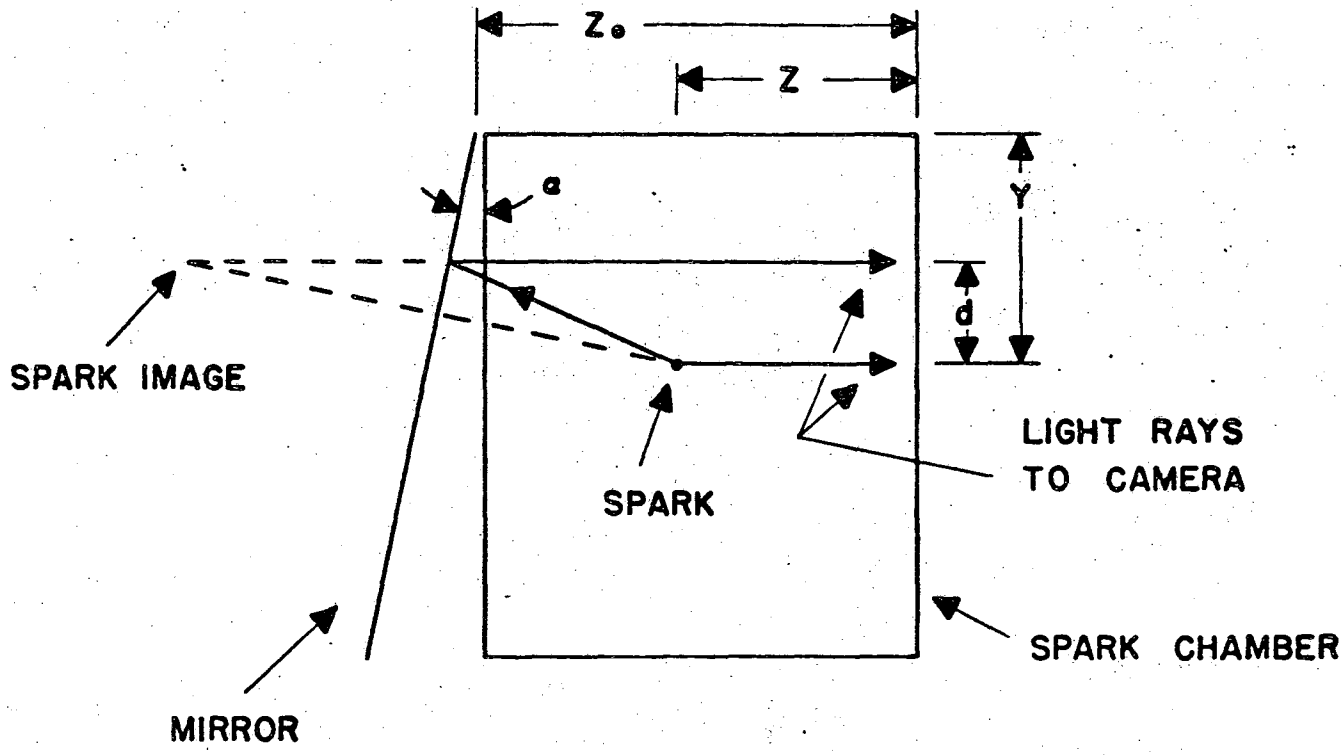

MUB-5219

Fig. 21

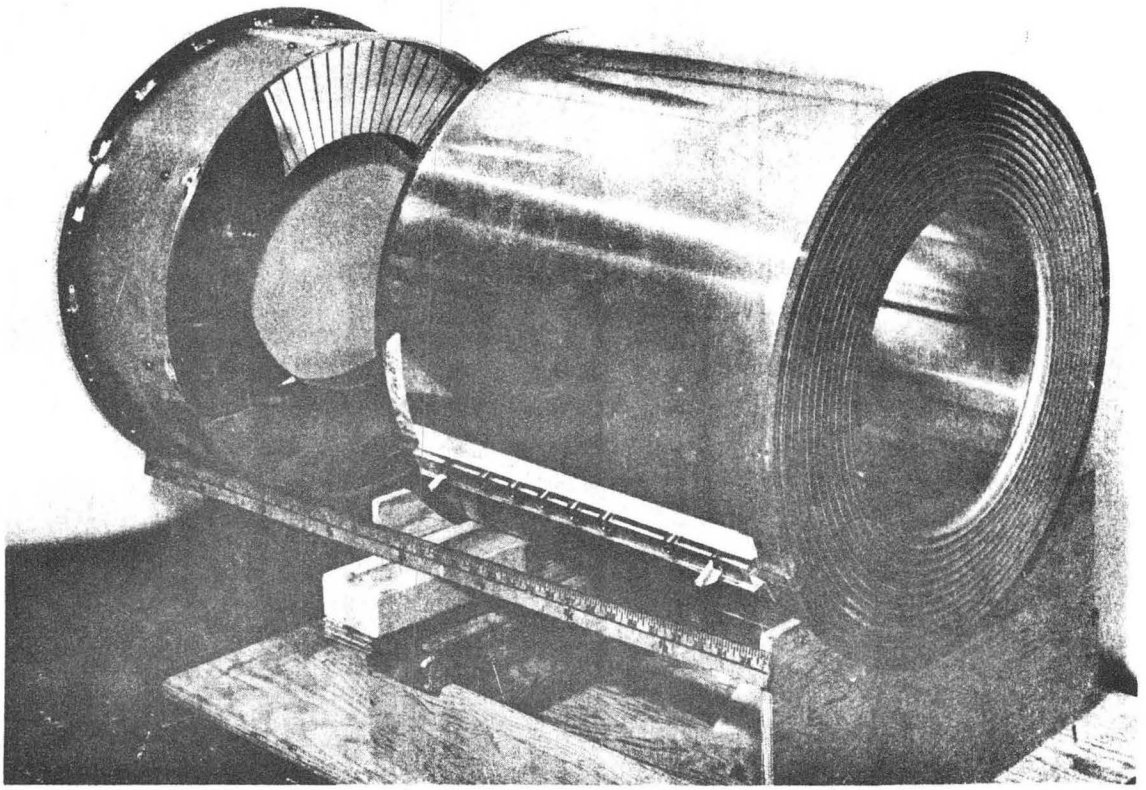

ZN-4685

Fig. 22

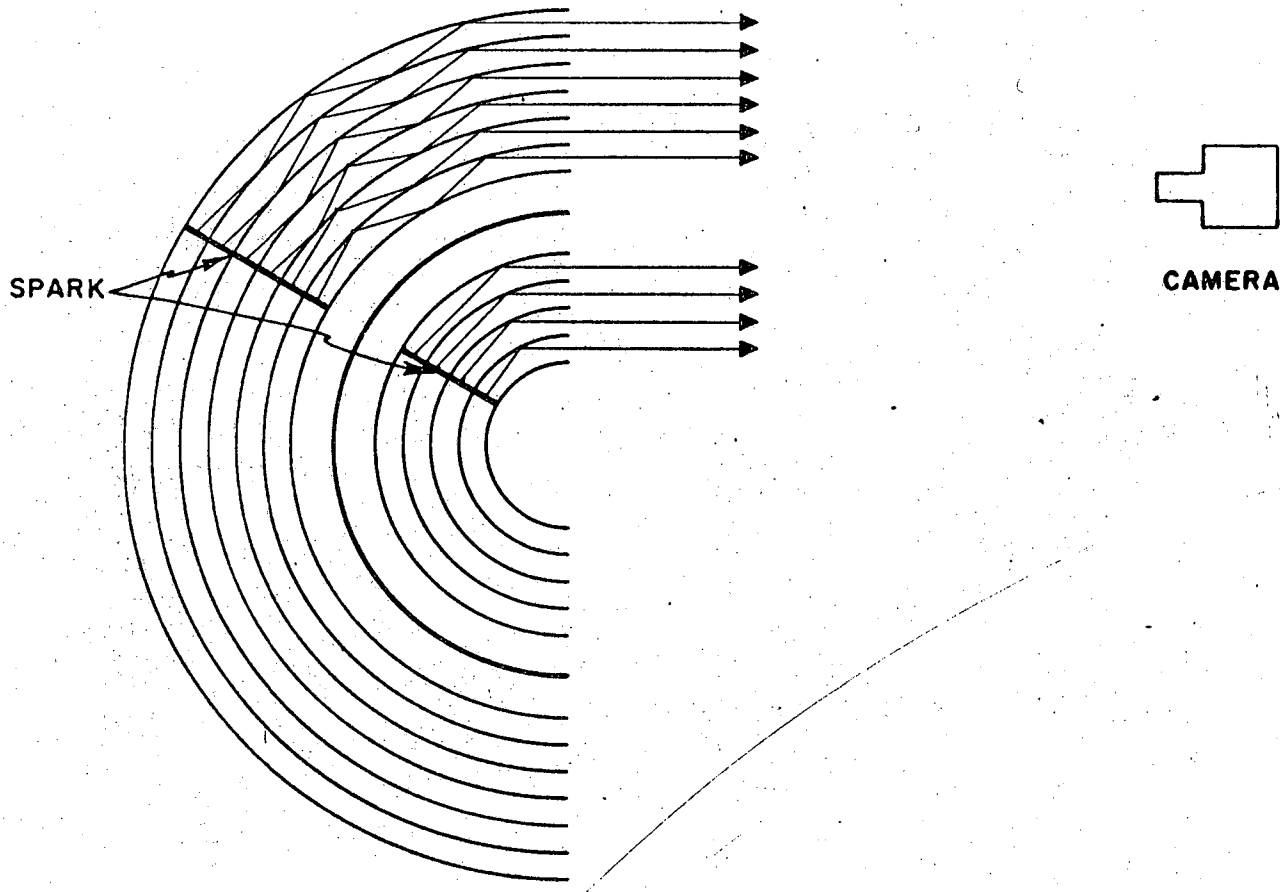

Fig. 23

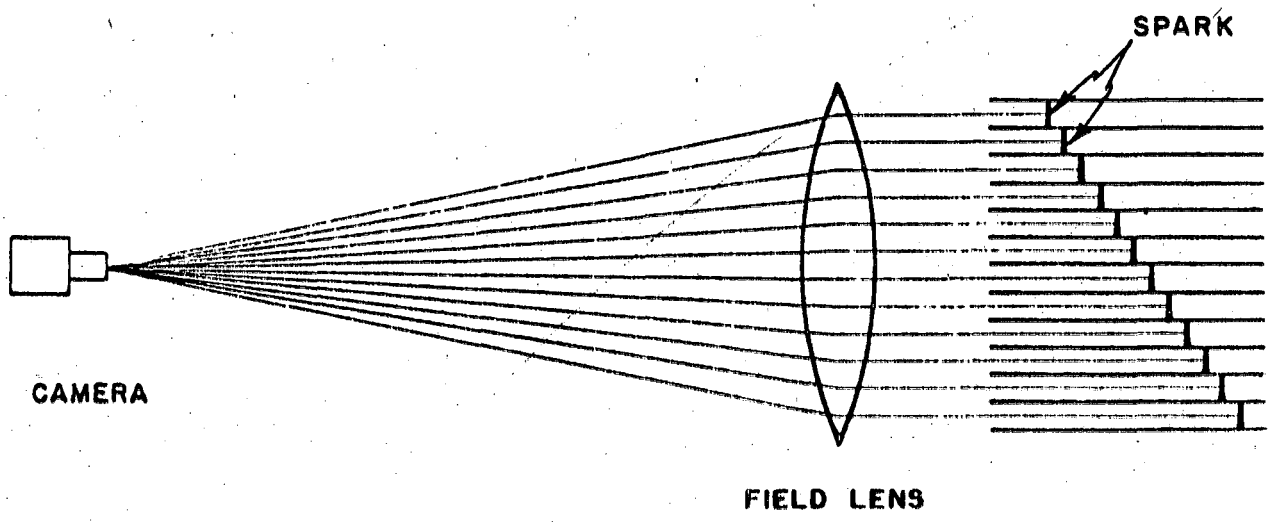

MUB-5221

Fig 24

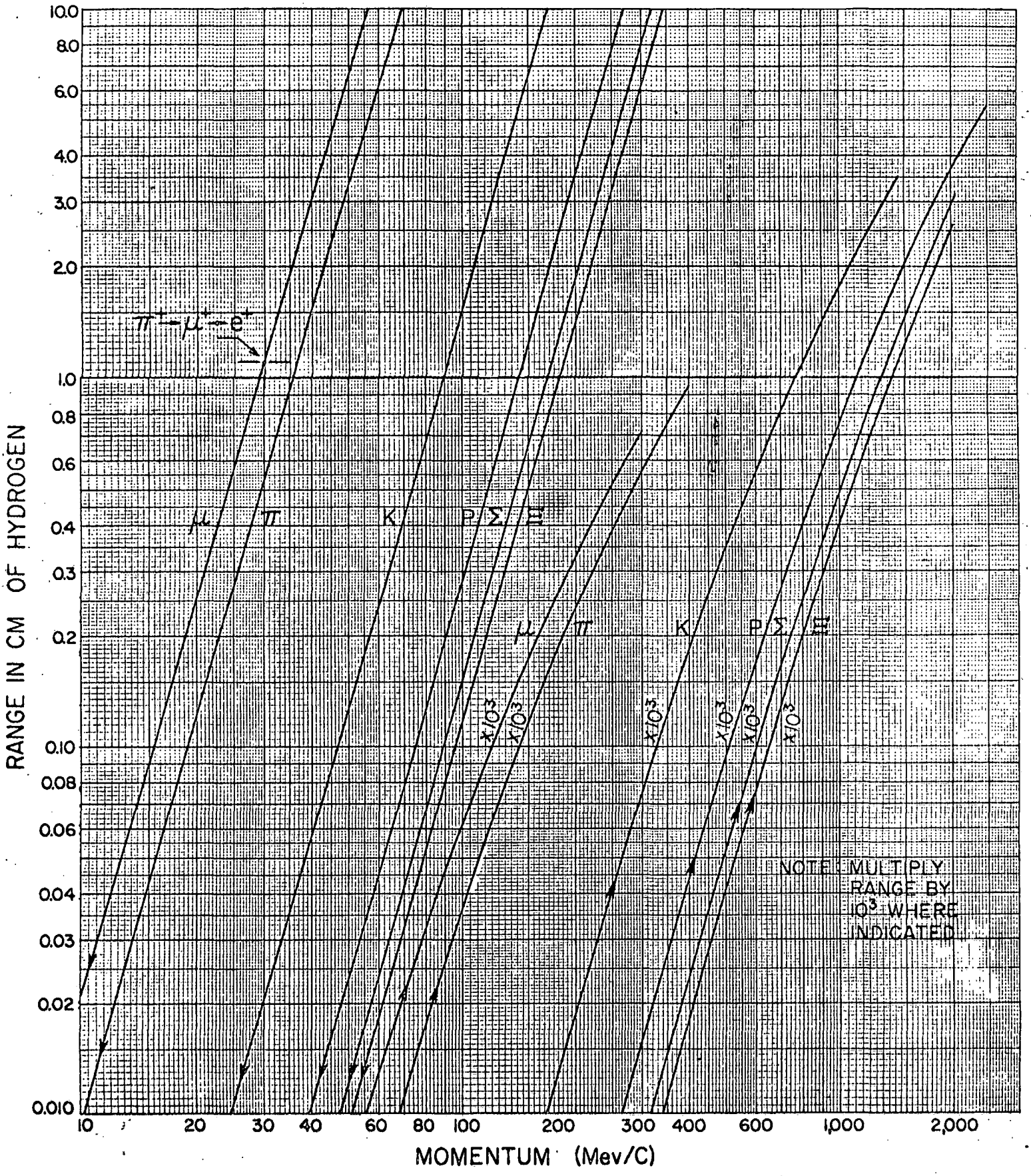

MUB-125

Fig. A-1

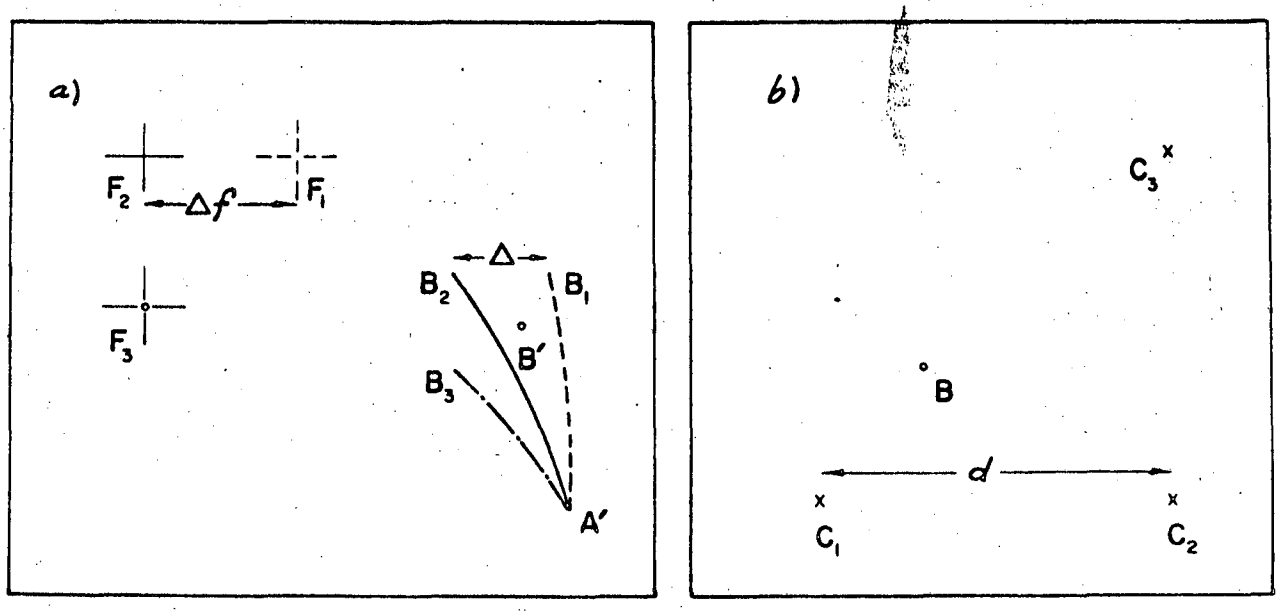

Fig. A-2

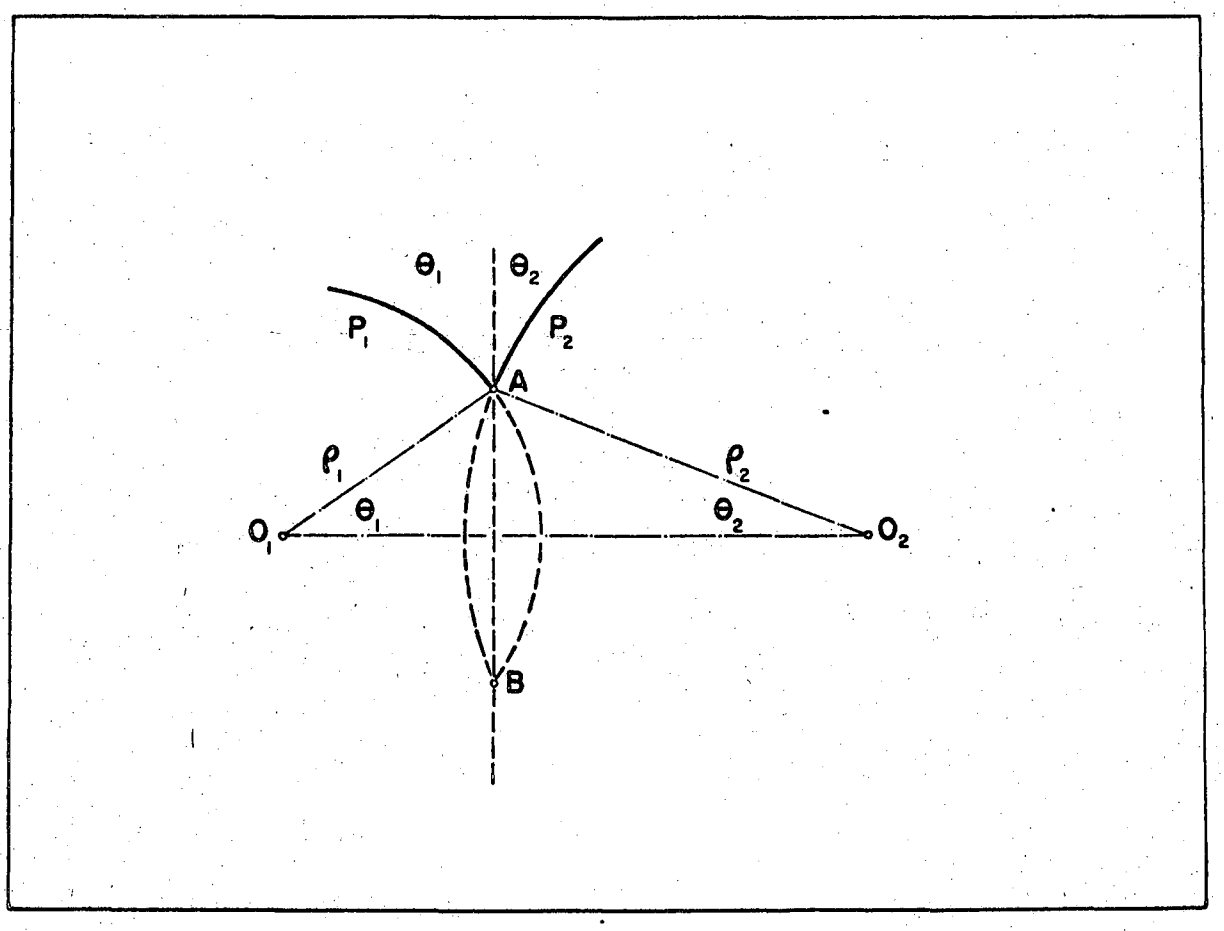

MUB-5158

Fig. A-3

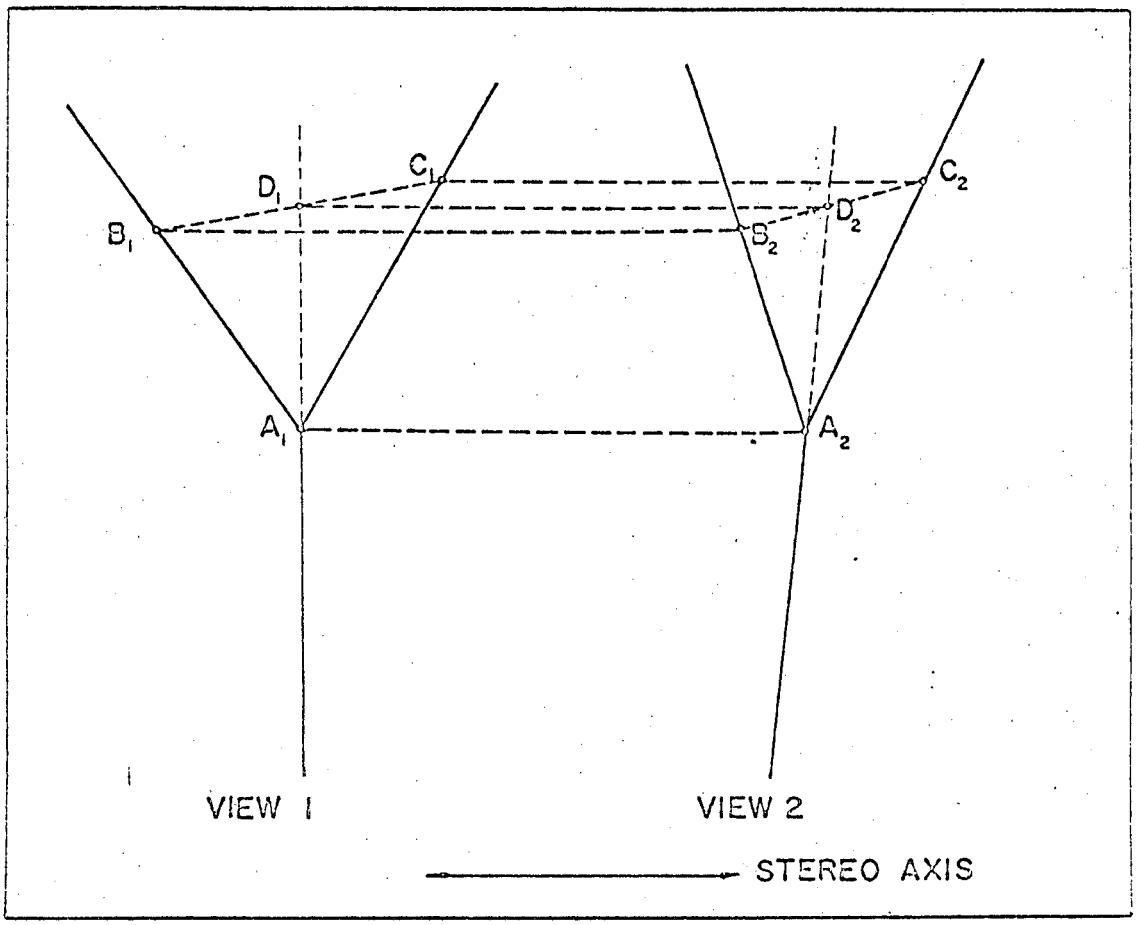

MUB-5151

Fig. A-4

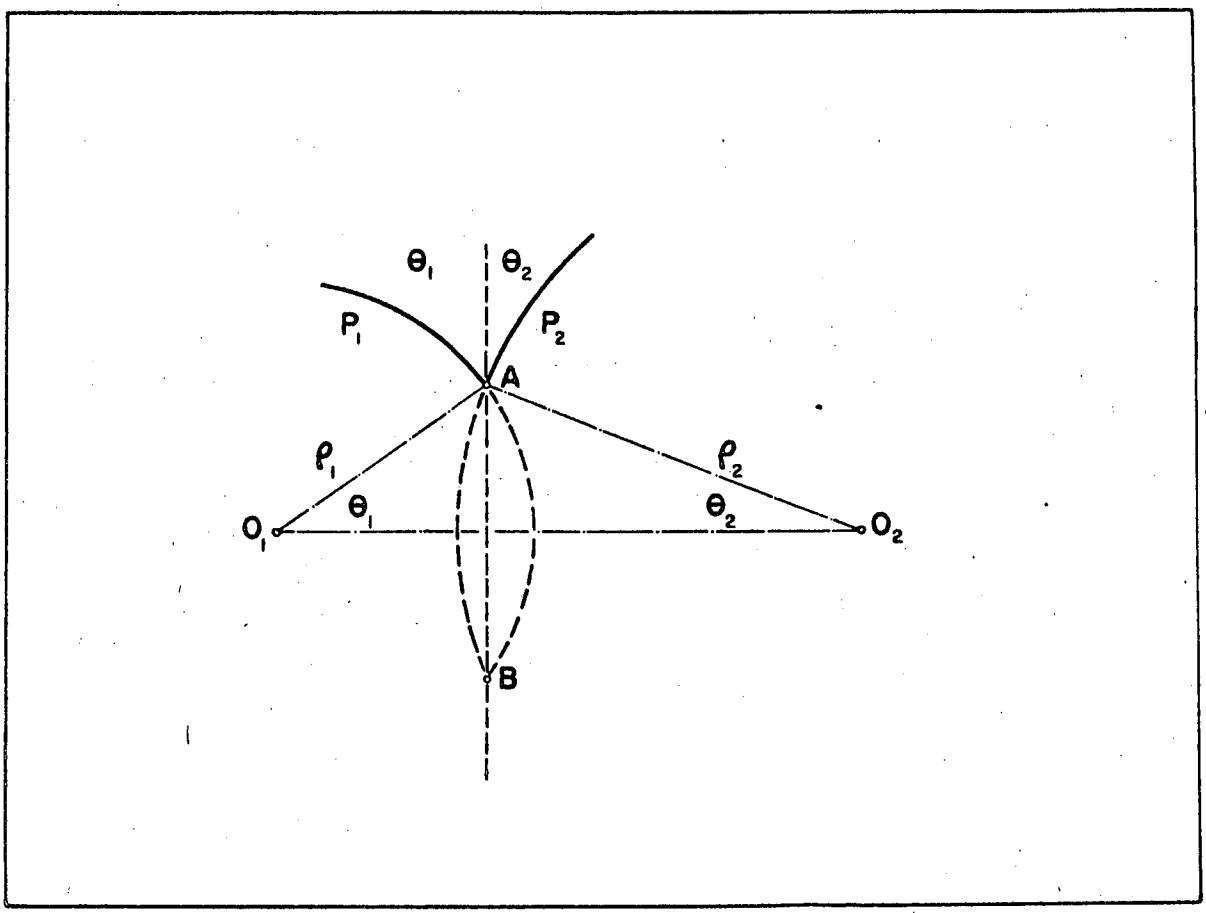

MUB-5158

Fig. A-3

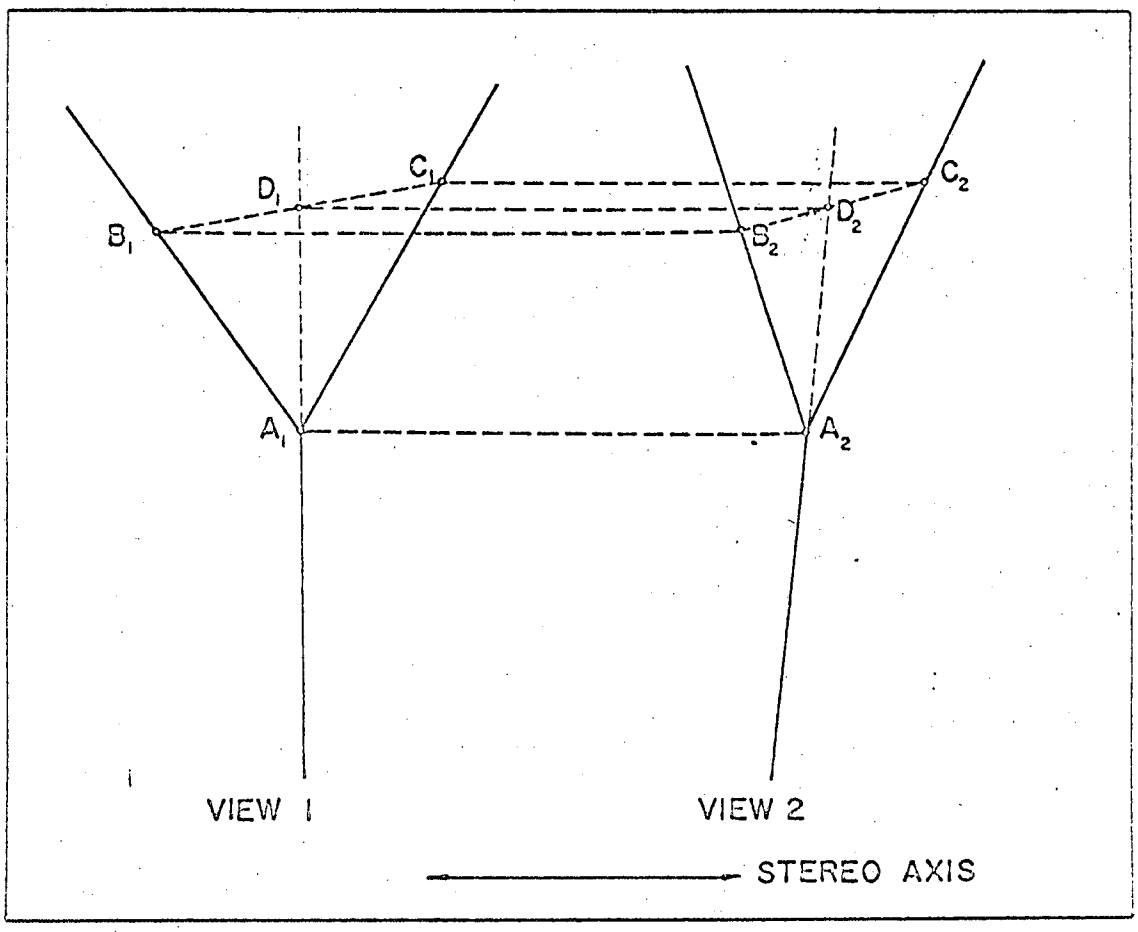

MUB-5151

Fig. A-4